UNIVERSITY OF OKLAHOMA

GRADUATE COLLEGE

EFFECT OF FLUID RHEOLOGY AND FLOW RATE ON WELLBORE CLEANOUT PROCESS IN HORIZONTAL AND DIRECTIONAL WELLS

A DISSERTATION

SUBMITTED TO THE GRADUATE FACULTY

in partial fulfillment of the requirements for the

Degree of

DOCTOR OF PHILOSOPHY

By

SARVESH NAIK
Norman, Oklahoma
2015

EFFECT OF FLUID RHEOLOGY AND FLOW RATE ON WELLBORE CLEANOUT PROCESS IN HORIZONTAL AND DIRECTIONAL WELLS

A DISSERTATION APPROVED FOR THE
MEWBOURNE SCHOOL OF PETROLEUM AND GEOLOGICAL ENGINEERING

BY

_____
Dr. Subhash N. Shah, Chair

_____
Dr. Ramkumar Parthasarathy

_____
Dr. Ramadan Ahmed

_____
Dr. Bor-Jier Shiau

_____
Dr. Maysam Pournik

Dedicated to my family, teachers and friends for their love, encouragement and support.

ACKNOWLEDGMENTS

There have been significant contributions by many people without whom this research would have not been possible.

I would like to express my sincere gratitude to Dr. Subhash Shah for his constant support and guidance during my research. His patience, motivation and encouragement helped me throughout my graduate program. I would also like to express my gratitude to Dr. Ramadan Ahmed for his comments on the research and help in designing the experimental setup. I would also like to thank Dr. Bor-Jier Shiau, Dr. Maysam Pournik and Dr. Ramkumar Parthasarathy for being a part of my committee and their recommendations.

I would like to thank Mr. Jeff McCaskill and Mr. Joe Flenniken for their expertise and help in conducting experiments at the Well Construction Technology Center (WCTC). Special thanks to Vineet, Govindu, Soham, Harsh and Aditya for their help in fabrication of the experimental setup and also in conducting the experiments. I would also like to thank Idowu and Xiaochun for the wonderful time we have had together.

Special thanks to my friends Eric, Himanshu, Subbu, Adarsh, Abhijit, Jyot, Dongre, Shantanu, Rohit, KV, Priyavrat, Ruchir, Lauren, Dhanya, Ankita, Sami and Janny, who have been my family away from home. You made my stay at OU a memorable one.

My sincere thanks to Peggy Rijken, Amit Singh and Oya Karazincir for their wonderful mentoring during my summer internships at Chevron ETC. Also, thanks to Sarkis Kakadjian and Siwar Trabelsi for providing an opportunity to intern with Trican Well Service. I would also like to thank the members of Coiled Tubing Consortium for their continued financial support towards this research.

Finally, I am forever thankful for the unwavering support and love from my family. Thank you Aai, Baba and Pranjali; I will always be indebted to you. I will always be thankful to my teachers from school and undergraduate university who have always believed in me.

Above all, thank you Almighty for everything.

TABLE OF CONTENTS

LIST OF TABLES

LIST OF FIGURES

ABSTRACT

Solids like milled plugs, produced sand or residual proppant are deposited in the wellbore during fracturing operation. These solids can impair hydrocarbon production or cause operational problems, and hence should be removed. Wellbore cleanout is the removal of such solids from the wellbore. Coiled tubing (CT) has found a niche as an economic option for wellbore cleanout and current worldwide estimates indicate cleanout operations account for almost 40% of all CT activities.

Several research efforts have been reported in the literature covering various aspects of wellbore cleanout. These include theoretical, empirical-based approaches or a combination of both to explain the dynamics of solid-liquid transport. Solids transport is affected by flow rate, fluid properties (rheology and density), solid properties (size and density) and wellbore configuration (inclination, annular geometry and eccentricity). A survey of literature suggests that flow rate and fluid rheology are dominant among these while others have a secondary influence on solids transport. A shortcoming in most studies is the failure to account for interaction between parameters. Furthermore, a significant number of investigations focuses on solids transport in drilling with limited information on fracturing operation. Although some success has been recorded, it can be stated that the current state of understanding of wellbore cleanout is incomplete and less than satisfactory.

A comprehensive experimental study of wellbore cleanout using CT was undertaken to understand the effects of flow rate and fluid rheology on solids transport in directional

and horizontal wells. An experimental setup with two interchangeable test sections was designed and fabricated to conduct solids erosion tests, which simulate the cleanout of a proppant (solids used in fracturing) bed in the wellbore under various operating conditions. Water, and 10 and 20 lb/Mgal guar fluids were evaluated at flow rates of 80, 100 and 120 gpm each and at inclinations of 45, 60, 75 and 90°. Additionally, solid erosion tests were carried out with a drag reducing fluid, 2.16 lb/Mgal HE 150 at 90°. The cleanout performance of fluid was determined by solids bed erosion and cleanout efficiency.

With increasing flow rate, the solids erosion rate and cleanout efficiency increased for all fluids and inclinations considered. Solids erosion rate and cleanout efficiency were higher at 120 gpm than 80 gpm for all cases considered. Better performance was obtained with water compared to polymeric fluids at 75 and 90° for the flow rates considered. At 45 and 60°, fluids with higher viscosity performed better than those with low viscosity. Thus, 20 lb/Mgal guar fluid performed better than other fluids with decreasing inclination.

For all flow rates considered, the rate of solids erosion for water increased with inclination whereas for polymeric fluids it increased with decrease in inclination. With decreased inclination, the cleanout efficiency increased with fluid viscosity. A 20 lb/Mgal guar fluid performed better at 45° at all flow rates considered.

The data of solids bed height as a function of circulation time was modeled using an exponential decay function. Using a statistical software MINITAB 16, the coefficients of

the correlation were obtained. This correlation would aid in predicting the bed height reduction and circulation time for various fluids at different rates and inclination. The correlation predicted the bed height within 10% deviation for all fluids at inclination of 75 and 90°. The deviation for 60° was higher since there was an unstable bed at this inclination which made the bed height predictions difficult.

Dimensional analysis was used to develop dimensionless groups, which were correlated using non-linear regression analysis to obtain correlations for inclinations of 60, 75 and 90°. One set of correlations were obtained for water and another set for polymeric fluids. These correlations can be used to predict solids bed height as a function of circulating time for different fluids and flow rates. The absolute percentage deviation of predictions with the experimental values are 18.13, 21.14, 20.85, 14.64, 21.57 and 8.82 % respectively.

CHAPTER 1

INTRODUCTION AND SCOPE OF RESEARCH

1.1 Introduction

Solids such as drill cuttings, milled plugs, produced sand or residual proppant can accumulate in the wellbore during drilling, production, stimulation and other operations. These solids can cause problems such as stuck pipe, lower drilling rate, lost circulation, additional pipe wear, and time for cleanouts (Kelessidis and Mpandelis 2003). They can also cause problems like premature packer setting, blocked screens, malfunctioning safety valves, and wear of equipment. With recent advancement in drilling operations, numerous horizontal and multi-lateral wells are being drilled and completed. These wells help to recover maximum hydrocarbons from existing surface facilities. With the increasing number of such directional wells having extended-reach laterals, the accumulation of solids in these laterals poses a serious challenge. Wellbore cleanout is the process of removing these solids from the wellbore. Several different approaches have been implemented to dislodge and circulate solid particles out of the wellbore. Among the different approaches, the use of Coiled tubing (CT) has emerged as the most convenient and economical approach. On a worldwide scale, 40% of all CT activities are related to wellbore cleanout (Aitken and Li 2013).

CT is a continuous milled tubular spooled on a reel, which is straightened before introducing into the wellbore and spooled back while removing from it. Being spooled on a reel enables CT to be mobilized faster and also tripping in and out of the wellbore is made easier. There is no need for making pipe connections, which reduces spillage and

the number of personnel required. However, CT, due to its small diameter, cannot handle very high flow rates or excessive surface pumping pressure. Due to the latter, it is a standard industry practice to move the CT (wiper trips) using forward and rear facing jetting nozzles to agitate the solids and re-entrain and transport solids out of the wellbore or casing. The common methods for cleanout with CT are forward and reverse fluid circulation modes, wiper trips, sand vacuuming, and venturi sand bailers (Li et al. 2010). In forward and reverse circulation modes, the CT is tagged to the top of solids bed, and fluid is circulated to fluidize the solids bed and then transported to the surface. In forward circulation, the fluid is pumped through the CT and solids are transported through the annulus between the casing/open hole and the CT. In reverse circulation, the fluid is circulated through the annulus and the solids are transported from within the CT. In wiper trip cleanout, the CT is pulled back as the fluid is circulated which helps to keep the solids in agitation at all times. The selection of the appropriate cleanout method depends on various logistical and technical issues. Logistical issues include equipment cost, CT reel weight, and, availability and cost of cleanout fluid. Technical issues include considering formation damage potential, bottomhole pressure, completion size and, size and type of solids (Li et al. 2010).

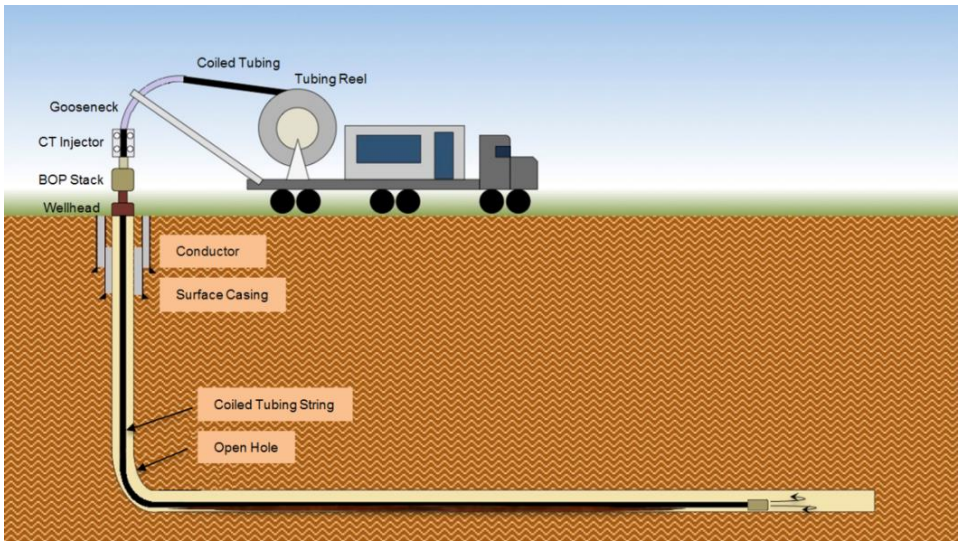

Figure 1.1: Wellbore cleanout process using CT

Apart from these issues, solids transport is affected by properties of fluid and solids, and wellbore parameters. A list of major factors affecting solids transport was given by Zamora and Paul (1990). They are as follows:

Fluid properties:

1. Rheology
2. Density
3. Annular velocity/velocity profile
4. Flow regime

Solid properties:

1. Size and shape
2. Density

Wellbore parameters:

1. Annular configuration
2. Inclination (angle measured from the vertical in degrees)

3. Eccentricity

Extensive research has been undertaken to study the effect of different parameters affecting solids transport. The research followed two major approaches: mechanistic modeling and experimental/empirical approach. Mechanistic modeling involves developing a set of mathematical equations by analysis of forces, stresses, and momentum acting during the solids transport process. The empirical approach involves gathering experimental data from solids transport tests and correlating them by dimensional analysis and theoretical reasoning. These correlations are valid for the range of operating conditions under which the data were gathered. The mechanistic modeling based approach offers advantages over the empirical approach, such as: the ability to make predictions outside the range of experimental data, develop a comprehensive understanding of the physical process involved, perform sensitivity analysis on parameters which are difficult to evaluate experimentally, and reduction in experimental work (Brown et al. 1989). Numerous mechanistic and experimental models are available in the literature to understand the solids transport phenomena. Cho (2001) suggested most of the mechanistic models fail to match the experimental or field data, for reasons such as:

1. Attempts to develop models covering a wide range of operating conditions (flow rate and inclination) and

2. Making inappropriate or too many assumptions, which may be in some cases completely wrong.

In spite of the many university and industry investigations conducted to study solids transport, mixed and ambiguous results have been obtained. In the oil and gas industry, certain accepted rules of thumb are used to compensate for the incomplete understanding of solids transport. For example, one common procedure is circulating two hole volumes at target depth; which may be insufficient to clean the wellbore. Also, different studies have conflicting views on whether fluids with high viscosity or low viscosity perform better, or whether laminar flow regime or turbulent flow regime will result in better cleanout. Thus, it may be stated that the solids transport is not completely understood, partly because of the effect of different variables which might be inter-related and due to different conditions under which the experiments are performed. The present research focuses on proppant cleanout with water and low viscosity polymer fluids. Proppants are solids used in hydraulic fracturing to keep the generated fractures open after pumping stops.

1.2 Problem Statement

With the increasing number of multi-stage fracturing operations performed in horizontal and deviated wells, there is a high probability of proppant settling in the wellbore. The proppant settle to form a solids bed, which can lead to lower hydrocarbon production. For such cleanouts, high viscosity fluids are generally not used due to formation damage issues. The important question to be answered is the type of fluid (water or low viscosity fluids) to be used for cleaning the solids bed. Another question to be answered is, what should be the circulation rate to clean the wellbore? In certain circumstances, a very high cleanout rate may not be recommended since it can affect the surface equipment by solids impingement. Hence, the engineer is usually faced with the question of circulation time

and pump rate to be utilized while cleaning the solids bed. Although there are many theoretical and experimental studies on solids transport, they are mainly focused on drill cuttings transport with drilling muds. The theoretical models are often complex and cannot be easily applied in the field. Hence, easy to use relations for determining the circulation time and flow rate for proppant cleanout with different fluids need to be developed with the help of experimental studies.

1.3 Scope of Research

The present study aims to provide an understanding of solids cleanout using water and low viscosity polymeric fluids. It will discuss the effect of fluid rheology and flow rate on solids cleanout in horizontal and inclined wells. The results from the study will help engineers to design a successful cleanout operation based on the available options.

An experimental setup with two different test sections, test section 1 and 2, was designed and fabricated for this study. Test section 1 was used for conducting tests in horizontal position and, test section 2 for conducting tests in both horizontal and inclined position. The cleanout fluids considered were water, 2.16 lb/Mgal HE 150, and 10 and 20 lb/Mgal guar fluids and solids used are 20/40 mesh proppant (average diameter = 630 microns) with relative density of 1.75 (density =14.6 lb/gal). The flow rates considered were 80, 100 and 120 gpm and inclinations are 45, 60, 75 and 90°. A total of 12 tests in section 1 and 36 tests in section 2 was performed.

As discussed in Section 1.3, different cleanout fluids are used for evaluating their cleanout performance. HE 150 is a 2-Acrylamido-2-methylpropane sulfonic acid (AMPS)

copolymer in liquid form and sold by Drilling Specialties Company. It contains 60% C12-C14 iso-alkanes by weight. The molecular weight ranges from 0.72 x 10^6 to 1.02 x 10^6 g/mol. The active polymer content in the suspension is 3.6 lb/gal. Table shows the physical properties of HE® 150.

Table 1.1: Physical properties of HE® 150

Quantity	Property
Color	Cream color
Flash point	188 °F
Specific gravity	0.96
pH	7
Polymer Activity	3.6 lb/gal

Guar gum is a galactomanan obtained from the endosperm of the *Cyamopsis tetragonolobus* seed. Galactomanans are polysaccharides consisting of a mannose backbone with galactose side groups. The principal backbone is a chain of (1-4)-β-D-mannopyranosyl units, with single (1-6)-α-D-galactopyranosyl units linked to the principal chain. The molecular weight of the polymer ranges from 5 x 10^5 to 8.0 x 10^6 g/mol. Guar gum used in this study is in form of liquid suspension, i.e slurry. The activity of the polymer was 4 lb/gal.

The solids used are 20/40 mesh proppant with an average diameter of 630 microns and a relative density range of 1.6 to 1.9. The proppant used was TerraProp Plus by Baker Hughes.

1.4 Approach

Solids bed was deposited in the annulus of the test section and cleanout fluid was re-circulated at specific flow rate to erode the bed. These solids erosion tests were performed by varying the fluid rheology, flow rate, and inclination while maintaining other parameters constant. A filter was placed downstream of the test section to separate the solids. The solids bed height with time was recorded for each experiment along the length of the test section. This data was then plotted as solids bed height versus time and the trend was fitted to an exponential decay equation using a statistical software to develop an empirical correlation. This correlation would be specific to a combination of fluid and flow rate. Additionally, inclination specific correlations were develop to predict the solids bed height as a function of circulating time for different fluids and flow rate.

1.5 Objectives

The primary objective of this study is to perform experimental studies on wellbore cleanout in directional wellbores using CT. Specific objectives are to:

1. Design and fabricate an experimental setup for solids erosion tests.
2. Perform transient solids bed erosion tests with fresh water, 2.16 lb/Mgal HE 150, and 10 and 20 lb/Mgal guar fluids and each at flow rates of 80, 100 and 120 gpm and inclinations of 45, 60, 75 and 90°.
3. Investigate the effect of fluid rheology and flow rate on solids bed erosion at different inclinations.
4. Develop empirical correlations to predict the solids bed height with time for different fluids and flow rates tested at inclinations of 60, 75 and 90°.

5. Develop correlations using dimensional analysis to predict solids bed height under various operating conditions.

This dissertation is divided into seven chapters. The various mechanistic models and experimental studies related to solids transport are discussed in Chapter 2. The effect of various operational parameters on solids cleanout are also discussed in this chapter. The descriptions of experimental setup, test procedures and data analysis are provided in Chapter 3. The results and analysis of solids erosion tests are discussed in Chapter 4. The development of empirical correlations and the dimensional analysis of variables affecting solids transport are described in Chapter 5. The field application and limitations of the model are discussed in Chapter 6. The conclusions and recommendations from this study are discussed in Chapter 7.

CHAPTER 2

LITERATURE REVIEW AND THEORY

This chapter provides a review of theoretical and empirical models developed to study solids transport. Solids transport in the wellbore depends on the fluid and solids properties, and wellbore geometry. This chapter also discusses the effect of different parameters affecting solids transport.

2.1 Theory

The analysis of solids removal process requires a good understanding of the forces acting on an individual solid particle. When fluid is pumped to clean the solids bed, a single particle resting on the bed is subjected to gravity, buoyancy, fluid drag, and lift force. The fluid drag and lift forces occur due to fluid flow over the solids bed. Above a critical value, these forces can initiate particle motion either by a rolling/sliding or lifting mechanism.

Gravity and buoyancy forces act opposite to each other and have opposite effect on solids transport.

The measure of force of gravity on a particle is given by its weight.

$$F_g = mg \tag{2.1}$$

The mass of particle can be expressed in terms of its density and volume.

$$F_g = \frac{1}{6}\pi {d_s}^3 \rho_s g \tag{2.2}$$

where, F_g = gravity force; m = mass of particle; d_s = diameter of particle; ρ_s = particle density; g = acceleration due to gravity.

Buoyancy is the upward force exerted by volume of fluid displaced by the partially or fully submerged particle. The measure of this force is given by the weight of displaced fluid.

$$F_b = m\frac{\rho_f}{\rho_s}g \tag{2.3}$$

Expressing the mass of particle in terms of its volume and density, Eq. 2.3 reduces to:

$$F_b = \frac{1}{6}\pi d_s^3 \rho_f g \tag{2.4}$$

where, F_b = buoyancy force; ρ_f = fluid density.

Solids are deposited when gravity dominates over buoyancy. Buoyancy of fluid is a function of its density. Hence, denser fluids can be more effective in solids transport. As discussed earlier, the drag and lift forces are a result of fluid flow over a solid body. These forces are a result of pressure and stress variations over the surface of solid particle due to fluid flow. They can be determined by integrating the wall shear stress and pressure distribution over the surface of particle. However, solution for these distributions are difficult to obtain mathematically or experimentally. Hence, experimentally obtained drag and lift coefficients are utilized to compute these forces. The fluid drag on the solid particle is given by,

$$F_d = \frac{1}{2}C_D \rho_f u^2 A_p \tag{2.5}$$

and the lift force is given by,

$$F_l = \frac{1}{2} C_L \rho_f u^2 A_p \quad (2.6)$$

where, C_D = drag coefficient; C_L = lift coefficient; A = projected area of the particle over the mean bed surface; u = fluid velocity.

Consider a solid particle at rest on a solids bed on verge of rolling (Fig. 2.1). The following equation represents the summation of the moment acting on point 'A':

$$F_D L_D + (F_L + F_B) L_G \geq F_G L_G \quad (2.7)$$

Particle motion occurs when the driving moment (due to fluid forces and buoyancy) generated at point 'A' overcomes the opposing moment due to gravity. The particle moves by sliding if the lift force is not sufficiently strong. When the lift force is sufficiently strong, the particle is lifted into the fluid stream and remains in suspension depending on fluid properties.

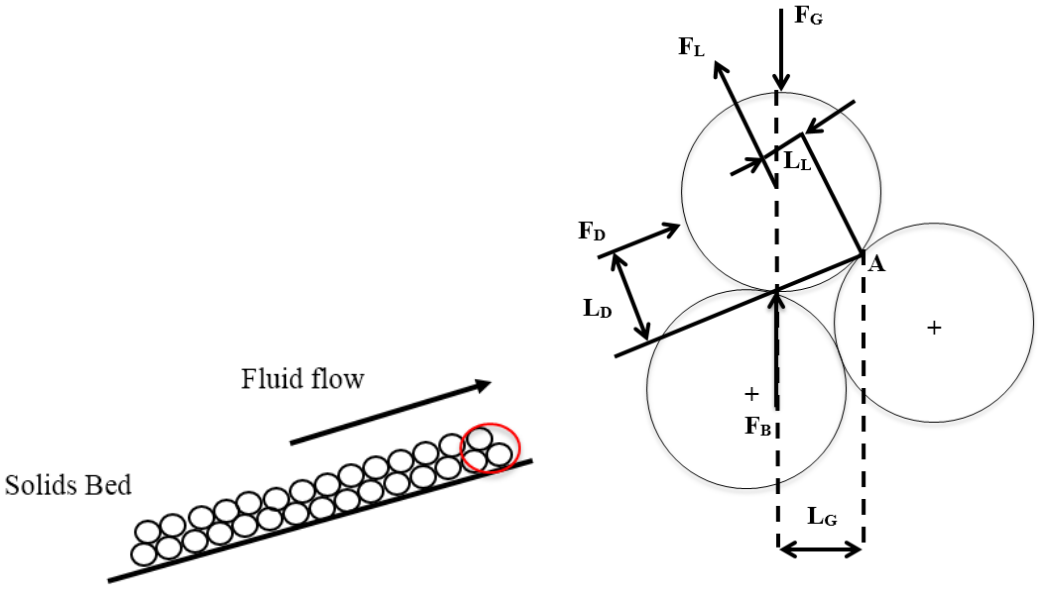

Fig. 2.1: Forces acting on a solid particle

2.2 Theoretical and Correlation Models

The study of solids transport follows two major approaches: mechanistic modeling and an experimental/empirical approach. Mechanistic models can be classified into two- and three-layer models based on number of distinct layers described in the model. Two-layer models describe the flow comprising of two layers. The top layer is either clear fluid or fluid with suspended solids and the bottom layer is a solids bed which may be stationary or moving slowly. The three-layer model consists of a stationary solids bed, above which exists a moving bed of solids. The top layer is a fluid layer which may have a suspension of some solid particles. These mechanistic models are based on mass balance equations for solids and fluids and momentum balance equations for the two- or three-layers resulting in a system of coupled algebraic equations. These equations are solved with the help of closure relations obtained from correlations in the literature.

Several two-layer models (Gavignet and Sobey 1989; Martins and Santana 1992) and three-layer models (Kamp and Rivero 1999; Ramadan et al. 2001; Cho et al. 2001) are available in literature. Kelessidis and Mpandelis (2003) suggest that the different two- and three-layer models vary primarily in the relationships used for the following:

1. Solids distribution in the heterogeneous solid-liquid layer
2. Interfacial friction between the fluid and moving solids bed
3. Terminal settling velocity of particles in fluid
4. Fluid friction between the fluid and pipe walls.

A brief description of the two- and three-layer models follows.

Gavignet and Sobey (1989) developed a two-layer model for solids transport during drilling by non-Newtonian fluids in eccentric annuli for deviated wells. The top layer consists of a clear fluid layer and the bottom layer is a moving bed of solids. The two modes of solids transport reported were saltation and sliding. Saltation occurs when the particle at the solid-fluid interface is lifted into fluid stream due to drag force, and sliding occurs when solids bed travel up or down the wellbore, depending on the magnitude of fluid forces exerted by fluid on it. The model predictions were used to study the effects of fluid velocity, viscosity and solids size on solids bed height. The solids bed height decreased with increasing fluid velocity. Viscosity was found to play a minor role in determining bed thickness. Higher flow rates were required to transport small cuttings compared to larger ones. The predictions from this model were compared with experimental data of Tomren et al. (1986). It was reported that the model over-estimated bed height since it did not account for solids transport by saltation mechanism. Also, there was no description of the stationary bed which occurs at a low fluid velocity at higher inclination.

Martins and Santana (1992) modified Gavignet and Sobey's model (Gavignet and Sobey 1989) to describe the stratified flow of solid and non-Newtonian fluid mixtures in horizontal and near horizontal eccentric annuli. This work was based on the model by Doron et al. (1987) for slurry flow in horizontal pipes. The bottom layer consisted of compact solids bed and top layer as heterogeneous suspension of solids and liquid. The solids concentration in the top layer was obtained by a concentration profile from diffusion equation. However, the procedure for calculating solids dispersion coefficient

in the diffusion equation was not provided. The predictions from this model were not compared with experimental or field data. The model did not account for slip between the velocity of solid and liquid and hence cannot be applied to inclined section. The recommendations from the model to solve drilling issues were to use larger diameter drill pipes, higher fluid density and flow rate. A computer simulator was generated from this model to aid in designing field operations.

Kamp and Rivero (1999) presented their two-layer model for calculation of solids bed height, pressure drop, and solids transport velocities at different rates of penetration and flow. It considered settling and re-suspension of solids at the interface of two layers. The model could be extended to account for slip velocities by using separate momentum equations for fluid and solid in heterogeneous layer or by using drift flux law. The predictions from the model were compared with results of the correlation model by Jalukar (1990). The model predicted a lower flow rate required to form a solids bed compared to the correlation model. The authors suggest that the correlation model has a tendency to over-predict flow rates. The particle transport was more efficient with larger particles, a fact which the authors disagree.

A significant shortcoming of two-layer models is the inability to model both, a moving bed and a stationary bed, in addition to fluid or suspension layer. These three layers were observed in experimental studies under various operating conditions. Hence, three-layer models were developed to overcome this shortcoming.

Doron and Barnea (1993) developed a three layer model to describe the solid-liquid flow in horizontal pipes. This model was a development over their previously published two-layer model (Doron et al. 1987). The predictions from the three-layer model was compared with their experimental data and the satisfactory agreement was reported. However, they did not consider annular flow, fluid rheology and rolling/lifting mechanism of solids transport.

Nguyen and Rahman (1998) presented a three-layer model to predict different modes of solids transport in highly deviated and horizontal annuli. The three layers were comprised of a particle bed of uniform concentration, a dispersed layer with variable solid concentration, and a fluid flow layer that could be a clear fluid or a turbulent suspension. The presence of a dispersed solid layer just above the interface of the solids layer was an improvement over the stationary cuttings bed. The thickness of the dispersed layer was obtained using Bagnold stresses (Bagnold 1954). Depending on the operating conditions, there may be five different modes of solids transport. The solution of each mode was discussed. The transition from two-layer to three-layer flow or vice-versa depending on operating conditions was presented. However, there was no comparison of the model predictions with experimental or field data. The different mechanism of transport such as rolling or lifting was not discussed. The settling velocity of particle was ignored, which limited the application of the model to horizontal or highly deviated wells. The procedure for calculating solids concentration in the heterogeneous layer was not provided.

Cho et al. (2001) presented a three-segment hydraulic model for two phase incompressible flow in annuli. The three segments described were a horizontal and near horizontal segment, a vertical and near-vertical segment and a transit segment. The model incorporated hindered settling by modifying the single particle settling velocity to account for concentration effects. The model predictions were compared with the experimental results of Tomren et al. (1986). It was suggested that the conventional mechanistic models, which described solids transport from vertical to horizontal as a function of wellbore deviation, could not properly characterize the cuttings transport mechanism. The dominant factors controlling cuttings transport vary with the wellbore deviation. The annular fluid velocity and fluid rheology were found to be the most important parameters for solids transport. The three-layer model does not change into a two-layer with increase in fluid velocity. Instead, a new two-layer was developed to account for the two layers.

Ramadan et al. (2005) presented a three-layer model for solids transport in horizontal and inclined pipes. This model can predict the annular pressure loss and average solids transport rate with Newtonian and power law fluids. It considered the settling behavior of particles to determine the solids concentration in the suspension layer. The authors compared the model predictions with their experimental data. The model predictions deviated from the experimental results for small particles with both Newtonian and power law fluids at near critical flow rates (flow rate at which solids start moving). This deviation at near-critical flow rates was attributed to formation of dunes and ripples, which was neglected in the model.

The experimental studies in solids transport can be classified as solids distribution and stationary hole cleaning tests (Li and Luft 2014). Solids distribution tests determine the steady state solids concentration under various operating conditions. Solids concentration are reported as solids bed height, annular volumetric concentration, area of wellbore covered by solids or weight of the solids remaining in the wellbore. Many researchers have focused on developing correlation models to predict critical velocity above which there is no formation of solids bed. These models are developed by either empirically correlating the experimental data or by analyzing the forces acting on the particle. However, these critical velocities are very high and cannot be usually achieved in the field. Hence, a solids bed is formed at these sub-critical flow rates. The height of the bed depends on the operating conditions. There are few correlations which predict the bed height at these sub-critical flow rates. Stationary hole cleaning test predicts circulation time required to completely clean or reduce the height of a solids bed to a desired value.

Peden et al. (1990) conducted experimental studies to investigate the influence of variables such as hole angle, fluid rheology, cutting size, drill pipe eccentricity, circulation rate, annular size and pipe rotation on cutting transport efficiency using the concept of Minimum Transport Velocity (MTV). The MTV is the critical annular velocity at which solids are moving upward either in suspension or by rolling. The hole can be cleaned efficiently if the annular velocity is higher than MTV. The model for calculating MTV was based on analyzing the forces acting a solid particle being transported upwards. The model prediction was compared with their experimental flow loop results obtained at The Heriott-Watt University. The experimental results matched

well with model predictions. The model predictions show that MTV for eccentric annuli are lower than those for concentric ones. The inclination range of 40 to 60° was found to be the most difficult to clean. The solids transport was strongly affected by turbulent intensity in the annulus. At all inclinations, smaller cuttings were transported effectively using a low viscosity fluid. In the inclination range of 0 to 50°, larger cuttings were effectively transported using higher viscosity fluids.

Larsen et al. (1997) studied the effect of fluid rheology, eccentricity, inclination, solids size, and flow rate by conducting more than 700 tests in a 35 ft, 5-in. x 2.375-in. annulus with varying pipe eccentricity and inclination range of 55 to 90°. They developed a correlation to predict critical transport fluid velocity (CTFV), which is the minimum fluid velocity required to maintain upward movement of cuttings, irrespective of the mode of transport. The CTFV was reported in the range of 3 to 4 ft/s depending on the value of various parameters, such as the fluid rheology, drilling rate, pipe eccentricity, and drillpipe rotation. They also developed a correlation for predicting solids bed area at sub-critical flow rates. Jalukar (1990) extended this correlation to account for different annular geometries.

Rubiandini (1999) presented a correlation to predict the minimum flow rate to transport solids from inclination 0 to 90°. The model used minimum transport velocity relation by Larsen et al. (1997) for inclination range of 55 to 90°. They modified the slip velocity model by Moore (1974) for vertical wells by accounting for change in inclination, drilling

rate and fluid density. By combining the two models (Larsen et al. 1997; Moore, 1974), they develop a unified models for minimum transport velocity at all inclinations.

Clark and Bickham (1994) presented a mechanistic model to predict minimum fluid velocity for solids transport and described transport mechanisms at different wellbore inclinations from bit to surface. Three different mechanisms of solids transport, namely, settling, rolling and lifting were discussed. For high inclination, transport was via rolling, whereas for intermediate inclination, lifting mechanism was dominant. At vertical or near vertical angles, transport was determined by relative velocity between the solid particle and fluid (settling). The model predictions were compared with experimental data obtained from 5 and 8-in. flow loop at University of Tulsa. The critical flow rate values (when all solids were moving upwards) from the model predictions were lower than the experimental data. The difference between model predictions and experimental values was due to the different criteria used to determine the critical flow rate. The criteria in model prediction was a minimum pressure drop whereas in experimental studies, it was visual observation.

Becker (1987) developed correlations to relate annular volumetric solids concentration to annular fluid velocity, wellbore inclination, fluid density and initial gel strength, and annular geometry. Six different correlations were developed for various ranges of inclinations (0 to 40°, 40 to 45°, 45 to 90°) and flow regimes (laminar or turbulent). It was reported that at inclination from vertical to 45°, solids transport performance was more effective when fluid was in laminar flow regime. Furthermore, when wellbore inclination was higher than 60° from vertical, solids transport performance was more

effective when fluid was in turbulent flow regime. Influence of fluid rheology on solids transport was considerably greater in the laminar flow regime in vertical wellbore, but fluid rheology had no significant effect on the solids transport when the flow regime was turbulent.

Duan et al. (2008) conducted an extensive study with three different solids size (0.017, 0.055 and 0.13-in.) in a field scale loop (8-in x 4.5-in, 100 ft long loop) to understand the effect of solids size, pipe rotation, fluid rheology, flow rate, and wellbore inclination. It was reported that smaller cuttings were easier to transport with polymeric fluids compared to water in horizontal wellbores. They developed a correlation for solids concentration and bed height in the annulus for field applications. They also matched their experimental data with a three-layer model of Ozbayoglu (2003) and the difference as high as 80% was observed with polymeric fluids. They developed a dimensionless bed height model as a function of flow rate, pipe size and cuttings size. Duan et al. (2009) proposed a critical re-suspension velocity (CRV) relation to initiate solids bed erosion by considering gravity, buoyancy, lift, drag and Van der Waals forces. From the investigation described above, it was observed that the critical deposition velocity (CDV) (when solids started to settle) was two to three times larger than CRV.

Ozbayoglu et al. (2010) conducted experiments using water for demonstrating light drilling mud flow conditions. ROP ranged from 10 to 100 ft/hr, flow rates varied from 40 to 250 gpm, and inclination varied from 50 to 90°. The drill pipe was fully eccentric for all experiments. Dimensional analysis was performed to predict the area of wellbore

covered by solids at sub-critical flow rates. By equating area of wellbore covered by solids to zero, they developed a correlation to predict critical fluid velocity to remove all solids.

Another area of research is the development of solids erosion models which predict the circulation time required for cleaning a solids bed during tripping operation (in drilling) or cleanout operation post-fracturing. Some of the models are by Martins et al. (1997), Adari (1999), Sapru (2001), Nguyen (2007), and Khan (2008).

Martins et al. (1997) conducted more than 60 solids erosion tests by varying fluid rheology, flow rate, wellbore inclination and annular configuration. They suggested an exponential type decay model to predict the decrease in solids concentration with time. It was reported that circulation for 10 minutes was sufficient to remove 66% of the total solids which could be removed, and five times the characteristic time (time constant) was sufficient to clean 99% of solids (which could be removed).

Adari (1999) proposed an exponential equation similar to the one proposed by Martins et al. (1997) to predict solids bed height as a function of time during bed erosion. This equation was applicable for a fixed combination of flow rate, fluid rheology and wellbore deviation. Using non-linear regression, a functional relationship was developed between fluid rheology, flow rate, solids bed height and circulation time required to clean the wellbore.

Sapru (2001) also conducted solids erosion tests with four different polymeric fluids and studied the effect of pipe rotation on the circulation time required to clean a solids bed. It was reported that increasing the pipe rotation speed improved solids transport. They also develop an exponential decay model, similar to the one developed by Adari (1999).

Khan (2008) developed a power law type of model to predict the decrease in solids bed height as a function of circulation time during bed formation and bed erosion process. These equations are related to a fixed combination of flow rate, fluid rheology and wellbore inclination.

Li et al. (2002) developed a proprietary computer model to predict the circulation time required for wellbore cleanout and studied the effect of fluid rheology, flow rate and wellbore inclination. The computer model divides the wellbore path into a certain number of control volumes and these volumes have homogenous properties. Fluid properties and flow rates are used to predict solids removal rate, which is then integrated in time to give solids concentration in each control volume.

2.3 Parameters affecting Wellbore Cleanout

It is evident that the efficiency of solids transport depends on fluid and solids properties and wellbore geometry. Depending on the operational conditions, there is a better control over some parameters in the field than others. Hence, it is essential to understand the effect of these parameters to perform a successful cleanout operation. A brief description

of the influence of these parameters on solids transport is discussed in the following sections.

2.3.1 Effect of fluid velocity

Fluid velocity is the most important parameter affecting solids transport. A high fluid velocity exerts high shear stress on the solids bed, which improves rate of solids transport. A high fluid drag (due to higher fluid velocity) also helps to transport suspended solids to a greater distance. Different studies have reported that high fluid velocities leads to improved solids transport (Tomren et al. 1986, Li and Walker, 1999).

The vertical component of fluid velocity changes with inclination (Fig. 2.2). A typical horizontal well has vertical, inclined, and horizontal sections. In the vertical section, solids transport occurs when the annular fluid velocity exceeds its settling velocity in the fluid. As a rule of thumb, in vertical annuli, fluid velocity should be twice the settling velocity of particles (Leising and Walton 2002).

In the inclined section, the vertical component of fluid velocity decreases. However, particle settling is still vertically downwards. Hence, the difference between solid settling velocity and vertical component of fluid velocity is reduced. If the vertical component of fluid velocity is not high, the particles may settle and form a bed on lower side of the wellbore. Once solids form a bed, the bed can slide up or down the wellbore depending on the fluid drag force. The fluid drag (interfacial stress) acts at the solid-liquid interface

and solids transport occurs by either by rolling/sliding or a suspension mechanism depending on fluid velocity.

The fluid velocity does not have a vertical component in the horizontal section. Two distinct mechanisms of solids transport in the horizontal position are rolling/sliding and suspension mechanisms. The fluid drag transports the solids by rolling/sliding mechanism. In turbulent flow, eddies contribute to solids suspension.

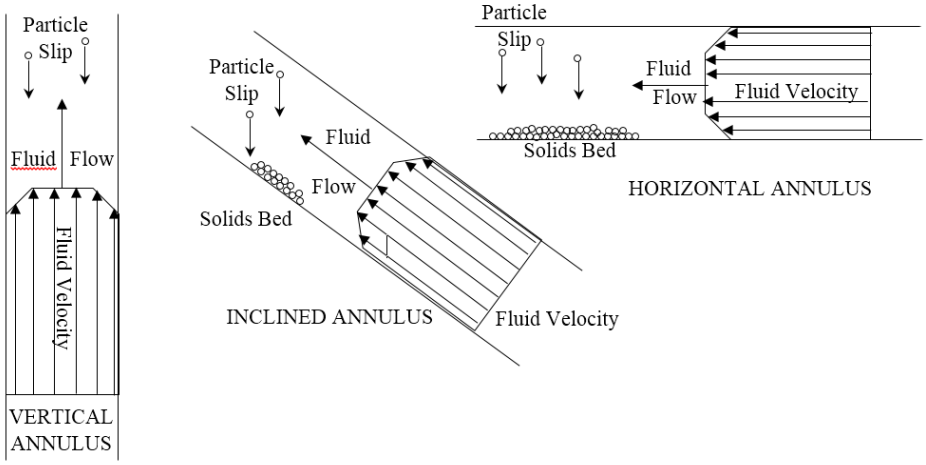

Fig. 2.2: Direction of solids settling relative to fluid flow

Ozbayoglu et al. (2004) reported that the velocity profile played an important role in solids transport. The annular velocity profile depends on fluid rheology, flow regime and eccentricity. The flow regime can be classified as laminar or turbulent based on the Reynolds number. The velocity profile is parabolic for laminar flow and flattens for turbulent flow for Newtonian fluids. The velocity profile is also affected by fluid rheology. Compared to Newtonian fluids, non-Newtonian fluids have a flatter velocity

profile. Higher the non-Newtonian nature of fluid, flatter is the velocity profile (Okrajini and Azar 1986). The flatter velocity profile ensures higher flow area being covered by higher point velocities. In a laminar flow regime, velocities are significantly lower at the wall boundaries. In a concentric pipe, velocity profile is symmetrical around the inner pipe. However, with an increase in eccentricity, the velocity profile skews towards the high side (Okrajini and Azar 1986). This translates to a higher flow rate in the wider annular area and lower flow rate at the bottom (where solids deposit). Hence, the fluid energy may be insufficient to erode a solids bed which is formed in the lower part of annulus. This effect is more pronounced in non-Newtonian fluids compared to Newtonian fluids.

2.3.2 Effect of fluid rheology

Fluids with different rheological characteristics are used in the oilfield operations, ranging from slick water to highly non-Newtonian polymeric systems for drilling, fracturing, cementing, etc. Figure 2.3 shows the rheogram for different fluid models. Many fluids used in the oil industry can be characterized by either Bingham Plastic model, Herschel Bulkley model, or Ostwald-de Waele power law fluid model.

The Bingham Plastic model is given by,

$$\tau = YP + PV(\gamma) \tag{2.8}$$

where, 'YP' = yield point, the minimum yield stress required for the fluid to flow; 'PV'=plastic viscosity; 'τ'= shear stress; and 'γ'= shear rate.

The Herschel Bulkley model for viscoplastic fluids is given by,

$$\tau = \tau_o + k\gamma^n \quad (2.9)$$

where, τ_o = yield stress; 'k'=fluid consistency index; 'n' = flow behavior index.

The Ostwald-de Waele model for pseudoplastic fluids is given by,

$$\tau = k\gamma^n \quad (2.10)$$

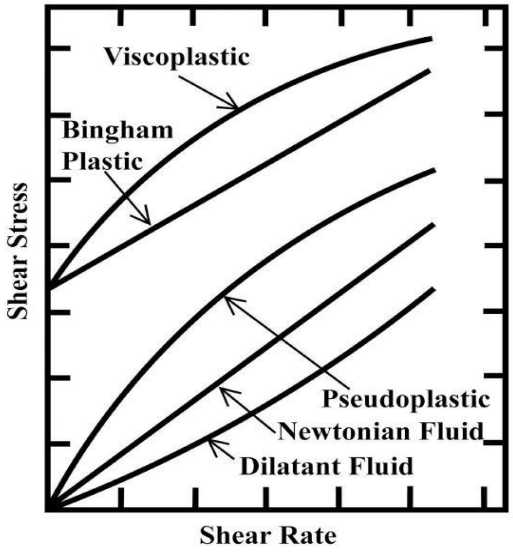

Figure 2.3: Rheogram for different fluid models

The non-Newtonian nature of the fluid is given by 'n'; lower the value of n, higher the non-Newtonian nature. The yield stress, τ_o is the minimum stress required for fluid to flow.

The effect of fluid rheology on solids transport depends on wellbore inclination, annular eccentricity, pipe rotation, and solids size. Numerous studies on the effect of fluid rheology under various operating conditions have been reported in the literature. Okrajni and Azar (1986) related the field measured rheological properties 'YP' and 'PV' of

Bingham plastic fluids to solids transport. They used the ratio 'YP/PV' to characterize the solids carrying capacity of fluid since it was difficult to characterize it with a single parameter, YP or PV. In turbulent flow regime, increasing YP and YP/PV of the fluid did not show any appreciable change in the solids concentration at all inclinations. This suggested that the rheological properties of fluid do not affect solids carrying capacity in turbulent regime. In the laminar regime, lower solids concentration was reported with increasing 'YP/PV' values for all inclinations. Higher YP/PV ratio indicates higher non-Newtonian characteristic resulting in a flat velocity profile which covers a higher annular area with increased velocity. In the laminar flow regime, increasing YP of the fluid decreased the solids concentration in low angle wells. However, for high angle wells (above 70°), increasing YP has no appreciable effect on solids concentration. The effects of fluid yield stress value and YP/PV ratio are more significant for lower annular fluid velocities.

Kenny et al. (1996) studied the hole cleaning capabilities of polymeric fluids by characterizing them using the Herschel-Bulkley model. Decreasing the value of 'n' causes a shift in the velocity profile in an eccentric annulus towards the wider area. Thus, the majority of flow is diverted to a wider area of the annular side with decrease in 'n', thereby requiring higher velocity to clean the solids. Increasing the value of yield stress, 'τ_o' increased the critical fluid velocity required for solids transport. Similarly increasing the fluid consistency index 'k', increases the critical fluid velocity required to clean the wellbore. It was suggested that all three parameters, τ_o, n and k should be considered together to evaluate solids transport efficiency.

Walker and Li (2001) studied the solids carrying capacity and erosion capabilities of the fluid. The fluids considered were water, polymer gels, and multiphase fluids system. They observed that shear stress at the bed interface plays a vital role important in solids transport for near-horizontal and horizontal wells. The polymeric gels have better solids carrying capacity but compared to water, they perform poorly at eroding the bed in horizontal or near horizontal wells. In an inclined section, polymeric fluids perform better at carrying the solids than water for the same flow rate. The fluid should have high solids carrying capacity but it is also important to erode the bed. For horizontal or near horizontal wells, the solids transport is more efficient if low viscosity fluid is pumped in turbulent flow than a viscous fluid in laminar regime. In vertical or near vertical flow, it is better to pump high viscosity fluids in laminar regime than low viscosity fluids in turbulent regime.

Li et al. (2005) evaluated the rheological properties of different biopolymers to relate them with the cuttings carrying capacity. Low shear rate viscosity (LSRV), i.e. the viscosity at shear rate of 0.06 sec^{-1}, should be higher for better suspension capabilities. Settling velocity tests carried out in these fluids indicated that the suspension capabilities increase with fluid's LSRV or elasticity. Seeberger at al. (1989) evaluated oil-based fluids for their solids transport capabilities, and concluded that LSRV and initial gel strength should be higher for improved solids cleanout.

2.3.3 Effect of fluid density

The increase in fluid density increases solids suspension capacity of fluid by reducing the settling velocity of particle (or increasing buoyancy). The fluid density can have both a positive and negative effect on hole cleaning. Fluids with higher density increase buoyancy effects but are difficult to pump in turbulent regime. Another disadvantage with 'weighted' fluids is the tendency of the weighting material to settle out of the fluid phase, which is known as 'sag'. The purpose of fluid density is to exert hydrostatic pressure, and hence is not changed for improving hole cleaning. However, a small increase in density was found to improve cuttings transport (Sifferman and Becker 1992).

2.3.4 Effect of wellbore inclination

The inclination of the wellbore from vertical is an important parameter affecting solids transport. The phenomena of solids transport varies with inclination and different modes of solids transport are encountered. Based on experimental observation on modes of transport, three different inclination ranges have been identified for investigation in the literature. The regions are:

1. Low (0 to 30°)
2. Intermediate (30 to 60°)
3. High (60 to 90°)

Different studies have shown that intermediate inclination in the range of 30 to 60° is the most difficult section to clean (Tomren et al. 1986; Peden et al. 1990, Sifferman and Becker 1992). The tendency to form a solids bed is higher in inclined section than in

vertical section since the vertical component of the fluid velocity is reduced. The solids bed has a tendency to slide down the wellbore and plug it at the 'heel'. This is avoided by the viscous drag force of the fluid. In order to keep the solids in suspension, the fluid velocity should be increased in the intermediate inclination wellbore section. Usually, in inclination angles between 30 to 60°, the solids beds slide down since the gravity acting on solids bed overcomes the friction force between bed and wall boundaries and fluid forces. Another phenomenon which comes into play is the Boycott effect, which states that settling in stagnant fluid is higher in well inclination angles between 40 and 50° than the vertical.

Tomren et al. (1986) conducted several solids transport tests in inclined wells and concluded that solids bed is formed at inclination more than 35°. Peden et al. (1990) studied the Minimum Transport velocity (MTV) as a function of different operational parameters. Based on experimental results, MTV required to initiate solids rolling up the annulus increased initially as the hole angle increased but reached a maximum value, after which it decreased. The critical angle was found to be in the range of 40 to 60° from vertical. The solids bed at these critical angles was unstable and they observed churning motion of particles. Brown et al. (1989) studied cuttings transport at inclination of 0, 20, 36, 52, 60, 79 and 90°. They identified the most critical section to clean to be in the range of 50 to 60° based on velocity required to clean these sections using fluids. Sifferman and Becker (1992) studied solids transport in the range from 45 to 90° from vertical. They identified the range from 45 to 60° as critical, since the bed formed has a tendency to crumble down and seal the hole. It was unstable bed and measuring the bed height was

difficult. Li and Walker (1999) observed that the most difficult angle to clean is 60° due to the formation of unstable bed. It was recommended to avoid building section at 60°. Once the bed is formed, it is more detrimental when the bed slides down.

2.3.5 Effect of wellbore geometry

The annular velocity and shear rate is dependent on wellbore geometry. The wellbore geometry includes the ratio of the inner pipe to wellbore diameter ratio. Irregular hole geometry can lead to formation of traps where cuttings can settle and could also cause casing seat, washouts, constrictions, etc. Drilling should be performed with a larger sized drillpipe in order to reduce the annular area and increase the fluid velocity. The higher the annular gap, the lower is the fluid velocity, and consequently, higher is the cuttings concentration.

2.3.6 Effect of eccentricity

Eccentricity is used to describe how off-center a pipe is within another pipe or the open-hole. A pipe would be considered to be fully (100%) eccentric if it was lying against the enclosing pipe or hole. A pipe would be considered concentric (0% eccentric) if it were perfectly centered in the outer pipe or hole. Negative eccentricity implies that inner pipe is resting on the upper half of outer pipe. Positive eccentricity implies that the inner pipe rests on the lower half of outer pipe. Eccentricity is defined by the following expression:

$$\varepsilon = \frac{2\delta}{d_2 - d_1} \tag{2.11}$$

Figure 2.4 describes the change in eccentricity based on the position of inner pipe relative to outer pipe. Eccentricity is the result of wellbore inclination and weight on tubing (bottomhole assembly). The solids transport efficiency decreases with increase in eccentricity. The velocity profile skews towards higher side of the wellbore due to eccentric annular configuration. Therefore, fluid velocity in the lower part, where there is solids bed, is not high. The concentric annular profile would lead to equal distribution of velocity and hence, solids would be cleaned more efficiently. However, it is not possible to control eccentricity in case of horizontal or extended reach well. The pipe will mostly be fully eccentric in these situations. The minimum transport velocity for cleaning the well increases with increase in eccentricity. Okrajni and Azar (1986) found that the effects of eccentricity are more pronounced in laminar flow with increasing inclination angle. Li and Walker (1999) confirmed that the decrease in velocity in the narrow gap of annular section is significant with high viscosity fluids. The effect of pipe eccentricity is more pronounced as the inclination angle is increased. The circulation volume required to clean the hole is about 40% more when the pipe has positive eccentricity (inner pipe is on the lower side) as compared to negative eccentricity.

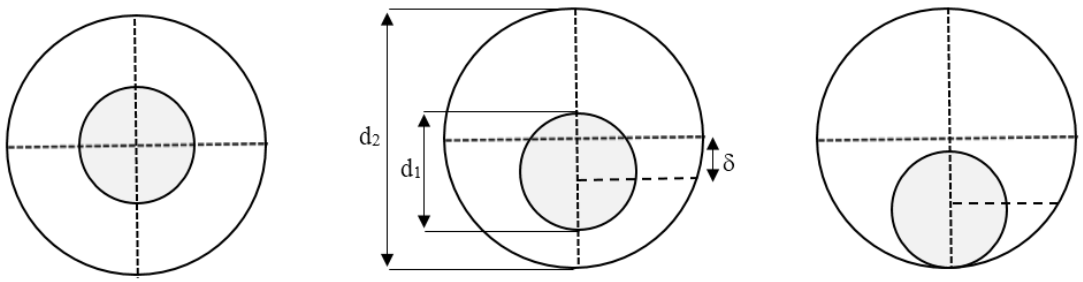

Fig. 2.4: Concentric, partially eccentric and fully eccentric annular geometries

2.3.7 Effect of solids size

The size of solids is also a major factor affecting cuttings transport. Studies to determine whether small or larger solids are easier to clean have provided conflicting results. Peden et al. (1990) conducted experimental studies and reported that smaller solids are easier to transport than larger ones, except at low inclinations with viscous fluid where larger ones are easier to transport.

Li and Wilde (2005) studied the effect of cuttings size by comparing the velocity required to prevent the formation of stationary bed. The three particle sizes studied were 0.006, 0.03, and 0.275-in. Smaller particles were difficult to clean out than larger ones when the particle size is larger than 0.02-in.; but for the particles smaller than 0.02-in, the smaller particles are easier to clean out.

Duan et al. (2008) investigated the effect of solids size with three different sized solids (0.0177, 0.055 and 0.130-in.) in 100 ft long, 8-in. x 4.5-in. annular flow loop. Smaller solids were easier to transport with polymeric fluids compared to water in a horizontal wellbore. The main factors affecting the transport of small solids were found to be fluid rheology and pipe rotation. The polymeric fluids transport small cuttings better than larger ones. Also, pipe rotation has a larger positive effect on transport of small sized solids than larger ones. Field results also indicate that smaller sized cuttings are difficult to transport.

Hence, the effect of solids size on cleanout depends on the range of solids size considered and the fluid rheology.

2.3.8 Effect of solids density

Higher density solids will lead to higher gravitational force acting on it, thus leading to higher settling rate and rapid formation of cuttings bed. Also, once the solids bed is formed, it will be difficult for fluid to lift and suspend the particles due to density difference.

Several conclusions can be drawn from this literature review. The solids transport in wellbore is influenced by several inter-related parameters (effect of fluid rheology changes with inclination and eccentricity). Also, the mode of transport for solids transport changes with inclination and hence, a single model to describe solids transport for all inclinations is difficult. Most of the models are applicable to drilling operations, i.e. solids (drill cuttings) are generated at a steady state and pipe rotation; whereas in cleanout operations, there is a solids bed and CT is unable to rotate. There are very few transient solids erosion model which relate to the removal of proppants from wellbore. Also, many experimental studies are focused on drilling operations by incorporating larger sized solids (drill cuttings) and drilling fluids (with yield stress), whereas wellbore cleanout operation involves removal of proppants by low viscosity polymeric fluids without yield stress.

CHAPTER 3

EXPERIMENTAL SETUP AND ANALYSIS

This chapter is divided into three sections. The first section describes the components of experimental setup and test sections 1 and 2, fabricated for this study. The second section outlines test procedures for performing cleanout experiments. The third section discusses analysis of bed height data obtained from the camera.

3.1 Design details

The setup was designed to enable conducting tests with variable inclination and annular configuration (different sizes of outer pipe and inner pipe). Two interchangeable test sections, 1 and 2, were designed to be part of this setup. The components of the setup are the support structure, hoisting system, test section, pumping system, instrumentation and data acquisition system. Test section 1 was used for conducting solids erosion tests in the horizontal position whereas test section 2 was used for conducting similar tests in both horizontal and inclined position. The length of test section 1 is 54 ft, and test section 2 is 34 ft long.

3.1.1 Support Structure

The support structure provides stability to the test section under all operating conditions. The support structure comprises of the base frame, a hinge system, and I-beams. The base frame, 12 ft x 5 ft, was constructed by welding iron channels. This frame was mounted on wheels and placed on the floor (Fig. 3.1). Three I-beams and a hinge system rests on the base frame. The central I-beam supporting the test section is 34 ft long and the two

side I-beams supporting the hydraulic cylinders (for use in future wiper trip experiments) are 16 ft long. The test section was clamped on the central I-beam. Since the length of test section 1 is 54 ft, 34 ft of this test section was supported by the central I-beam and the additional 20 ft length was supported by iron channel stands. One end of the three I-beams was welded to the hinge system to facilitate rotation during experiments with inclination (Fig. 3.2). The hinge system consists of two hinges placed 4.5 ft apart with a solid iron shaft (2 7/16-in. OD) inserted through them. The hinges have internal bearings for smooth rotation of the shaft. The free end of central I-beam was connected to a pulley (mounted on top of a vertical beam) by a steel rope for hoisting during experiments with inclination. The base frame supports only 12 ft of I-beams, whereas the remaining portion is supported by iron channel stands (Fig. 3.3). The I-beams are raised with pulley-winch system for conducting experiments in the inclined position whereas the base frame remains on ground at all times.

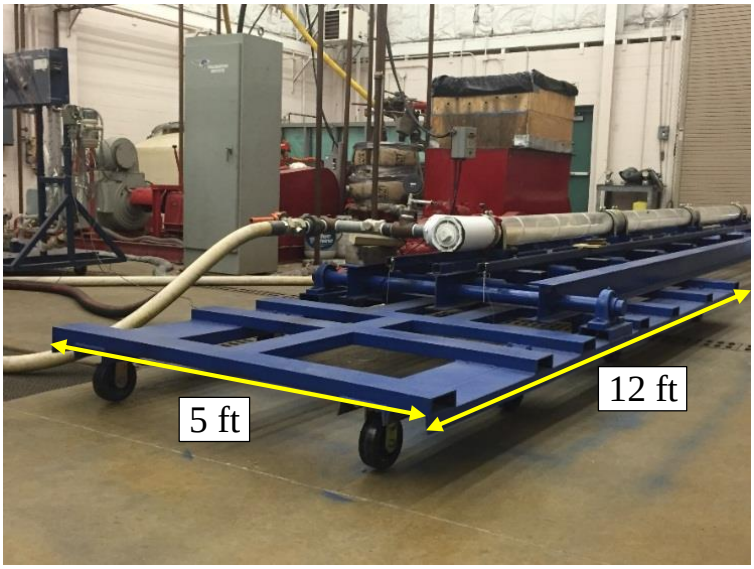

Figure 3.1: Base frame for the support structure

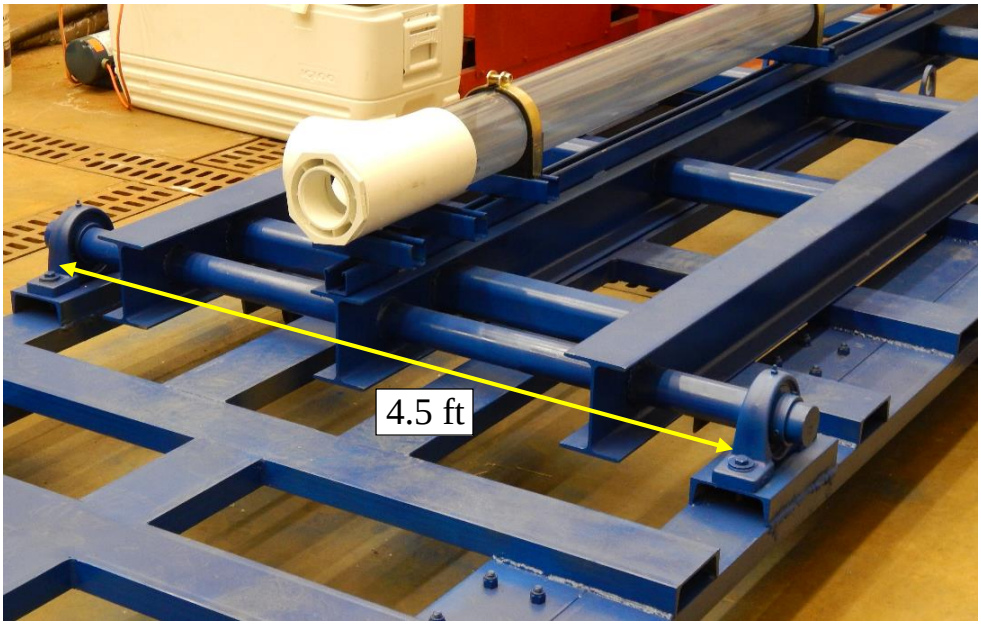

Figure 3.2: Hinge system

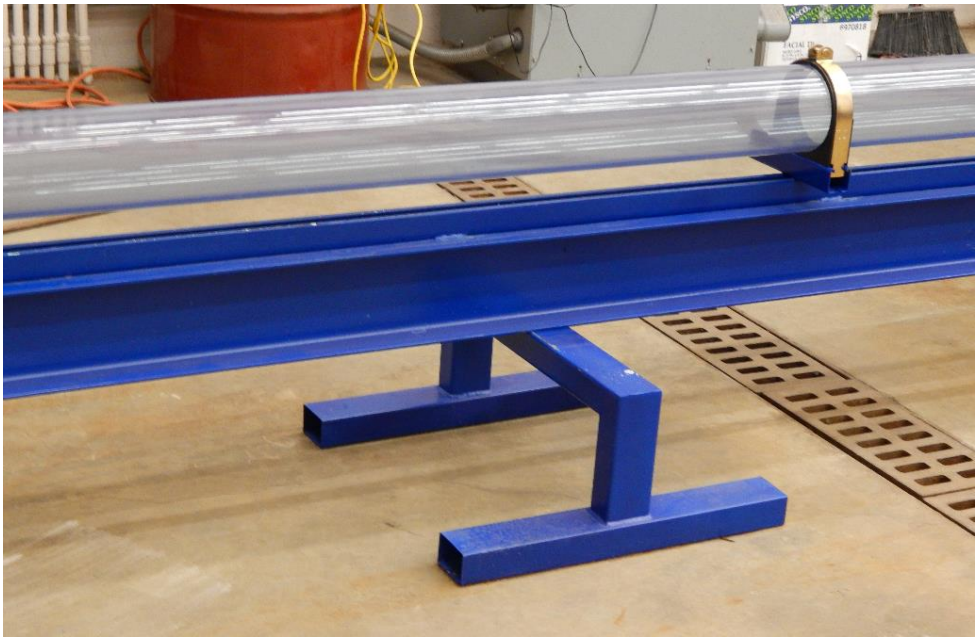

Figure 3.3: I-Beam supported by iron stand

3.1.2 Hoisting System

The hoisting system was used to lift one end of central I-beam for achieving necessary inclination. It consists of a vertical beam, roller arrangement and pulley-winch system. The vertical beam is a 32 foot long hollow square beam with 1 ¾-in. seam cut on one side (Fig. 3.4). The vertical beam was welded on a base plate and bolted to the ground and supported by two bracings at the top (Figs. 3.5 and 3.6). The roller arrangement consisted of two 6-in. diameter wheels with a 3/4-in. OD shaft inserted through them. The roller was placed inside the vertical beam through the seam to guide the vertical motion of central I-beam (Fig. 3.7).

A pulley and winch system was used to lift the free end of central I-beam (Fig. 3.8). A steel rope, passing over the winch and pulley, was hooked to central I-beam via chains (Fig. 3.9).

Figure 3.4: Vertical beam

Figure 3.5: Base support for vertical beam

Figure 3.6: Top support (bracing) for the vertical beam

Figure 3.7: Roller-track system

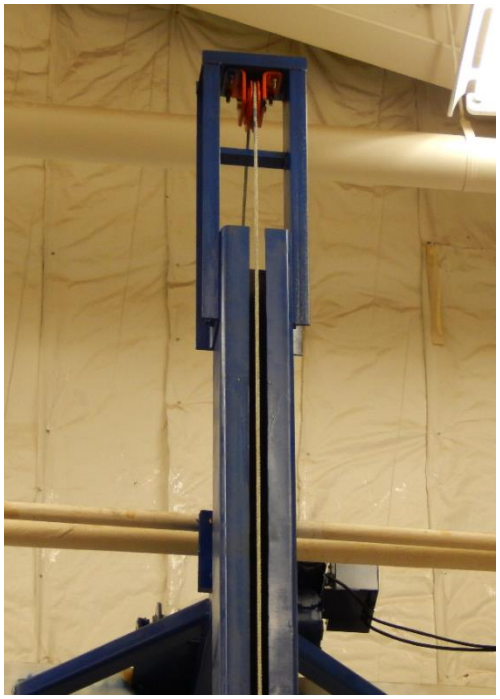

Figure 3.8: Pulley-winch system

Figure 3.9: Chain-steel rope system

3.1.3 Test Section

Test section 1 is 54 ft long with 5.5-in. OD x 5-in. ID PVC outer pipe and 2 3/8-in. OD inner CT. It could only be used for conducting horizontal tests. The height of the roof restricted the use of test section 1 for conducting tests at inclination. Hence, a new shorter test section 2 with 34 ft of 5.5-in. OD x 5-in. ID acrylate outer pipe and 2 3/8-in. OD inner CT was assembled for conducting tests at inclination. Acrylate outer pipe was used in test section 2 since it is more clear compared to PVC and hence, better suited for flow visualization. The outer pipe was placed on central I-Beam with strut and clamp arrangement (Fig. 3.10). This arrangement ensured that the outer pipe was stationary under operating conditions. Since acrylate and PVC pipes were available in 6 and 10 ft sections, several sections were coupled with a Straub connection to form a tight seal (Fig. 3.11). The inner tubing was fabricated by welding 25 ft sections of 2 3/8-in. tubing and trimming the remaining portion to achieve the desired length (54 ft for test section 1 and 34 ft for test section 2). Blinds were welded at ends of the inner tubing to ensure that the flow is restricted to the annular section between the outer pipe and inner tubing. A T-connection was attached on both ends of the test section to connect the inlet and return lines (Fig. 3.12). A rupture disc (set at 140 psi) and a relief valve (set at 110 psi) was installed upstream of the test section to ensure safe operating conditions at all times (Fig. 3.13). A filter system comprising of 3 ft x 3 ft wooden box with an inner lining of 50 mesh size steel sieve was constructed (Fig. 3.14). This filter was mounted downstream of the test section on top of fluid tank to filter slurry during the tests.

Figures 3.15 and 3.16 show the complete setup with test section 1 and 2. After assembling the test section, water was pumped at various rates while checking for leaks. No leaks were observed in the system, and hence it was considered ready for testing.

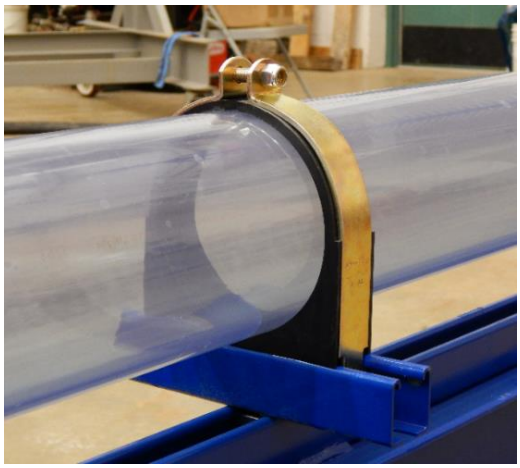

Figure 3.10: Strut and clamp system

Figure 3.11: Straub connection

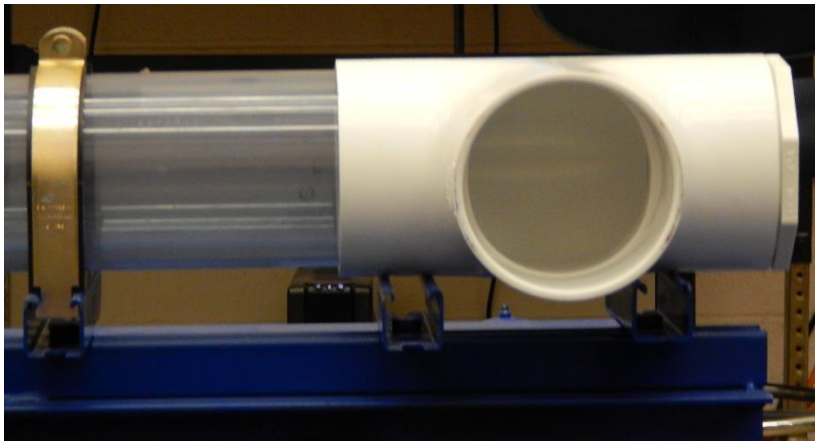

Figure 3.12: T-connection at the end of the test section

Figure 3.13: Relief valve and rupture disc

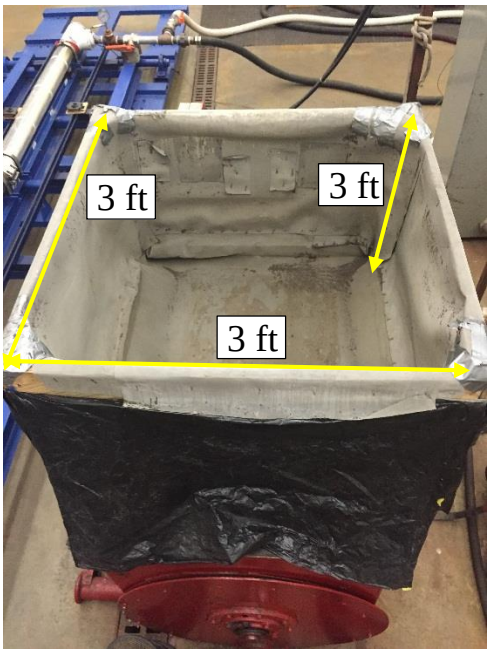

Figure 3.14: Filter for separating solids

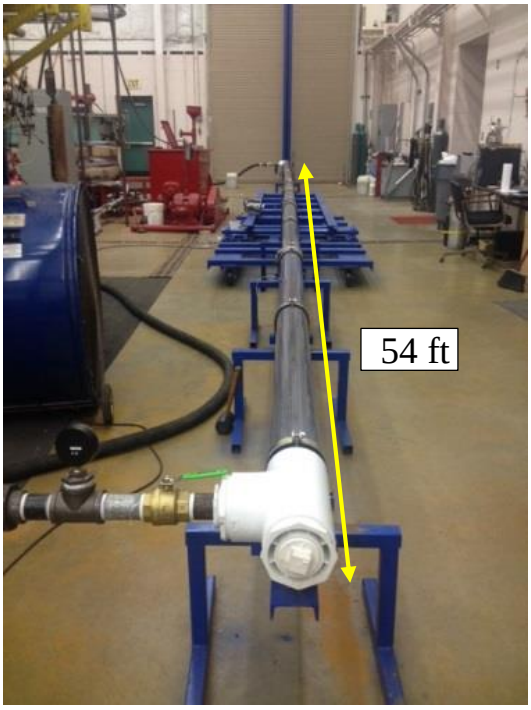

Figure 3.15: Test section 1 (54 ft)

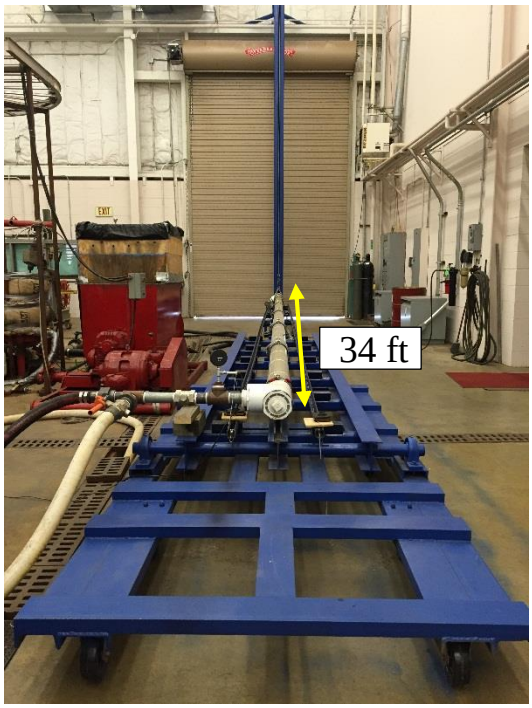

Figure 3.16: Test section 2

3.1.4 Pumping system and instrumentation

Solids are injected into the test section using a 55 gal tank equipped with a Lightnin blender, and cleanout fluid is prepared in a 220 gal tank equipped with a ribbon blender. The ribbon blender is useful to mix polymeric fluids without any mechanical degradation. Two pumps are placed in series to circulate cleanout fluid through the test section. A 6P10 Moyno pump with a maximum flow rate of 140 gpm at 600 psi was used to pump the cleanout fluid. A 5M Deming centrifugal pump was used to boost the suction pressure of Moyno pump. Figures 3.17 and 3.18 show the centrifugal and Moyno pump. A Coriolis flow meter was placed upstream of test section to provide the data of flow rate, fluid density, and temperature. A track system with a small pulley at the end was fabricated and installed on both sides along the length of test section. Two video cameras for flow visualization were maneuvered along the track using a thread and pulley arrangement

(Fig. 3.19). These cameras record the bed arc length readings measured using paper scales attached across test section. The scales were placed 1.5 ft apart along the test section (Fig. 3.20). Gate valves were used for test section isolation and flow diversion.

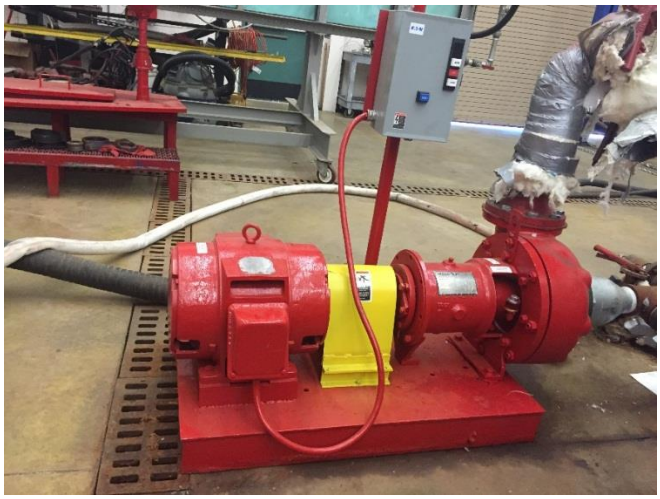

Figure 3.17: Deming Centrifugal pump

Figure 3.18: Moyno pump

Figure 3.19: Track system

Figure 3.20: Paper scales across the test section

3.1.5 Data acquisition and recording

A new data acquisition system was purchased from National Instruments (NI CDAQ-9188) (Fig. 3.21). The data from the flow meter was gathered via this new system. The system has dedicated channels for gathering different output signals from various

instruments; 32 channels for voltage, 16 channels for current, 4 channels for thermocouple and 8 channels for frequency input.

Figure 3.21: Data Acquisition System (NI CDAQ- 9188)

The schematic of the flow loop is shown in Figure 3.22.

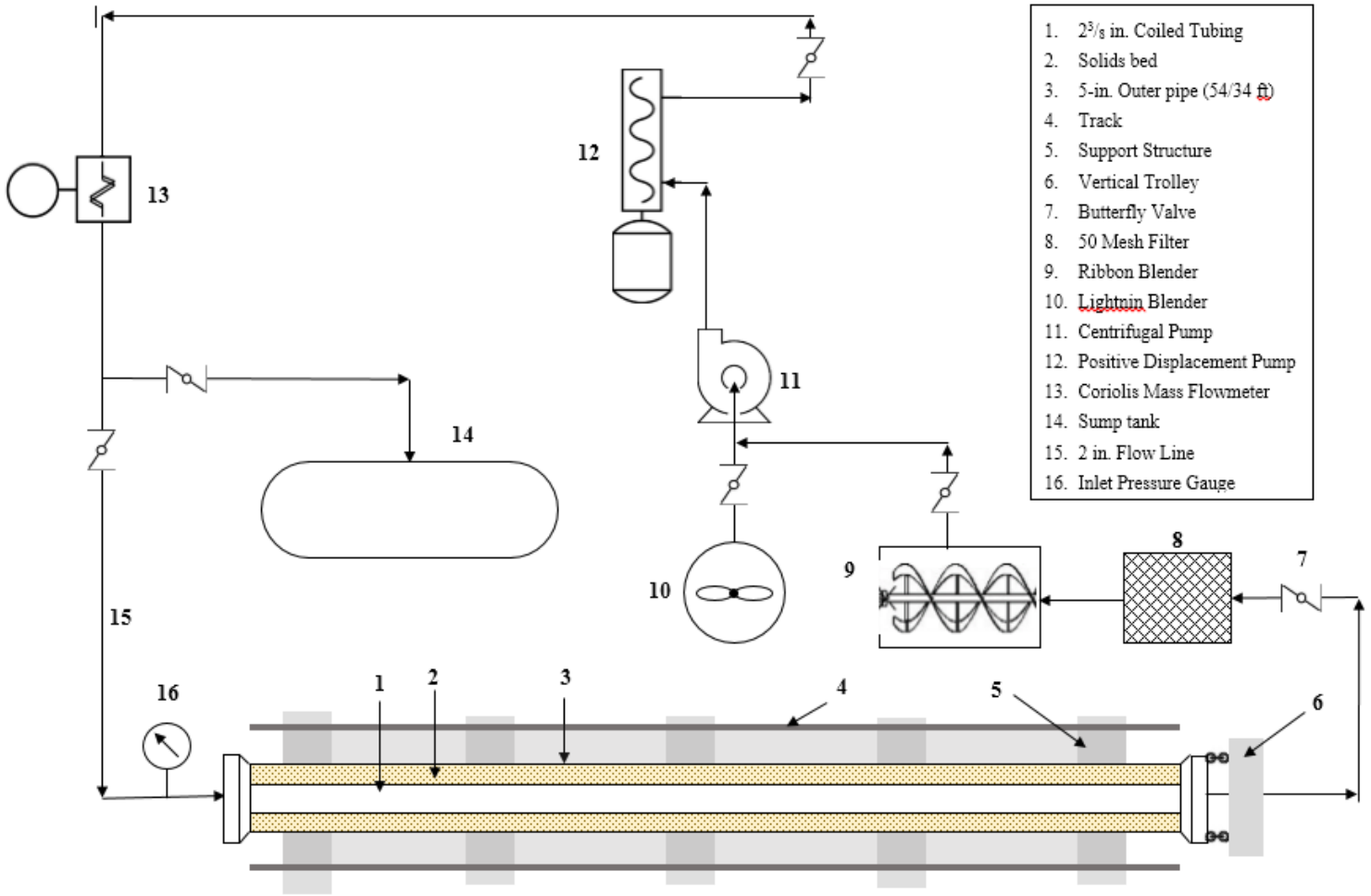

Figure 3.22 Schematic of the flow loop

3.2 Test Procedures

The procedure for conducting solids bed erosion test consisted of three steps. First, depositing a solids bed, followed by preparation of cleanout fluid and then, circulating the cleanout fluid at the desired flow rate and wellbore inclination. The detailed test procedure is as follows:

Step 1. Deposition of solids bed in the test section

1. Water from 55 gal blender was re-circulated through the annulus of the test section at 50 gpm.
2. Once the test section was filled with water, solids were slowly added to blender while re-circulating through the test section.
3. For test section 1, solids were added until the average bed height in test section was approximately 2.8-in., since it ensured that the inner pipe was completely covered with solids.
4. For test section 2, 200 lbs of solids were added to blender while re-circulating through the test section (which also ensured the inner pipe was completely covered with solids).
5. The solids settled in the test section forming a bed.
6. The test section was then isolated, and bypass lines were flushed with water.
7. The arc length of solids bed along the outer pipe circumference was recorded at 35 locations on one side for test section 1, and 42 locations (21 on each side) on both sides of test section 2, each 1.5 ft apart using paper scales fixed on the test section (Fig. 3. 20).
8. The initial arc length was the average of all readings taken along the test section.

It is easier to clean test section 2 after completing the test, since it can be inclined and the remaining solids are thereby easier to remove. Hence, adding 200 lbs of solids ensured uniform starting condition for all experiments conducted in test section 2. However, it was difficult to remove all solids from test section 1 since it cannot be inclined. Hence, in test section 1, solids were added till the average bed height was 2.8-in. to ensure uniform starting condition. For inclined tests, the solids bed is deposited in the horizontal position and then test section is raised to desired inclination.

Step 2. Preparation of cleanout fluid

1. Two hundred gallons of fresh water was filled in 220 gal ribbon blender.
2. If the test was conducted with a polymeric fluid, then the required amount of polymer was added to fresh water while agitating fluid at moderate speed.
3. The fluid was mixed for an hour to ensure complete polymer hydration.
4. Fluid rheology measurements were performed before and after the test using 6 speed, model 35 Fann viscometer equipped with 1/5th spring.

Step 3. Erosion of solids bed

1. The test fluid was pumped through test section and bypass lines at 10 gpm to flush out water.
2. The test fluid was then diverted to bypass line where the flow rate was increased to a desired value.
3. The flow was then diverted to test section and stop watch was started.

4. The bed arc length was recorded 1 min after the flow through test section followed by recording at every 2 mins. The readings were recorded using the camera moving along track. The bed arc length was determined by taking the average of the readings taken along test section at a given time.
5. The test was continued for 30 mins and flow was then diverted to bypass line.
6. The final bed arc length (average of all readings) was then recorded.

Water was then pumped through test section to flush the polymeric fluid and remaining sand. This procedure was repeated for each test.

3.3 Bed Height Calculations

The bed arc length along the circumference was recorded using camera on both sides of the test section 2. The arc length was recorded manually only on one side for test section 1 since the track system was not assembled while this section was used. The arc length, 'a', was measured from the top of outer pipe. The bed arc length from the bottom is b = 8.64 - a, where 8.64 is half-circumference of outer pipe (Fig. 3.22). The relationship between the radius, bed arc length and central angle (when measured in radians) is:

$$b = r \phi \qquad (3.1)$$

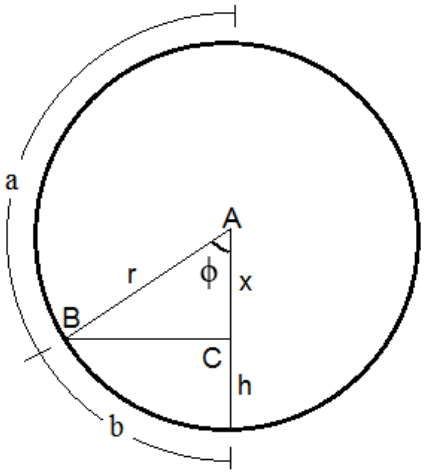

Figure 3.23: Cross section of outer pipe

The triangle ABC in Fig. 3.4 is a right-angled triangle and hence, using trigonometric relations, we get, $\cos \phi = x/r$.

Thus,

$h = r - x$

$h = r - r \cos \phi$

or,

$h = r - r \cos (b / r)$. (3.2)

The correct bed-height is obtained by accounting for the thickness of outer pipe. Hence, subtracting the thickness of outer pipe from the calculated bed height we obtain,

$h_c = h - 0.25\text{-in.}$ (3.3)

For example, if the bed height reading recorded at a given time is a = 5.24-in. then,

$b = 8.64 - 5.24$

or,

$b = 3.40\text{-in.}$

The corrected bed height is then calculated as,

$h = 2.75 - 2.75 \cos (3.40 / 2.75)$;

or,

$h = 1.85$-in.

Then,

$h_c = 1.85 – 0.25$

or,

$h_c = 1.6$-in.

The corrected bed height readings recorded are then plotted as a function of time, and correlations are developed to relate solids bed erosion as a function of time. The corrected bed height 'h_c' will be hereon denoted by 'h' (i.e. all values of h have been corrected for outer pipe thickness).

CHAPTER 4

RESULTS AND DISCUSSION

4.1 Rheological characterization

The fluids employed in the field for cleanout operations are water, and low concentration polymeric fluids. Water, 2.16 lb/Mgal HE 150 (only in test section 1), and 10 and 20 lb/Mgal guar fluids were evaluated for their efficiency as cleanout fluids. Water is a Newtonian fluid; its viscosity is independent of shear rate. The polymeric fluids, HE 150 and guar fluids, are non-Newtonian and their viscosity depends on the applied shear rate.

The rheology of polymeric fluids, before and after test, was determined at ambient conditions with a $1/5^{th}$ spring model 35 Fann viscometer (Fig. 4.1). It is a coaxial cylinder type rotational viscometer equipped with a R1B1 bob and cup geometry, and suitable for measurements in the shear rate range of 5 - 1022 sec^{-1}. Table 4.1 shows the specifications of viscometer. The test fluid is contained in the annular space between cylinders. The rotation of outer cylinder (sleeve) at known velocity causes the fluid to exert a viscous drag, which in turn imparts a torque on inner cylinder or bob. This torque is transmitted to spring and its deflection is the dial reading of viscometer.

Figure 4.1: Model 35 Fann viscometer

The fluids studied were found to be pseudoplastic/shear-thinning and could adequately be described by power law or Ostwald-de-Waele rheology model. The relationship of shear stress and shear rate of a power law fluid is given as:

$$\tau = k\dot{\gamma}^{n} \tag{4.1}$$

where, τ = shear stress (lb_f/ft^2); $\dot{\gamma}$ = shear rate (sec^{-1}); k = fluid consistency index (lb_f-s^n/ft^2); n = flow behavior index (dimensionless)

The relationship of wall shear stress and wall shear rate of a power law fluid is given as:

$$\tau_w = K_v\dot{\gamma}_w^{n} \tag{4.2}$$

where, τ_w = wall shear stress (lb_f/ft^2); $\dot{\gamma}_w$ = wall shear rate (sec^{-1}); K_v = viscometer flow consistency index (lb_f-s^n/ft^2).

Wall shear stress and wall shear rate was calculated from the viscometer dial readings (θ) and speed of the rotating sleeve of viscometer (RPM) using the following equations:

$$\tau_w = 0.01066N\theta_i \tag{4.3}$$

$$\dot{\gamma}_w = 1.703\ \text{RPM} \tag{4.4}$$

where, τ_w = wall shear stress (lb_f/ft^2); N = spring number (0.2 for $1/5^{th}$ spring); θ_i = dial reading at i^{th} rpm; $\dot{\gamma}_w$ = wall shear rate (sec^{-1}); RPM = revolutions per minute of model 35 Fann viscometer.

The flow behavior index, *n*, and consistency index for viscometer, K_v, of fluids are determined by plotting the wall shear stress vs wall shear rate on a log-log scale. The viscosity of a non-Newtonian fluid is shear dependent, hence the use of term 'apparent'. For a shear thinning fluid, the viscosity increases with decrease in shear. Apparent viscosity of a power law fluid is calculated using the equation:

$$\mu_a = 47880 K_v \dot{\gamma}_w^{n-1} \quad (4.5)$$

where, μ_a = apparent viscosity (cP); K_v = viscometer consistency index (lb_f-s^n/ft^2); $\dot{\gamma}_w$ = wall shear rate (sec^{-1}).

Tables 4.2 and 4.3 list the average values of n, K_v and μ_a (@ 511 sec^{-1}) measured for fluids, before and after the test, for experiments conducted in test sections 1 and 2. The shear rate of 511 sec^{-1} is used since apparent viscosity of polymeric fluids is commonly reported at this shear rate value.

Table 4.4 lists the range of Reynolds number for the tests. The two boundary conditions are the wellbore without solids and wellbore with a solids bed height of 2.75-in. The solids bed height of 2.75-in. ensures the inner pipe is completely covered by solids.

Table 4.1: Specifications of model 35 Fann Viscometer

Instrument	Geometry	Dimensions, mm	Shear Rate Range (sec^{-1})
Fann 35 Viscometer	Diameter of Bob	D_b = 34.49	5.1 - 1022
	Diameter of Cup	D_c = 36.83	
	Ratio of bob and cup diameter (β)	D_b / D_c = 0.9365	

Table 4.2: Rheological characterization of fluids evaluated in test section 1

Fluid	Flow rate (gpm)	Flow behavior index, n	Fluid consistency index, Kv ($lb_f.sec^n/ft^2$) ($x10^{-4}$)	Apparent viscosity μ_a @ 511 sec^{-1}, (cP)
2.16 lb/Mgal HE - 150	80	0.687	4.09	2.72
	100	0.724	3.70	3.42
	120	0.690	4.26	2.77
10 lb/Mgal Guar	80	0.718	7.09	5.77
	100	0.668	9.27	5.43
	120	0.705	7.30	5.32
20 lb/Mgal Guar	80	0.665	23.55	14.22
	100	0.629	29.84	14.20
	120	0.543	52.19	14.39

Table 4.4: Rheological characterization of fluids evaluated in test section 2

Fluid	Inclination	Flow rate (gpm)	Flow behavior index, n	Fluid consistency index, Kv ($lb_f.sec^n/ft^2$) ($x10^{-4}$)	Apparent viscosity μ_a @ 511 sec^{-1}, (cP)
10 lb/Mgal Guar	45°	80	0.661	8.62	4.96
		100	0.670	7.67	4.69
		120	0.663	8.63	4.99
10 lb/Mgal Guar	60°	80	0.654	8.75	4.85
		100	0.646	8.85	4.66
		120	0.661	7.71	4.46
10 lb/Mgal Guar	75°	80	0.664	8.60	5.03
		100	0.660	7.81	4.50
		120	0.652	7.89	4.31
10 lb/Mgal Guar	90°	80	0.670	7.67	4.69
		100	0.673	7.63	4.74
		120	0.637	8.94	4.49
20 lb/Mgal Guar	45°	80	0.683	19.14	12.16
		100	0.582	36.61	12.96
		120	0.597	33.09	12.48
20 lb/Mgal Guar	60°	80	0.606	28.60	11.60
		100	0.583	35.59	12.63
		120	0.569	38.14	12.41
20 lb/Mgal Guar	75°	80	0.567	35.63	11.48
		100	0.577	38.53	13.17
		120	0.596	33.33	12.45
20 lb/Mgal Guar	90°	80	0.576	33.22	11.31
		100	0.586	35.48	12.82
		120	0.639	25.88	12.99

Table 4.4: Range of Reynolds number for different fluids

Flow Rate, gpm	Water	2.16 lb/Mgal HE 150	10 lb/Mgal Guar	20 lb/Mgal Guar
80	5047-64433	5694-8076	3314-4526	1023-1295
100	6306-80510	7610-10788	4469-6100	1404-1778
120	7563-96586	9645-13667	5706-7785	1820-2303

4.2 Results of solids erosion tests

The performance of cleanout fluids is evaluated on the basis of bed erosion curves and cleanout efficiency. Bed erosion curve is the plot of solids bed height as a function of circulation time. Cleanout efficiency is the ratio of weight of solids collected in filter (at the end of the test) to the total weight of solids initially loaded in test section.

$$\text{Cleanout Efficiency}(\%) = \frac{\text{Weight of solids collected in filter}}{\text{Weight of solids initially loaded in test section}} \text{ x } 100 \qquad (4.6)$$

Figures 4.2 through 4.5 show the solids bed observed after circulating the cleanout fluid for 1 minute at inclination of 45, 60, 75 and 90°. Cleanout efficiency was useful for determining the performance of different fluids at inclination of 45°, where there was no formation of solids bed. At inclination of 45°, most of the solids in test section form a heterogeneous suspension and no solids bed was observed. The heterogeneous suspension was due to higher vertical component of fluid velocity at 45° compared to those at higher inclinations. At inclination of 60°, there was a solids bed which had a tendency to slide. This unstable bed coupled with fluid flow caused dunes and a highly uneven solids bed. At inclinations of 75° and 90°, there was a formation of stable solids bed which does not slide. The results of solids erosion test conducted in test sections 1 and 2 are presented in Secs.4.2.1 through 4.2.3. The two test sections 1 and 2 are abbreviated as TS 1 and TS 2 in the bed erosion and cleanout efficiency plots. For keeping the initial bed height similar, the initial bed height readings for any given case are normalized to the highest initial reading in a particular set. This ensures that in any plot, the starting point for the curves is the same. Also, at inclination of 60°, all the solids fall to the inlet and there was no distribution of solids along the test section. Hence, at 60° the initial bed height is 2.75-in.

which is the average of the initial bed height reading for all tests with inclination 75 and 90°.

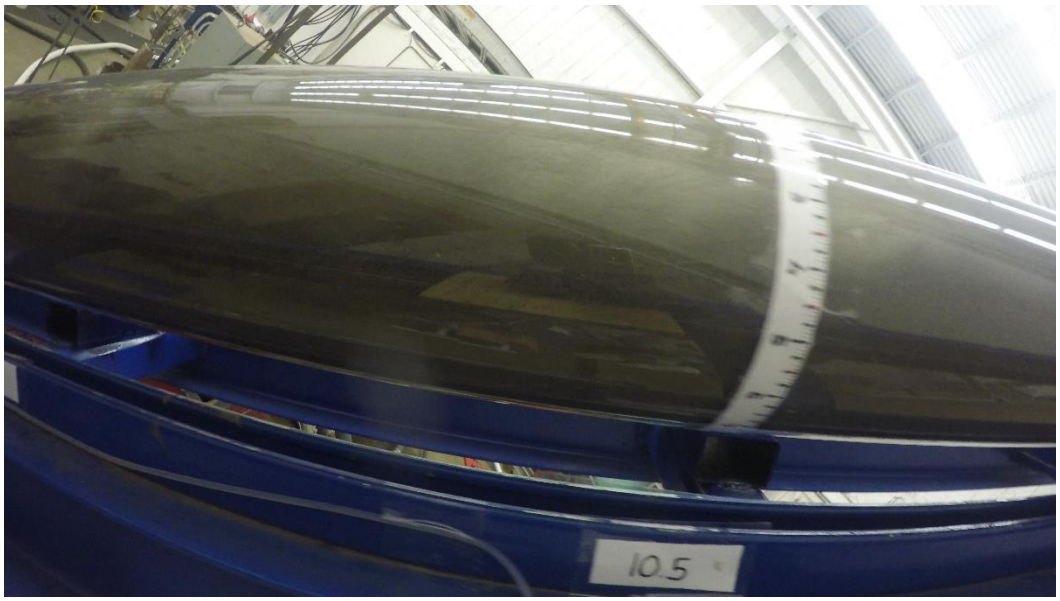

Fig. 4.2: Solids bed observed at inclination of 45°

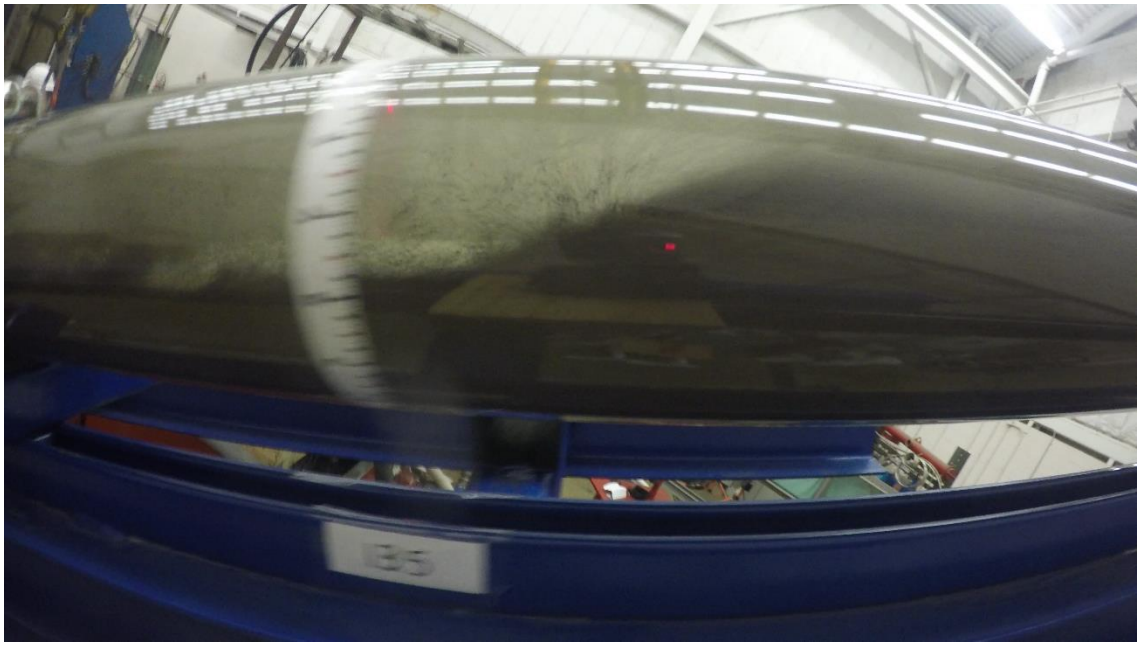

Fig. 4.3: Solids bed observed at inclination of 60°

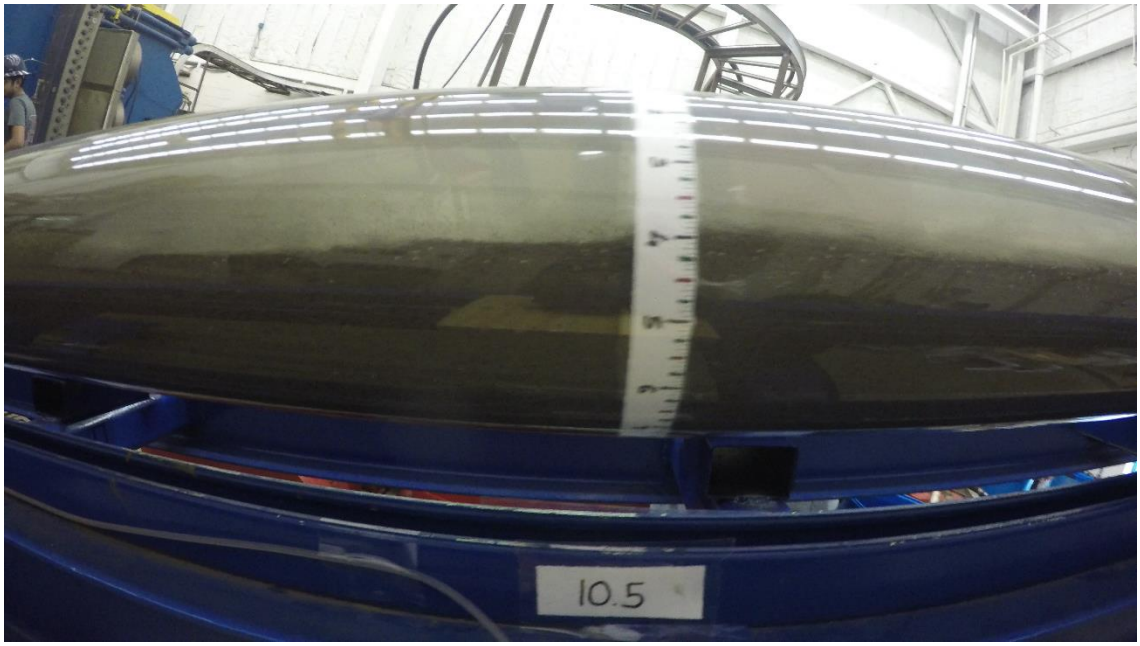

Fig. 4.4: Solids bed observed at inclination of 75°

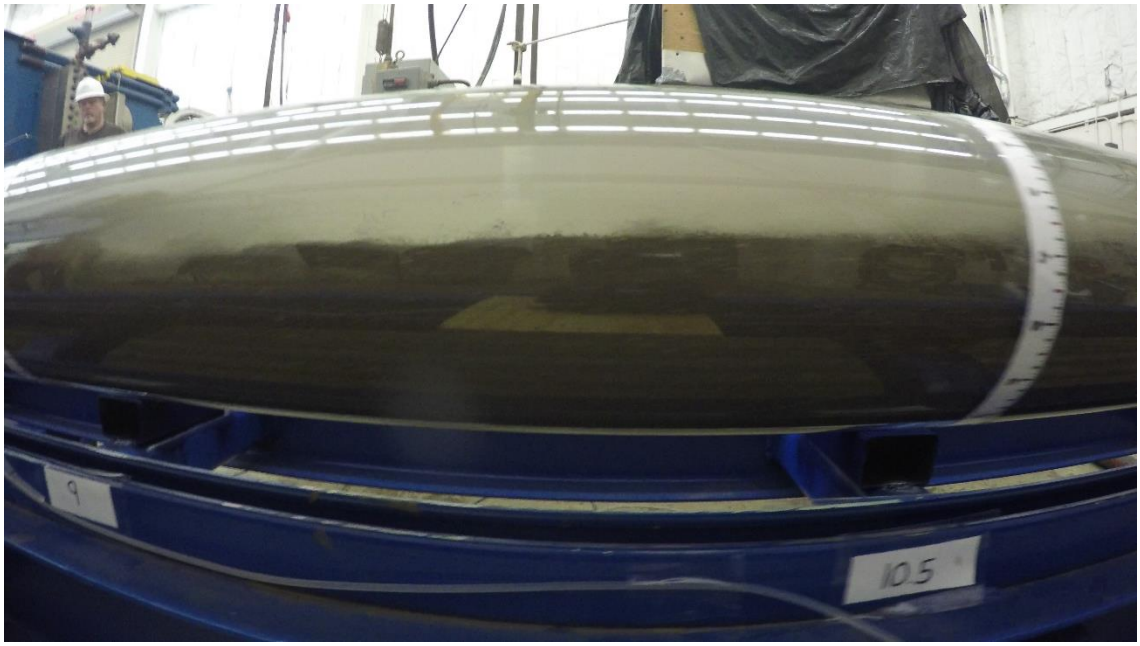

Fig. 4.5: Solids bed observed at inclination of 90°

The reported average bed height does not convey the non-uniformity of bed height along length of the wellbore. Figure 4.6 shows an error graph with the standard deviation of the mean (average) bed height. Standard deviation is a widely used measurement of variability or diversity used in statistics. It shows how much variation or "dispersion" there is from the average (mean, or expected value). A low standard deviation indicates that the data points tend to be very close to the mean, whereas high standard deviation indicates that the data are spread out over a large range of values. The vertical bar denotes the standard deviation for the calculated average bed height, i.e. the variation of the bed height used to calculate a given average bed height. The initial variation in bed height is lower and increases as circulation begins.

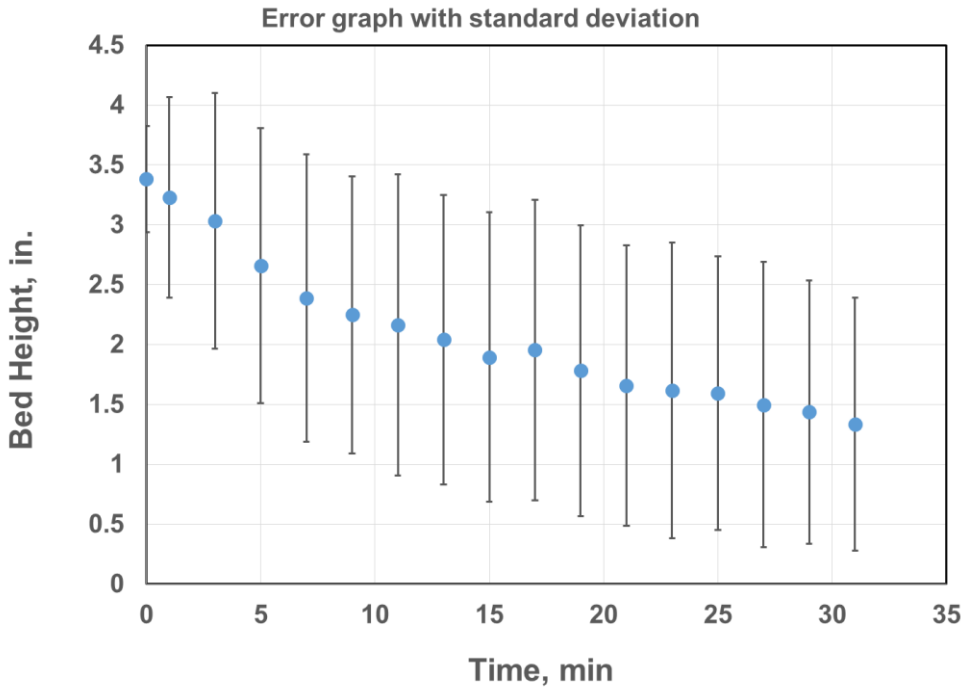

Figure 4.6: Standard deviation for average bed height for water at 80 gpm and 90°

4.2.1 Bed erosion curves and cleanout efficiency for various flow rates

The bed erosion curves for different fluids at 80, 100 and 120 gpm and at 60°, 75° and 90° are shown in Figures 4.7 through 4.10 (for water), 4.12 through 4.15 (for 10 lb/Mgal guar), 4.17 through 4.20 (for 20 lb/Mgal guar) and 4.22 (for 2.16 lb/Mgal HE 150) respectively. With increasing flow rate, rate of solids erosion increased for each fluid at all inclinations. At lower inclination of 60°, solids are transported by rolling or sliding mechanism (for solids in the bed) and by entrainment in the fluid stream. The vertical component of fluid at 60° is higher than 75 and 90°, leading to entrainment of some solids into fluid stream. Solids are also entrained into fluid stream by eddies in case of turbulent flow with water. The amount of solids entrained by eddies depends on turbulent intensity of fluid. Increasing flow rate increases turbulent intensity of the fluid. The fluid drag on entrained solids increases with flow rate, thereby transporting them to a greater distance. At inclination of 75 and 90°, most of the solids are transported by rolling or sliding mechanism as the vertical component of fluid velocity is low. The rate of solids transport via rolling and sliding is directly proportional to interfacial shear stress exerted by fluid on solids bed. Interfacial stress acting on solids bed is directly proportional to flow rate; increasing the flow rate increases interfacial stress leading to improved solids transport. Figures 4.11, 4.16 and 4.21 shows the cleanout efficiency of water, 10 and 20 lb/Mgal guar at different inclinations and flow rate respectively. It is observed that cleanout efficiency also increases with flow rate for all fluids and inclinations considered.

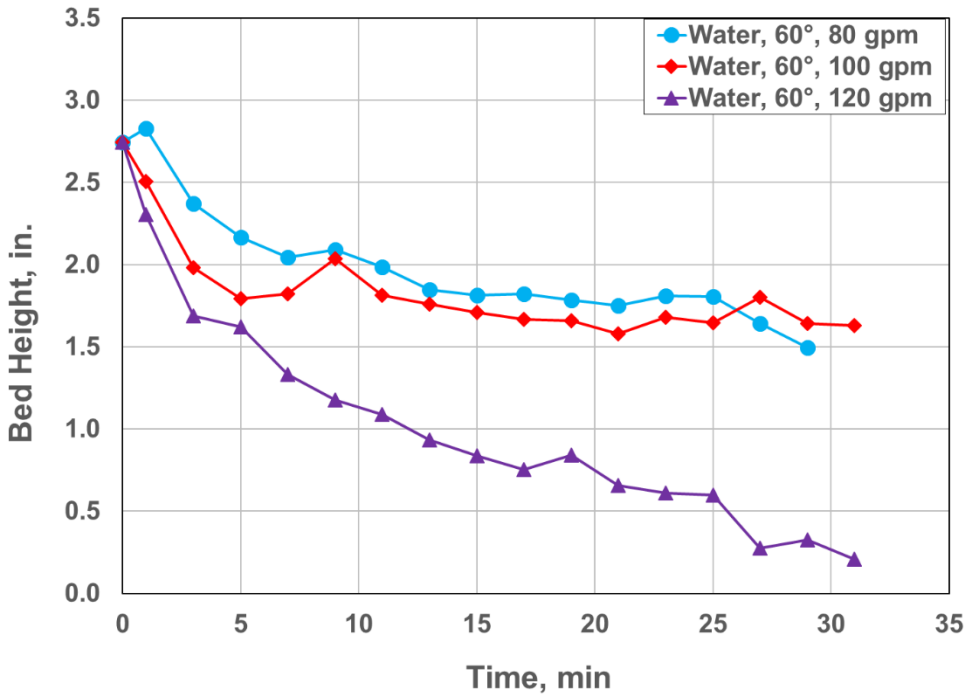

Figure 4.7: Bed erosion curves with water as cleanout fluid at 60° (TS 2)

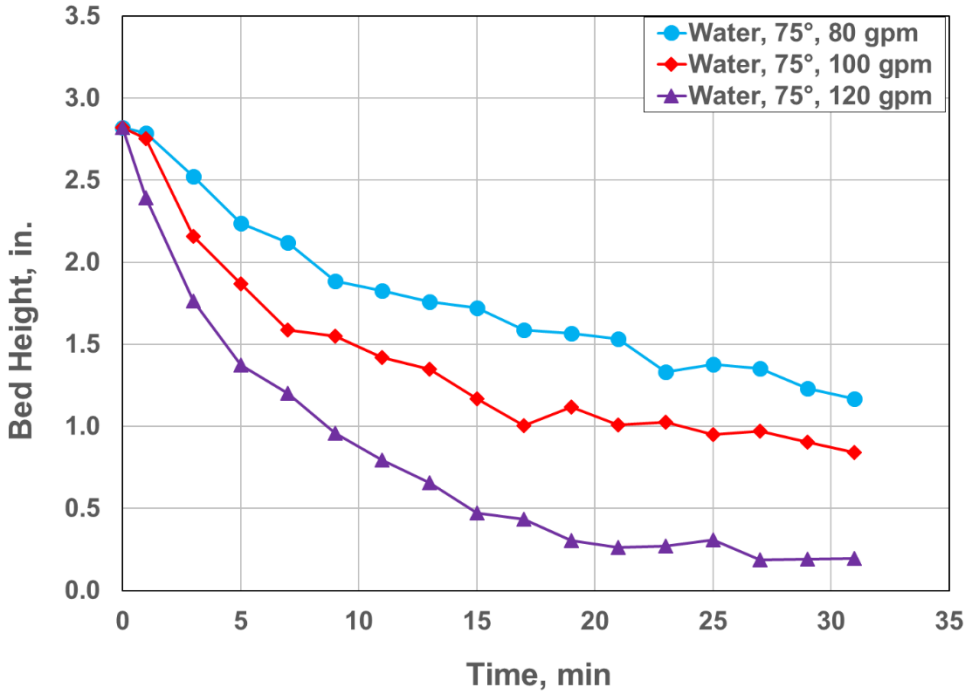

Figure 4.8: Bed erosion curves with water as cleanout fluid at 75° (TS 2)

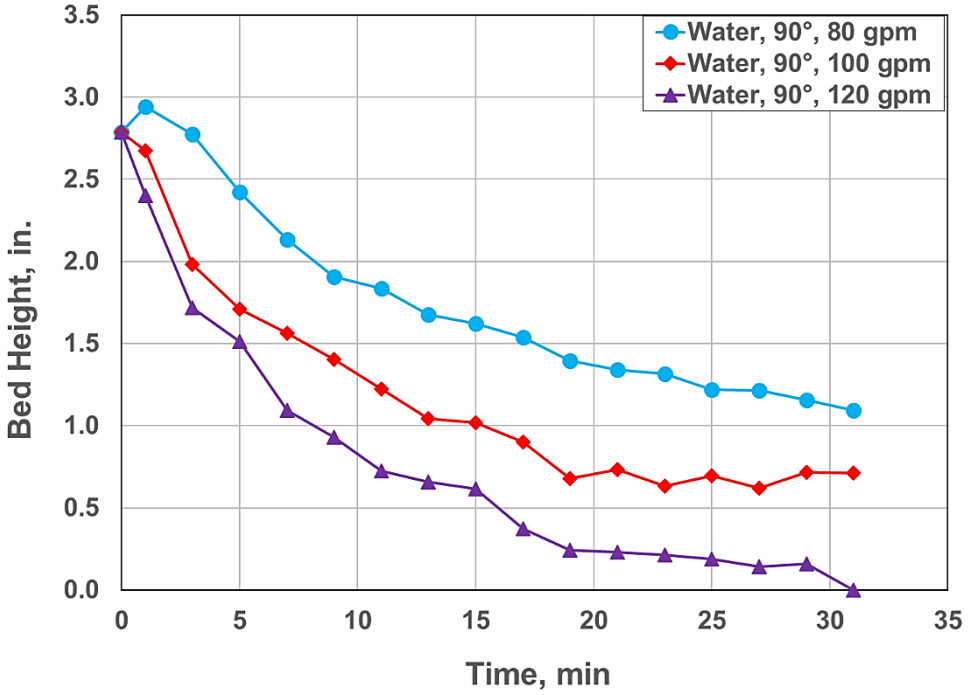

Figure 4.9: Bed erosion curves with water as cleanout fluid at 90° (TS 2)

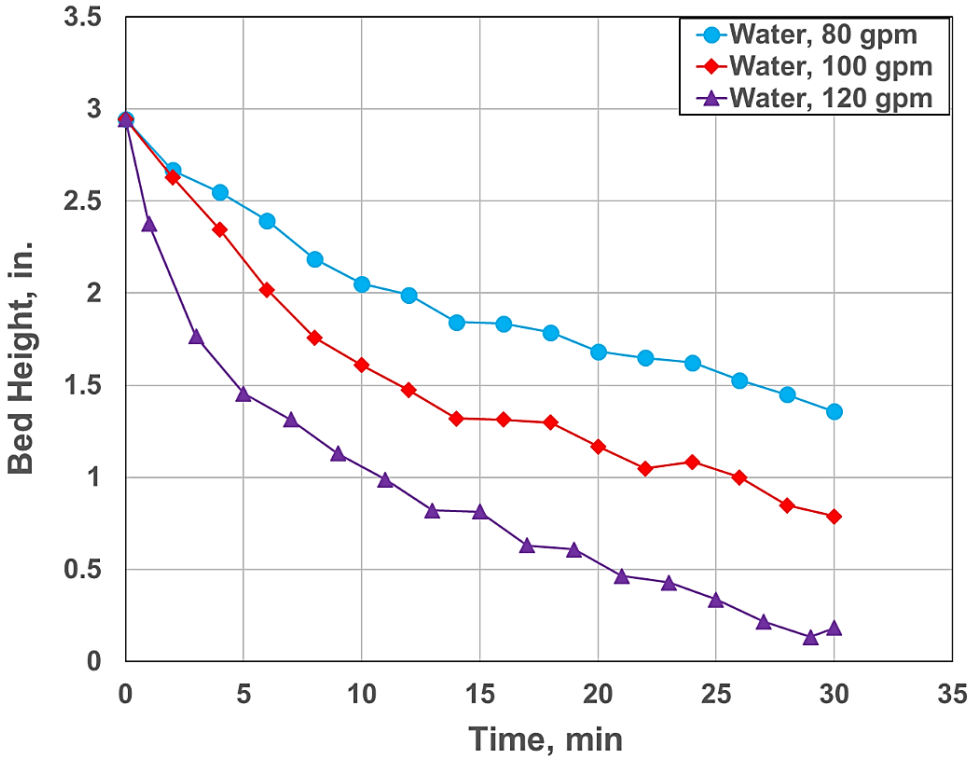

Figure 4.10: Bed erosion curves with water as cleanout fluid at 90° (TS 1)

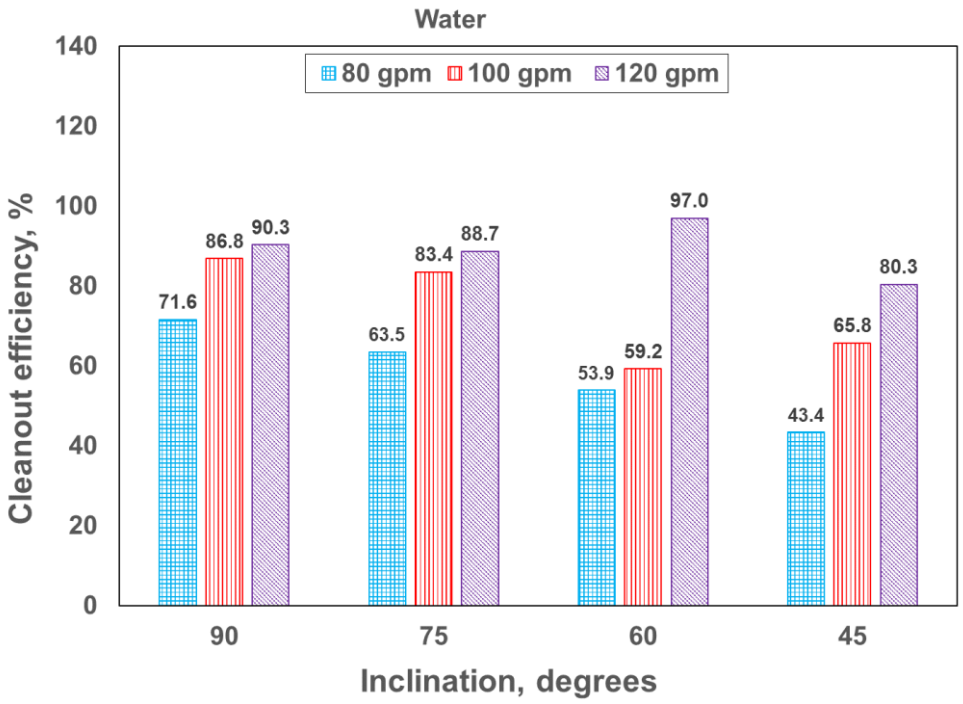

Figure 4.11: Cleanout efficiency of water at different inclinations and flow rates (TS 2)

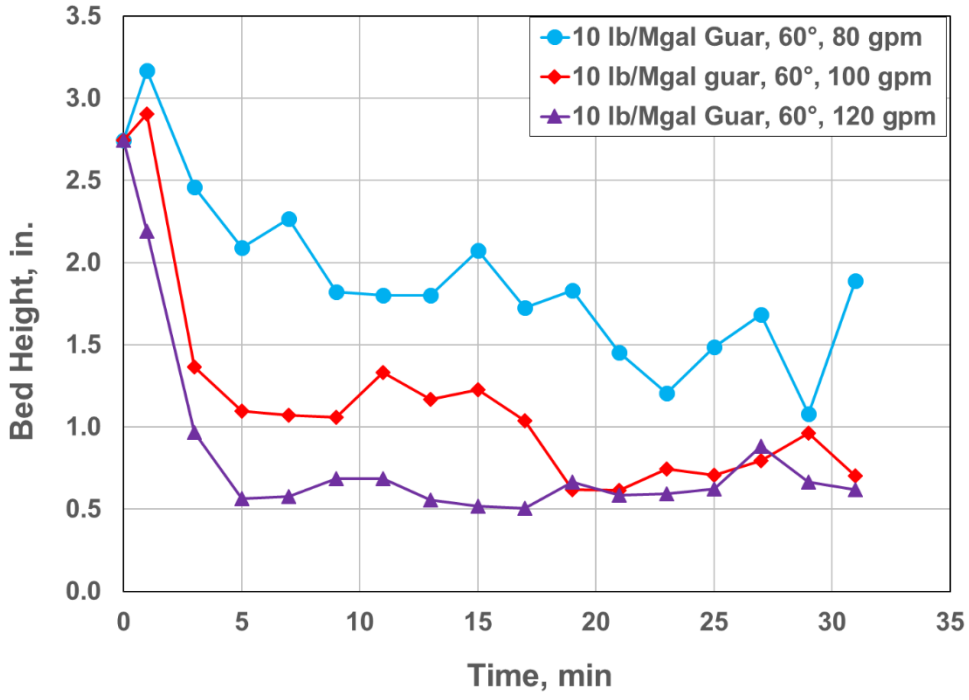

Figure 4.12: Bed erosion curves with 10 lb/Mgal guar as cleanout fluid at 60° (TS 2)

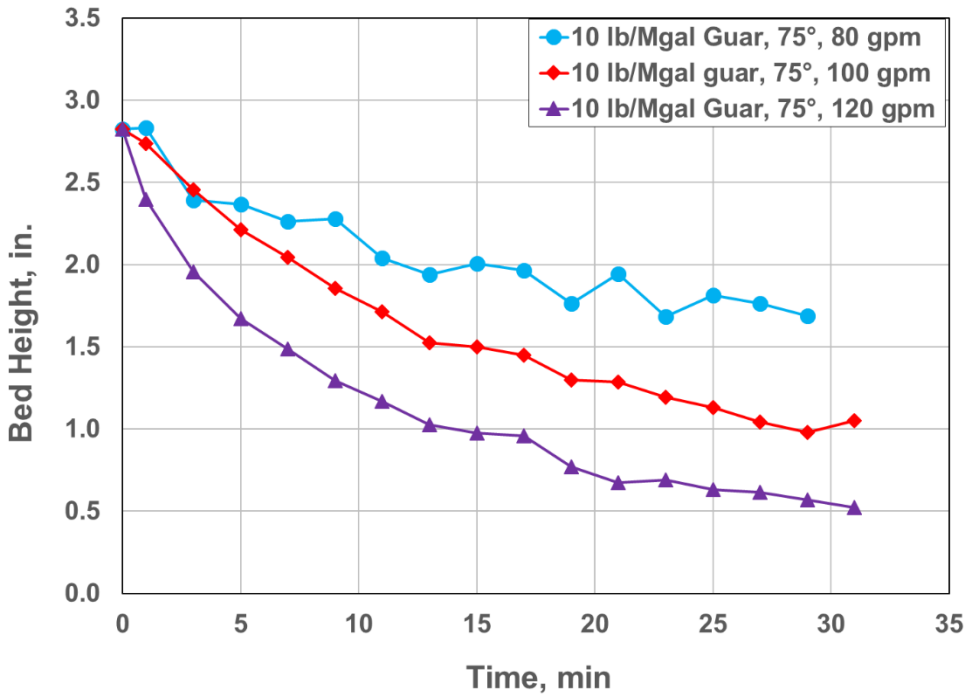

Figure 4.13: Bed erosion curves with 10 lb/Mgal guar as cleanout fluid at 75° (TS 2)

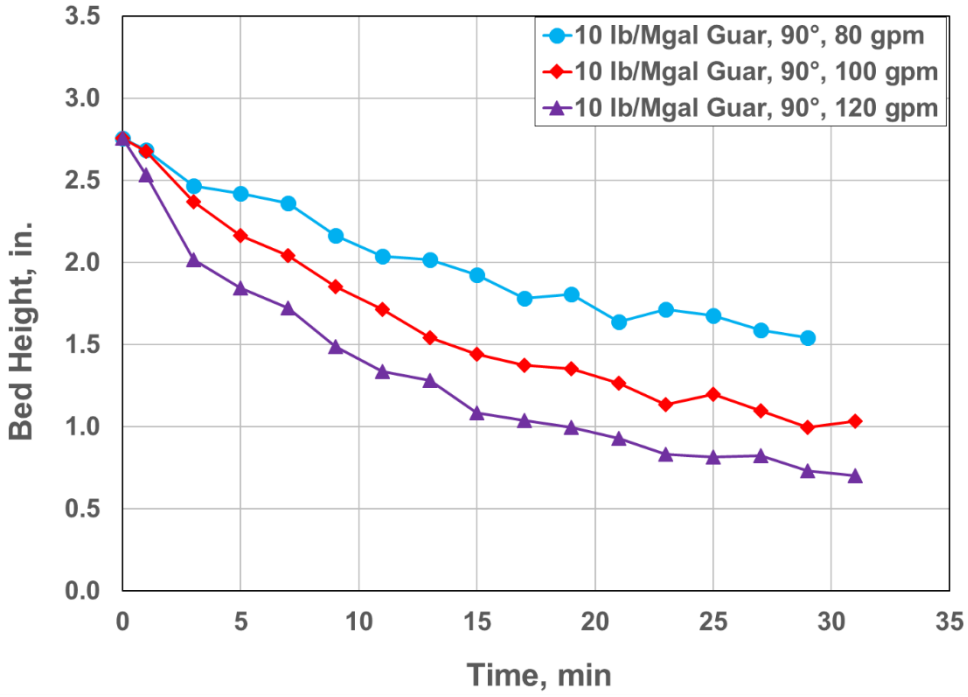

Figure 4.14: Bed erosion curves with 10 lb/Mgal guar as cleanout fluid at 90° (TS 2)

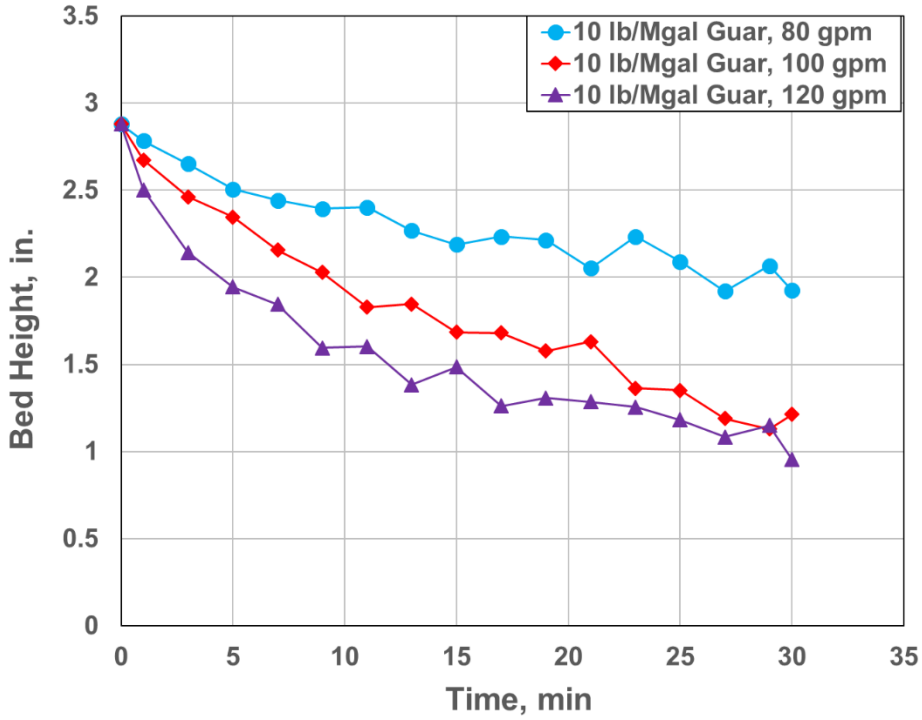

Figure 4.15: Bed erosion curves with 10 lb/Mgal guar as cleanout fluid at 90° (TS 1)

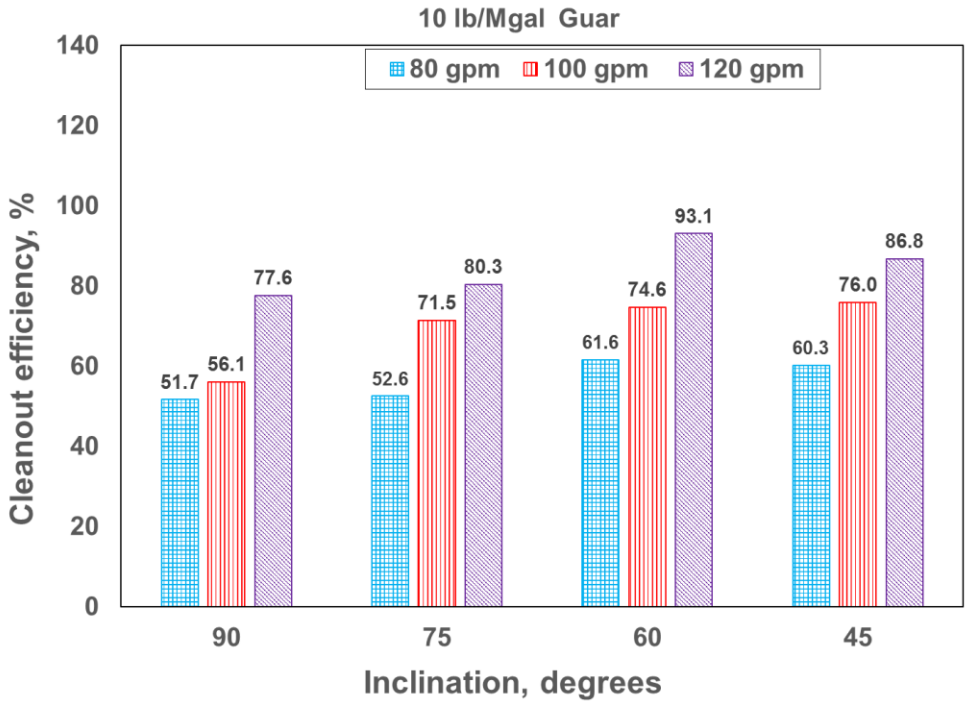

Figure 4.16: Cleanout efficiency of 10 lb/Mgal guar at different inclinations and flow rates (TS 2)

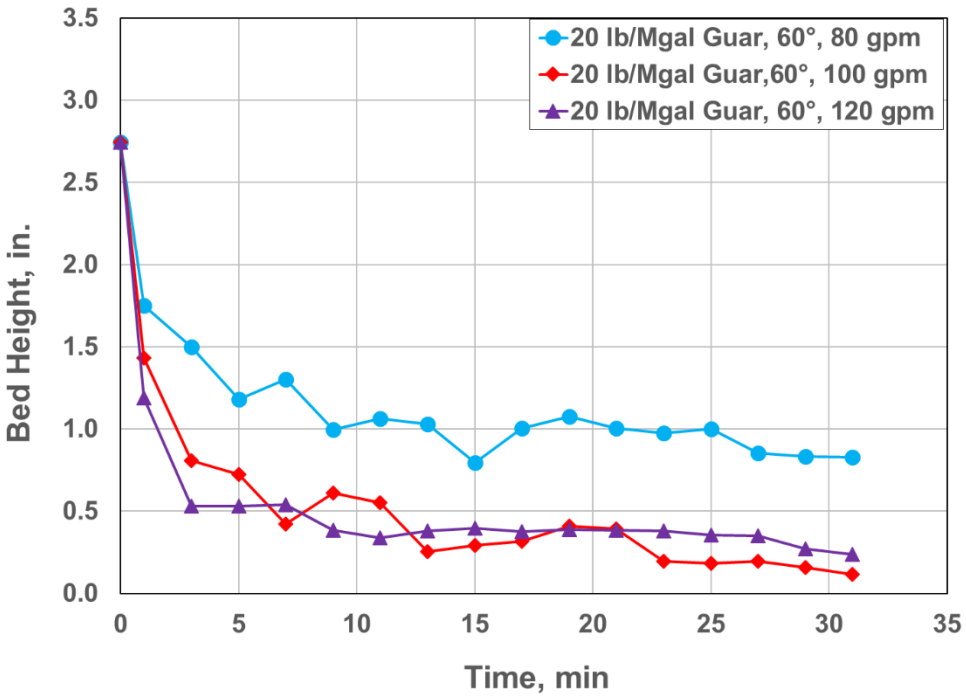

Figure 4.17: Bed erosion curves with 20 lb/Mgal guar as cleanout fluid at 60° (TS 2)

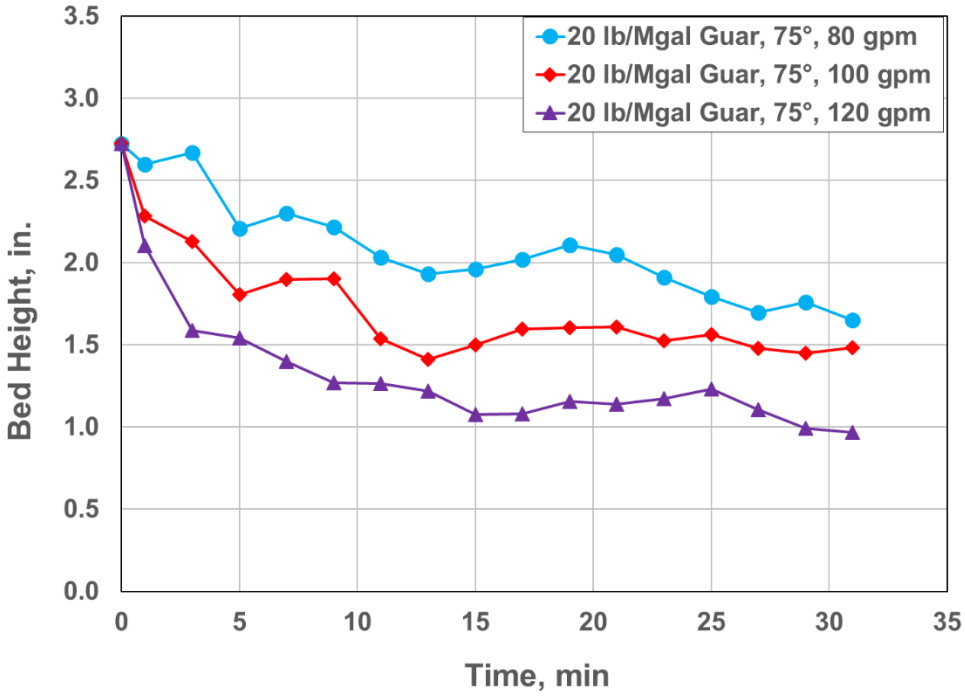

Figure 4.18: Bed erosion curves with 20 lb/Mgal guar as cleanout fluid at 75° (TS 2)

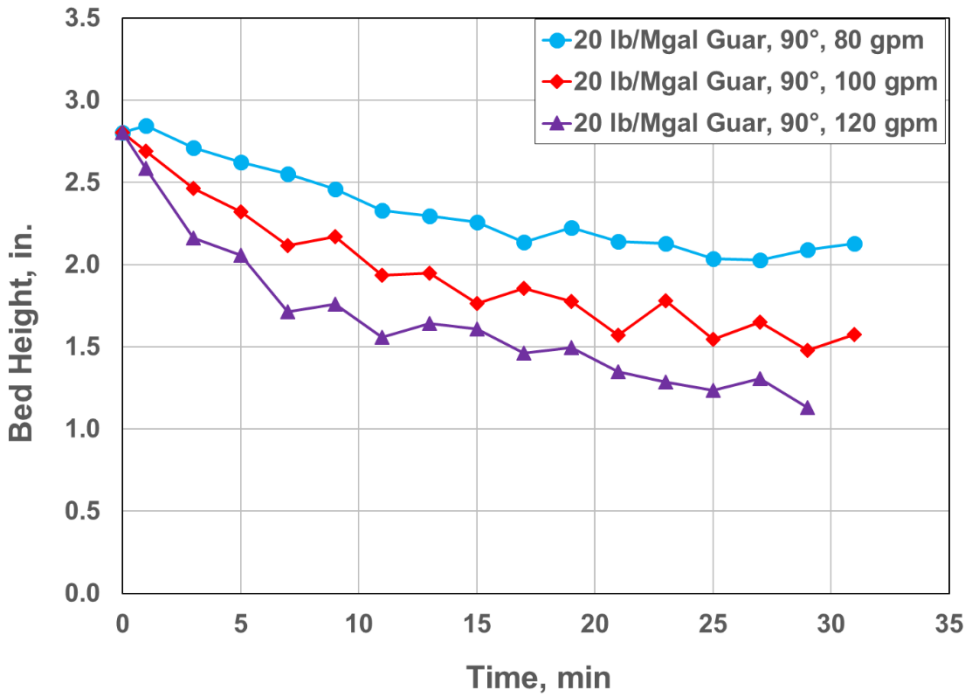

Figure 4.19: Bed erosion curves with 20 lb/Mgal guar as cleanout fluid at 90° (TS 2)

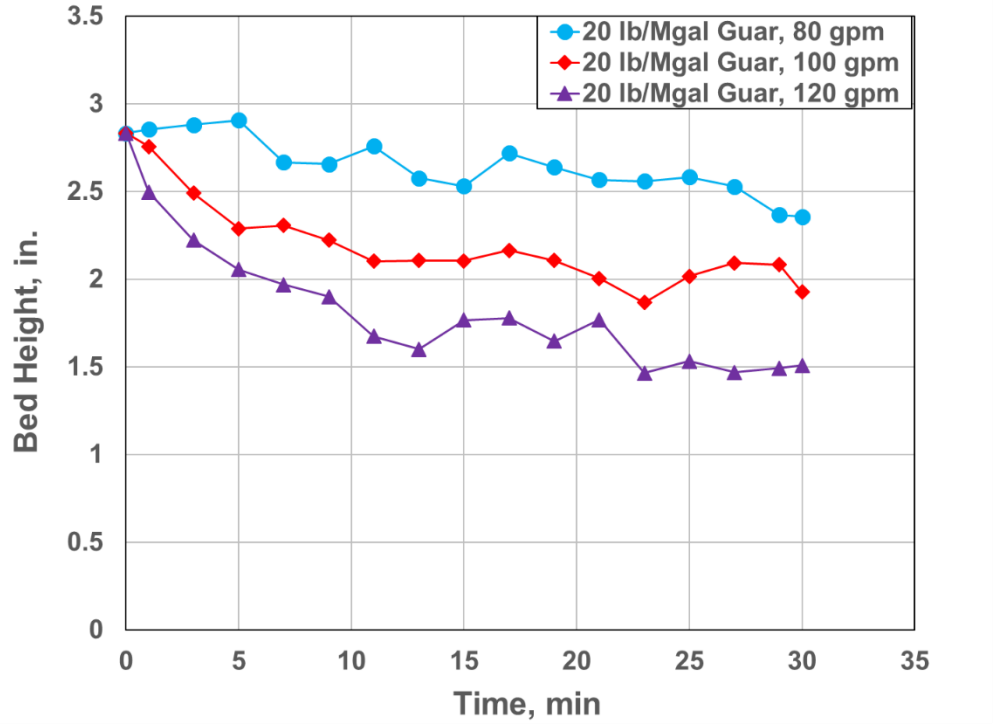

Figure 4.20: Bed erosion curves with 20 lb/Mgal guar as cleanout fluid at 90° (TS 1)

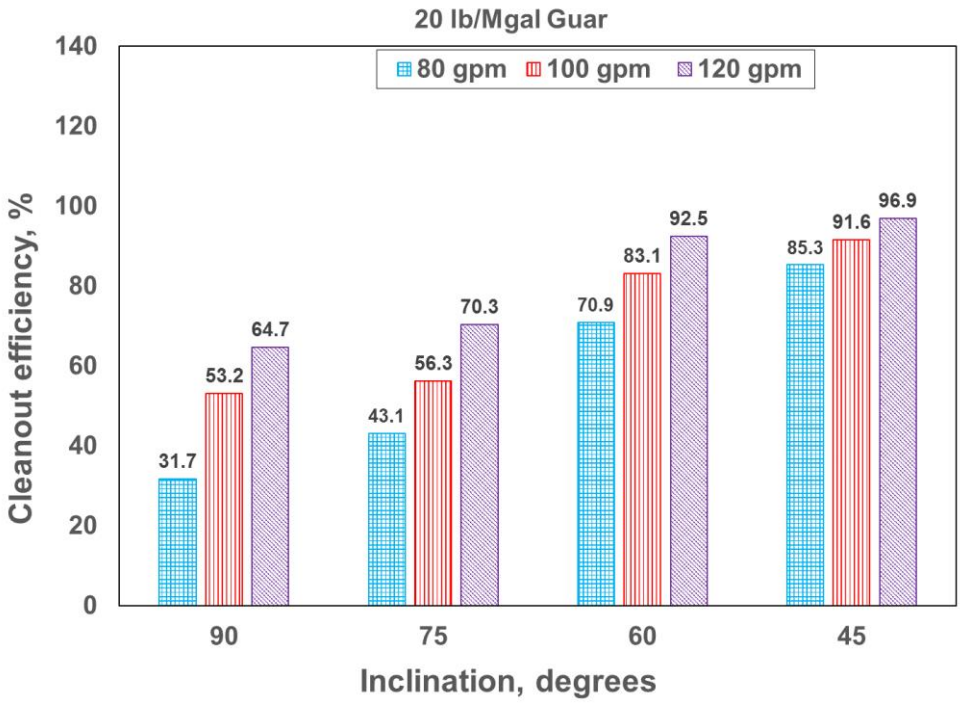

Figure 4.21: Cleanout efficiency of 20 lb/Mgal guar at different inclinations and flow rates (TS 2)

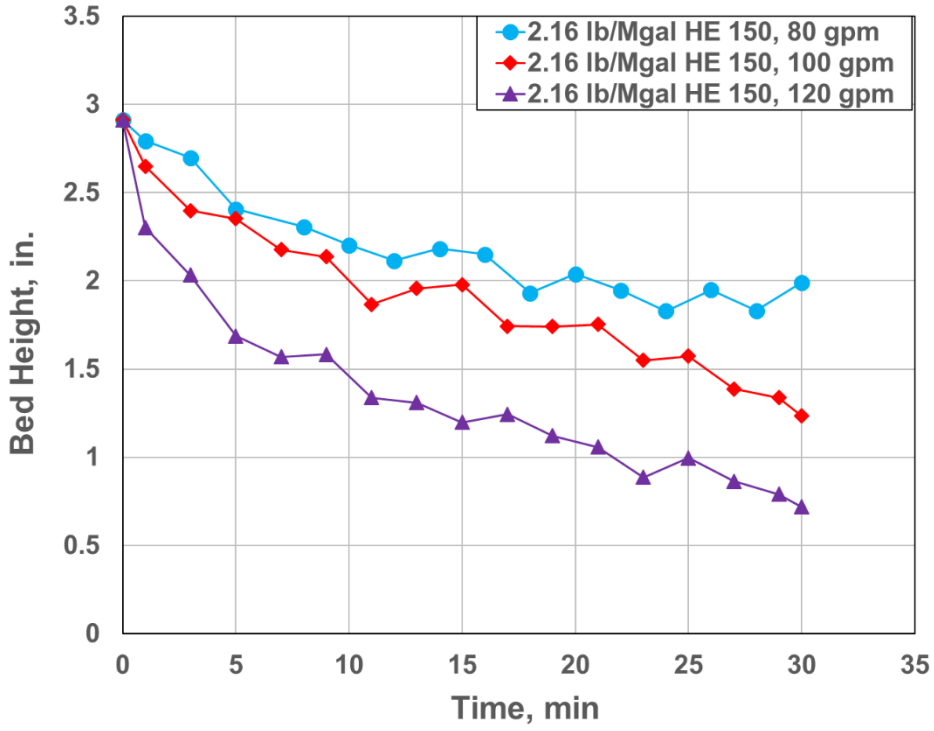

Figure 4.22: Bed erosion curves with 2.16 lb/Mgal HE 150 as cleanout fluid at 90° (TS 1)

4.2.2 Bed erosion curves and cleanout efficiency for various fluids

Bed erosion curves for water, 10 and 20 lb/Mgal guar fluids at flow rates of 80, 100 and 120 gpm and at different inclinations are shown in Figures 4.24 through 4.26 (for 60°), Figures 4.28 through 4.30 (for 75°), and Figures 4.32 through 4.37 (for 90°). Figures 4.32 through 4.37 includes bed erosion curves for 2.16 lb/Mgal HE 150 at inclination of 90°. Figures 4.23, 4.27, 4.31 and 4.38 show the cleanout efficiency of different fluids at inclinations of 45, 60, 75 and 90°.

The effect of fluid rheology on bed erosion depends on flow rate and inclination. Fluids with higher viscosity perform better than low viscosity fluids at 45° for all flow rates based on the cleanout efficiency values. The difference in cleanout efficiency of three fluids decreases at higher flow rates. As discussed earlier, solids form a heterogeneous suspension at 45°, and it has a tendency to settle to the bottom. A fluid with higher viscosity will help to keep the solids in suspension and reduce its settling rate. Alternatively, a higher drag force will also aid in solids transport. Hence, with increase in flow rate the difference in efficiency reduces as the increased fluid drag compensates for the reduced viscosity. However, 20 lb/Mgal guar fluid shows a better overall performance than 10 lb/Mgal guar fluid and water at 45° for all flow rates considered.

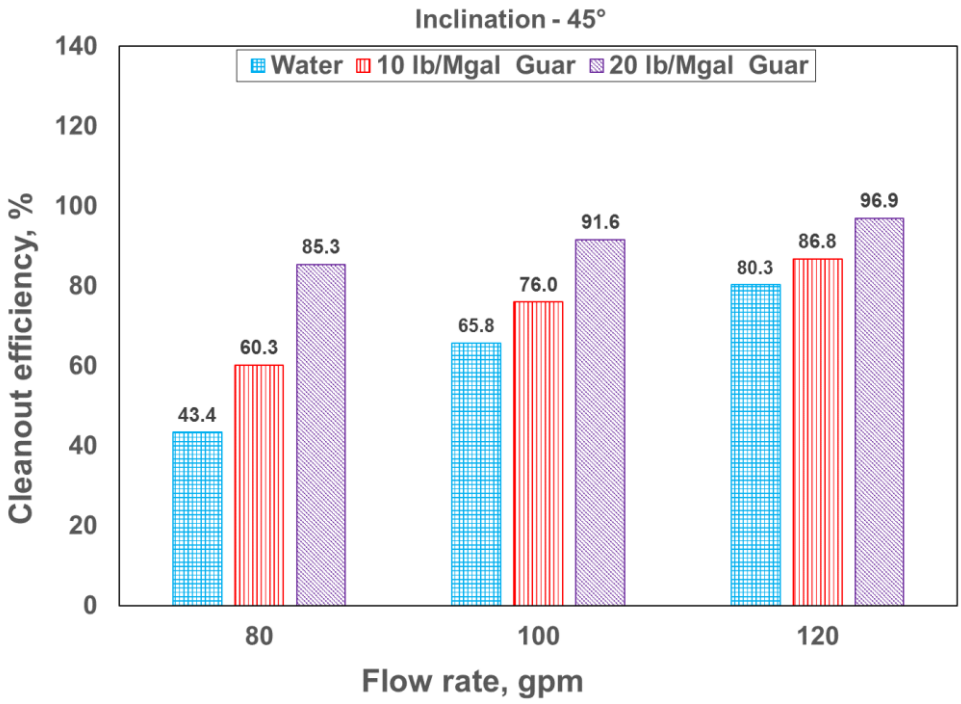

Figure 4.23: Cleanout efficiency of different fluids at 45° (TS 2)

Increasing the inclination from 45° to 60°, solids settle due to gravity to form a sliding bed. At 60°, fluids with higher viscosity (20 lb/Mgal guar) perform better than those with low viscosity (water and 10 lb/Mgal guar). The rate of solids erosion increases with viscosity at all flow rates. The cleanout efficiency also increases with viscosity at 80 and 100 gpm. At 120 gpm, the cleanout efficiency is similar to all three fluids since higher drag force compensates for lower viscosity in case of water and 10 lb/Mgal guar. Also, the efficiency is similar (92-97%) as most of the solids from test section are removed and the remaining solids are deposited in narrow gap at the bottom. Thus, it can be said that both high viscosity fluid at lower rates and low viscosity fluids at higher flow rates have comparable performance at 60°.

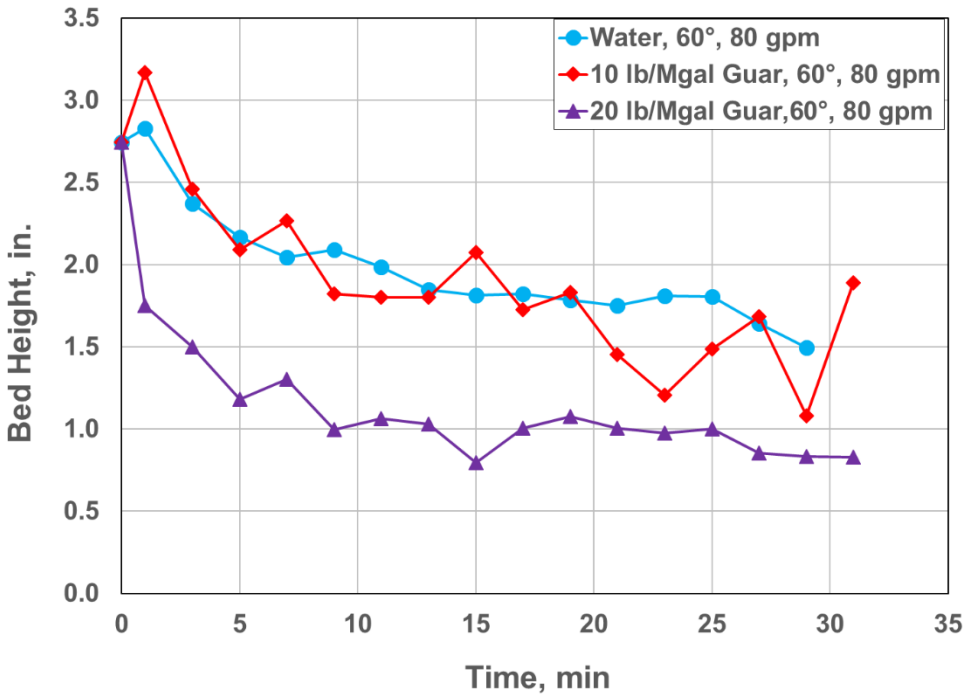

Figure 4.24: Bed erosion curves for different fluids at 60° and 80 gpm (TS 2)

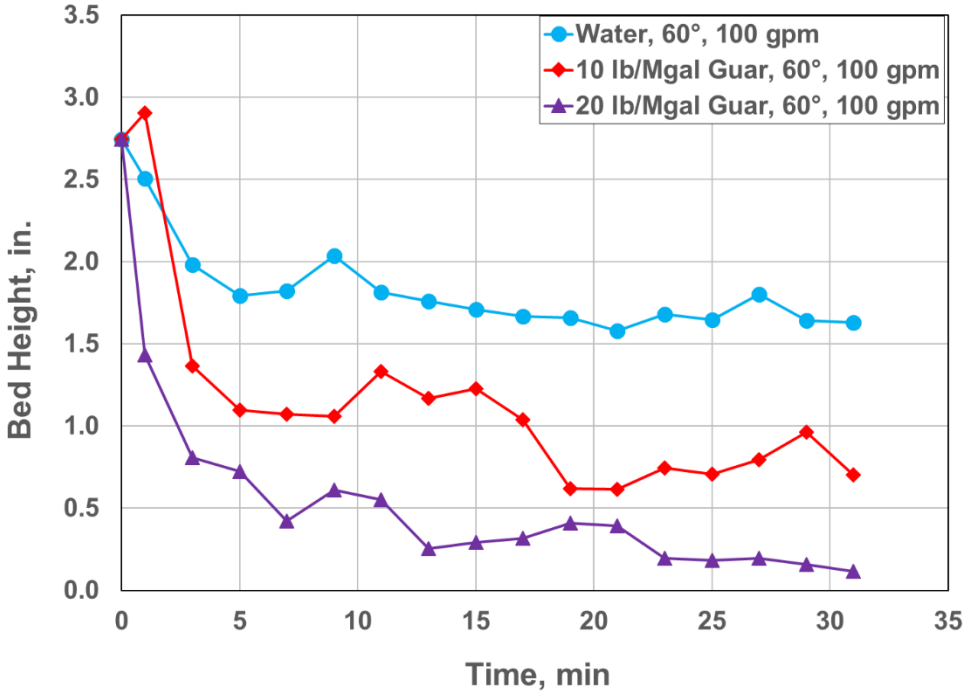

Figure 4.25: Bed erosion curves for different fluids at 60° and 100 gpm (TS 2)

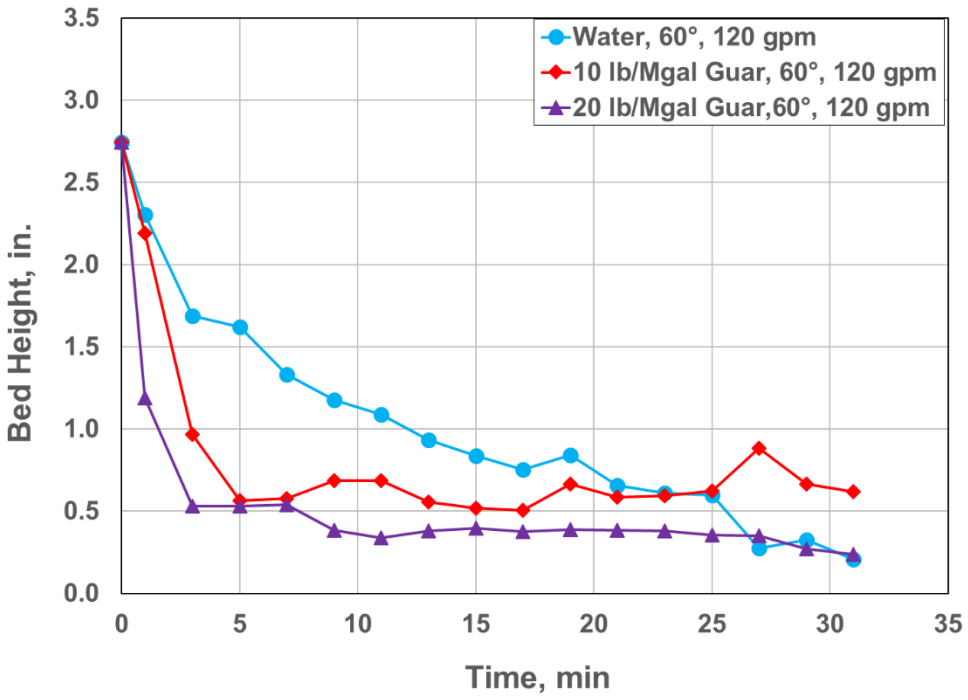

Figure 4.26: Bed erosion curves for different fluids at 60° and 120 gpm (TS 2)

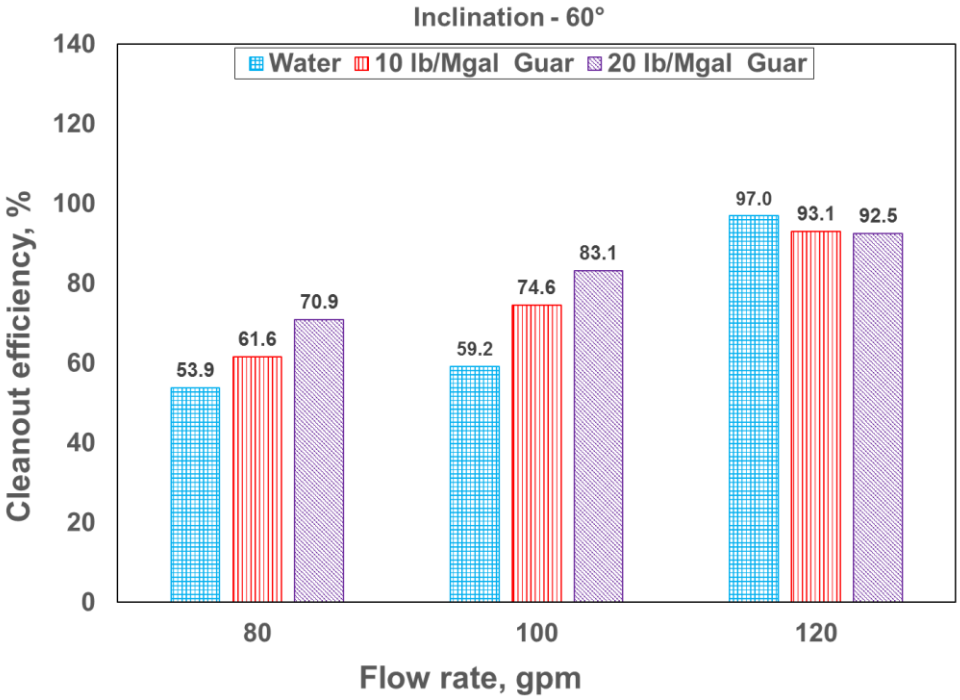

Figure 4.27: Cleanout efficiency of different fluids at 60° (TS 2)

Water showed better performance compared to both polymeric fluids at 75 and 90° for flow rates considered. At higher inclination (75-90°), the solids bed does not have a tendency to slide. Water and low viscosity fluids perform better at solids erosion at these inclinations; since for a given flow rate they can exert higher interfacial stress compared to higher viscosity fluids. Since, most of the solids are transported via rolling or sliding mechanism, higher turbulence (in case of water or low viscosity fluid) will improve solids transport. Since, solids are not entrained into fluid stream at 75 and 90° for the flow rates considered, viscosity did not play a major role in solids transport. This trend can be observed from bed erosion curves and also from cleanout efficiency values.

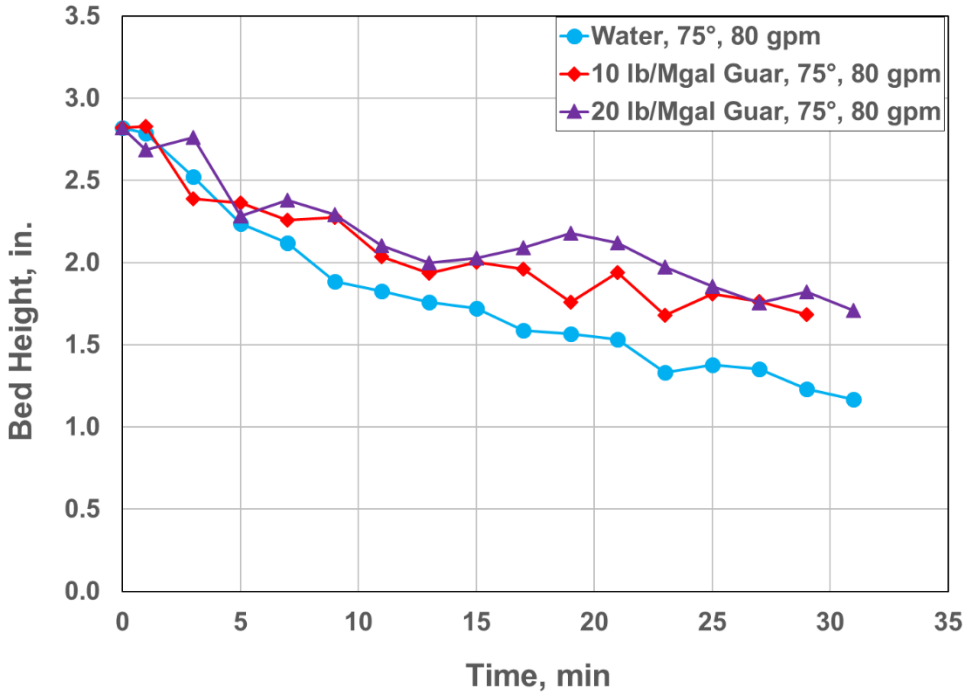

Figure 4.28: Bed erosion curves for different fluids at 75° and 80 gpm (TS 2)

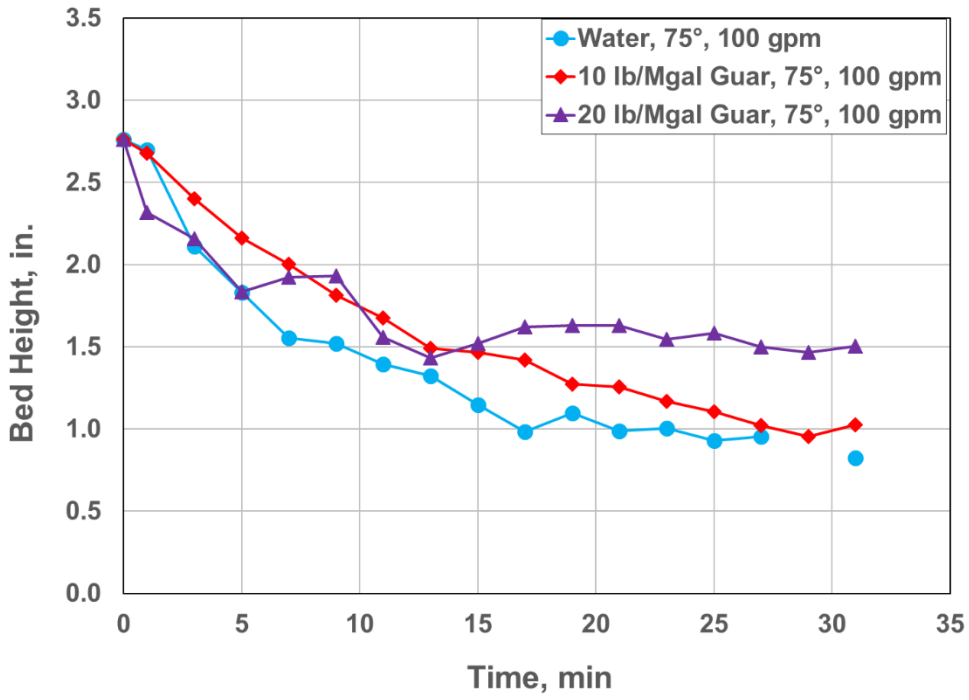

Figure 4.29: Bed erosion curves for different fluids at 75° and 100 gpm (TS 2)

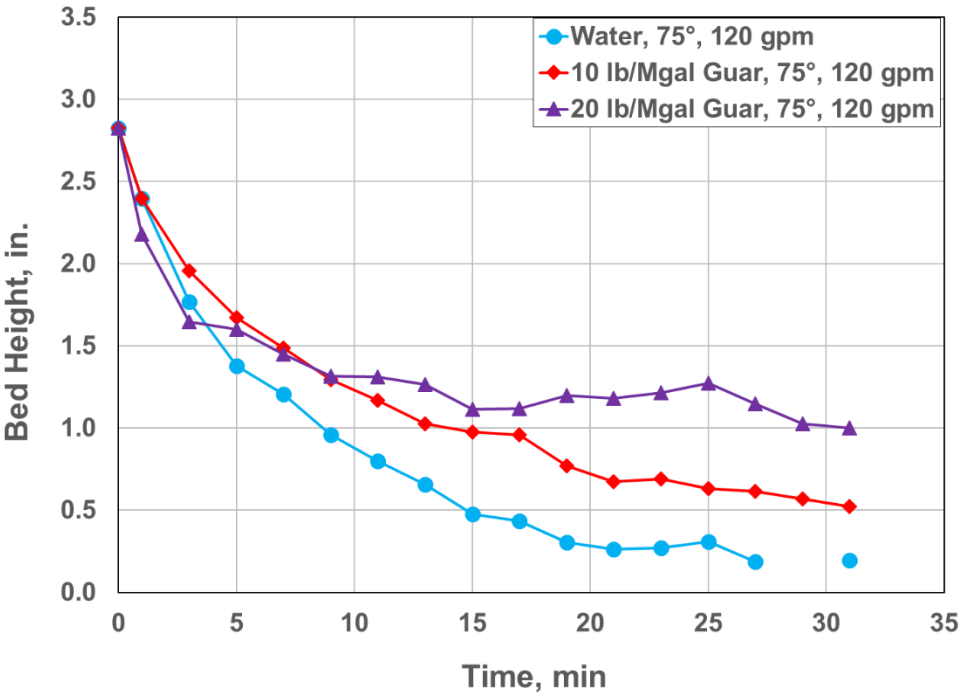

Figure 4.30: Bed erosion curves for different fluids at 75° and 120 gpm (TS 2)

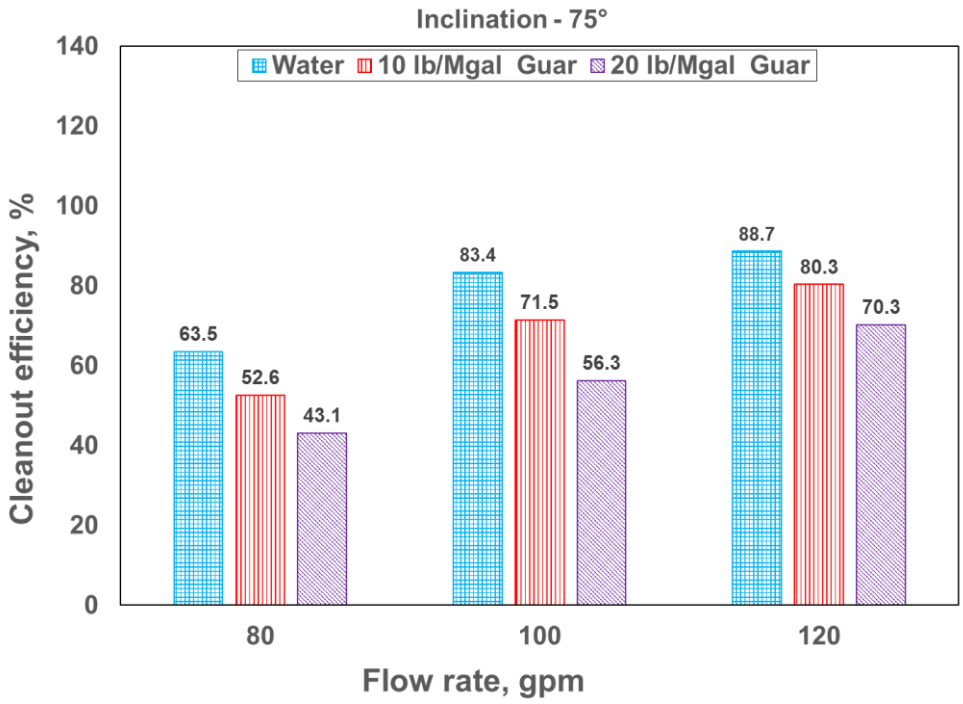

Figure 4.31: Cleanout efficiency of different fluids at 75° (TS 2)

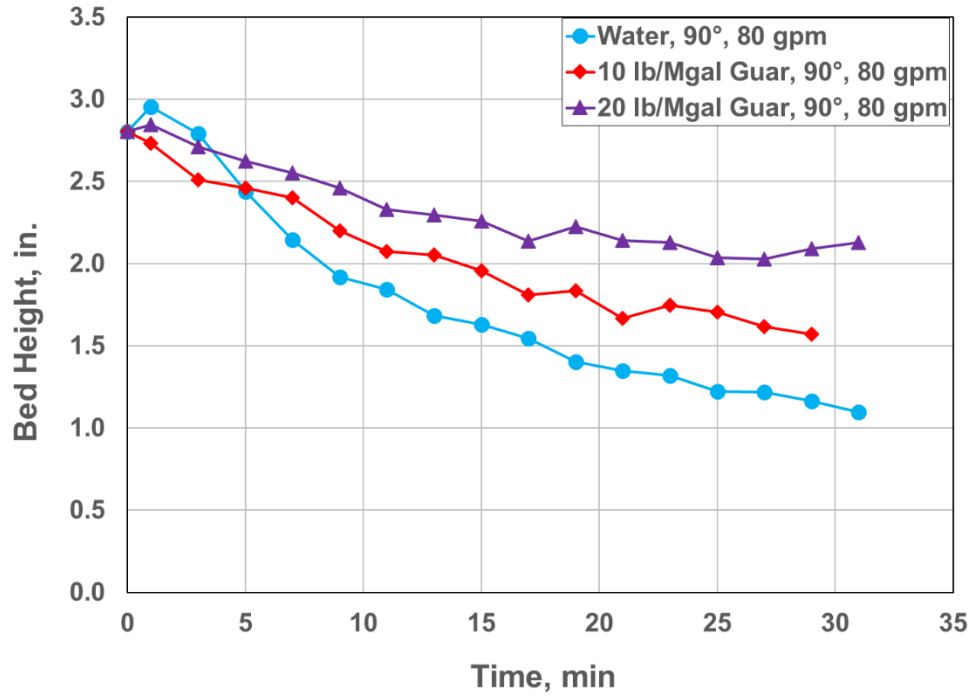

Figure 4.32: Bed erosion curves for different fluids at 90° and 80 gpm (TS 2)

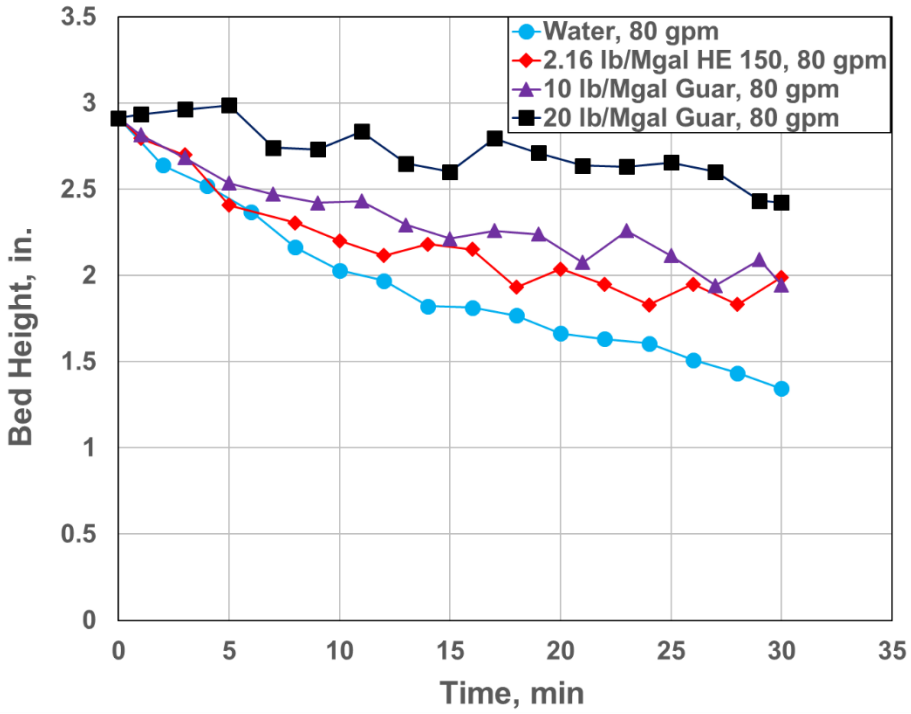

Figure 4.33: Bed erosion curves for different fluids at 90° and 80 gpm (TS 1)

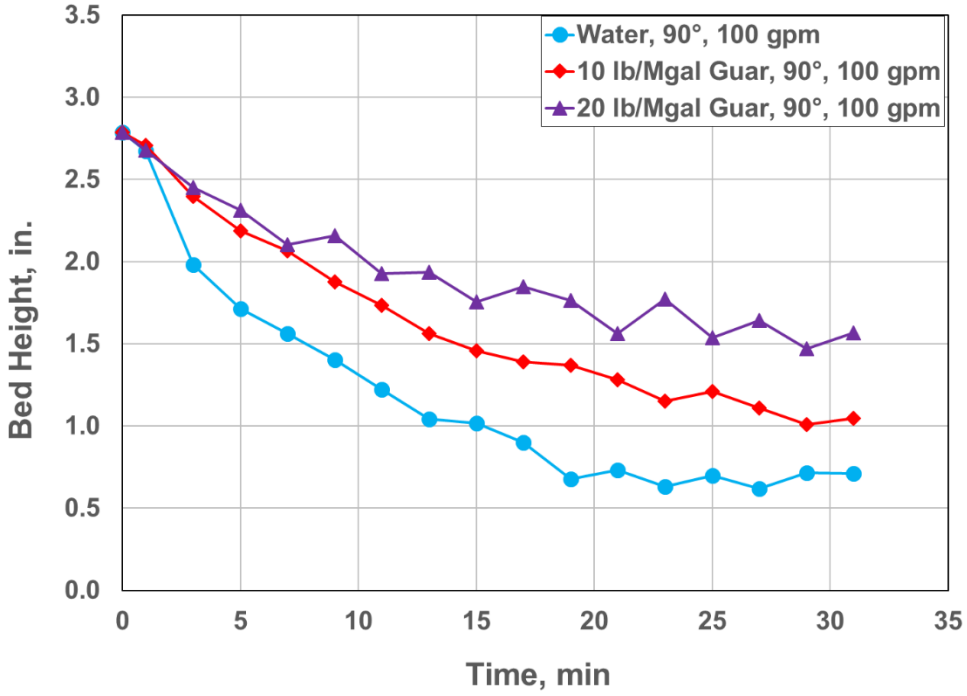

Figure 4.34: Bed erosion curves for different fluids at 90° and 100 gpm (TS 2)

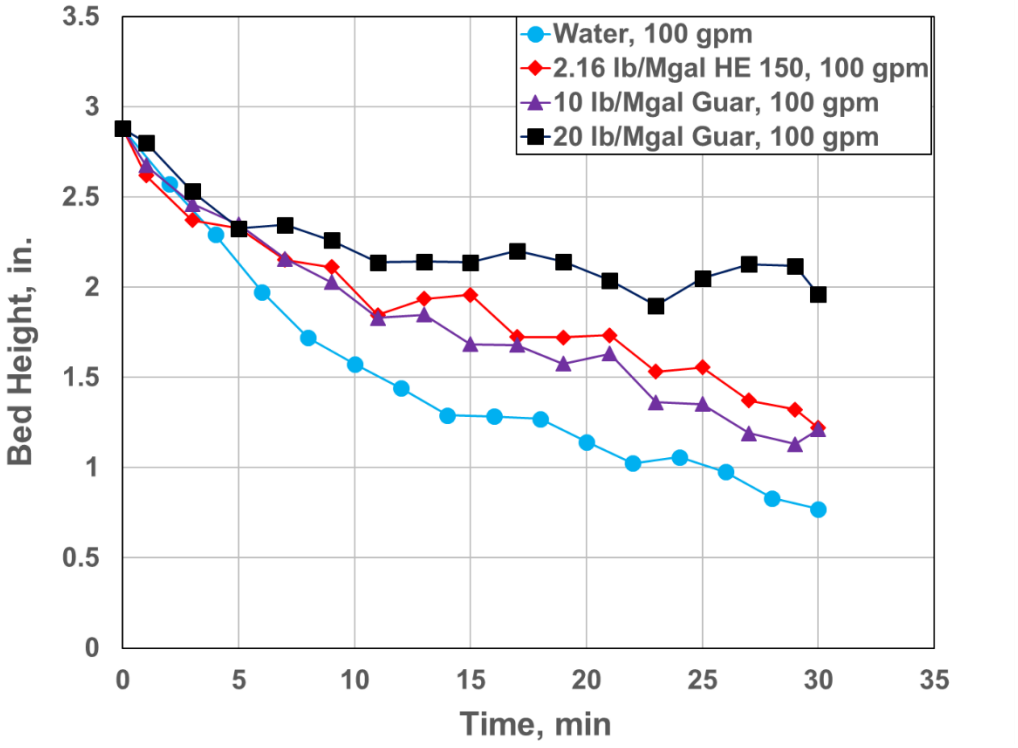

Figure 4.35: Bed erosion curves for different fluids at 90° and 100 gpm (TS 1)

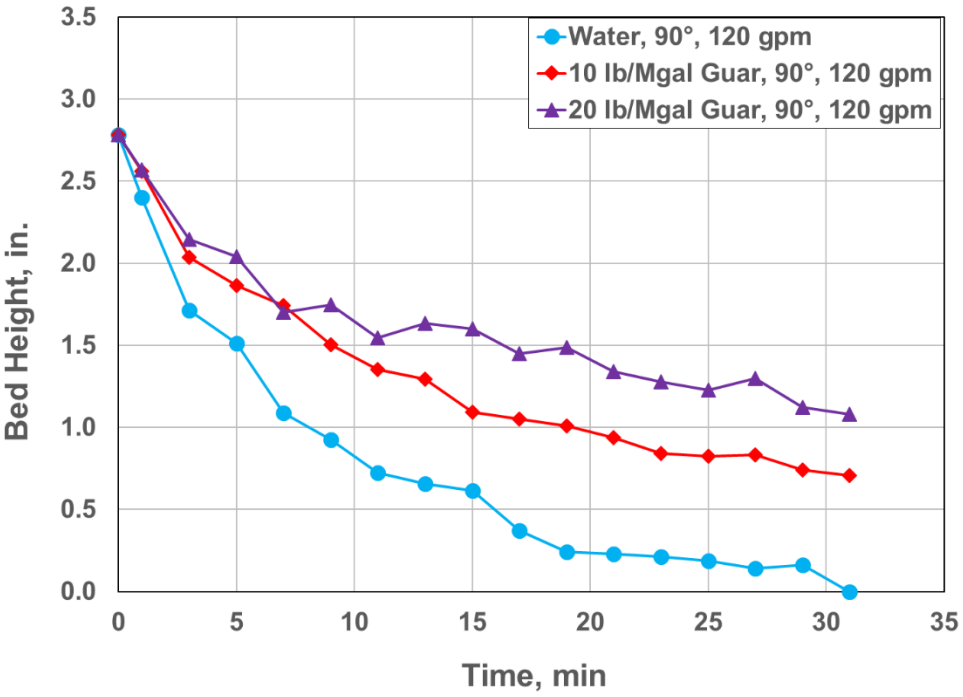

Figure 4.36: Bed erosion curves for different fluids at 90° and 120 gpm (TS 2)

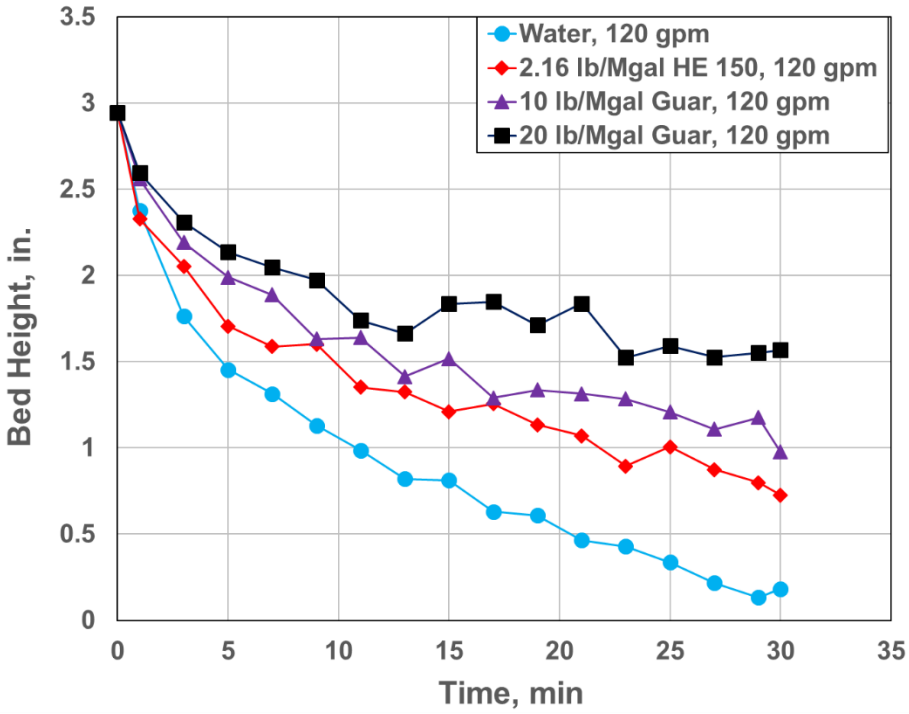

Figure 4.37: Bed erosion curves for different fluids at 90° and 120 gpm (TS 1)

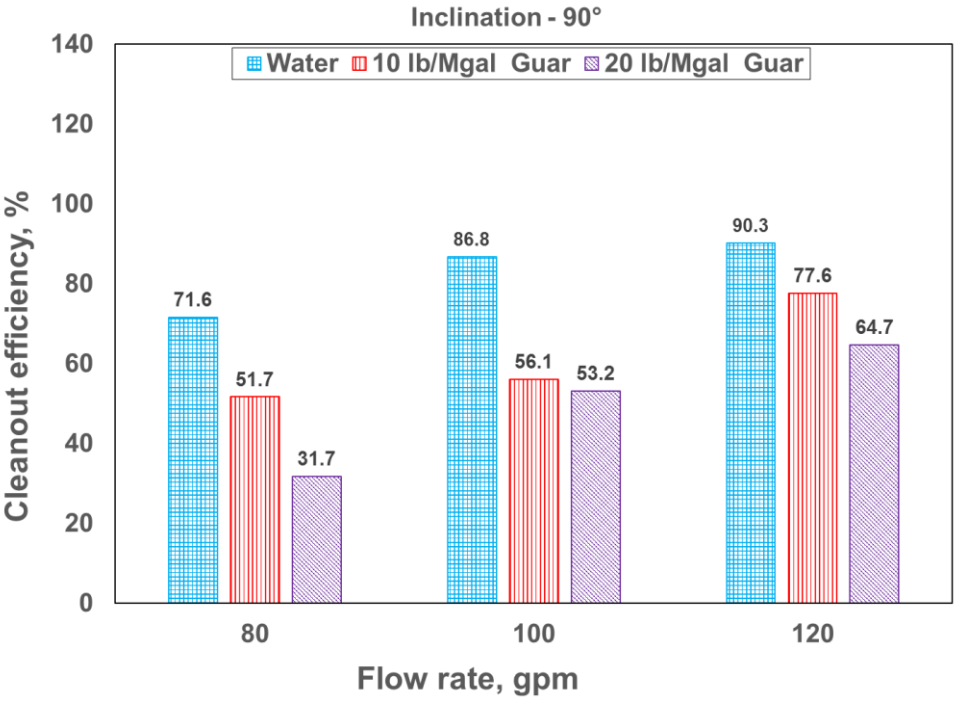

Figure 4.38: Cleanout efficiency of different fluids at 90° (TS 2)

4.2.3 Bed erosion curves and cleanout efficiency for various inclinations

Bed erosion curves for water, 10 and 20 lb/Mgal guar fluids at 60°, 75° and 90° at three flow rates are shown in Figures 4.39 through 4.41 (for 80 gpm), Figures 4.43 through 4.45 (for 100 gpm), and Figures 4.47 through 4.49 (for 120 gpm). Figures 4.42, 4.46 and 4.50 show the cleanout efficiency at flow rates of 80, 100 and 120 gpm.

The effect of inclination on solids transport depends on fluid rheology and flow rate. At 80 gpm, the rate of solids erosion for water increased with inclination (from 60° to 90°) whereas for polymeric fluids it increased with decrease in inclination (from 90° to 60°). With decrease in inclination, solids are entrained into fluid stream due to higher vertical component of fluid velocity. Fluids with higher viscosity can effectively suspend these solids and transport them out of wellbore. Also, the cleanout efficiency of water increased with inclination at 80 gpm. For 10 lb/Mgal guar fluid, the efficiency was similar at 75° and 90°. It slightly increased at 60° and remained constant at 45°. With 20 lb/guar fluid, the efficiency increased with decreasing inclination. Hence, higher viscosity fluids perform better than low viscosity fluids with decreasing inclination at 80 gpm.

Similarly, at 100 gpm, the rate of solids erosion with water increased with inclination whereas for polymeric fluids it increased with decrease in inclination. The cleanout efficiency with water decreased with inclination whereas it increased for 10 and 20 lb/Mgal guar fluid.

At 120 gpm, the rate of solids erosion with water increased with inclination whereas for polymeric fluids it increased with decrease in inclination. The cleanout efficiency of water is nearly constant up to 60°, but decreases at 45°. This may be due to settling of suspended solids in water compared to viscous polymeric fluids. Similarly, the efficiency of 10 lb/Mgal guar fluid decreased at 45°. Thus, flow rate of 120 gpm was insufficient to compensate for low viscosity of water and 10 lb/Mgal guar fluid compared to 20 lb/Mgal guar. The efficiency of 20 lb/Mgal guar fluid continuously increases with decreasing inclination. Thus, with decreasing inclination, higher viscosity fluids perform better. However, increasing the flow rate can compensate for lower viscosity at 60°.

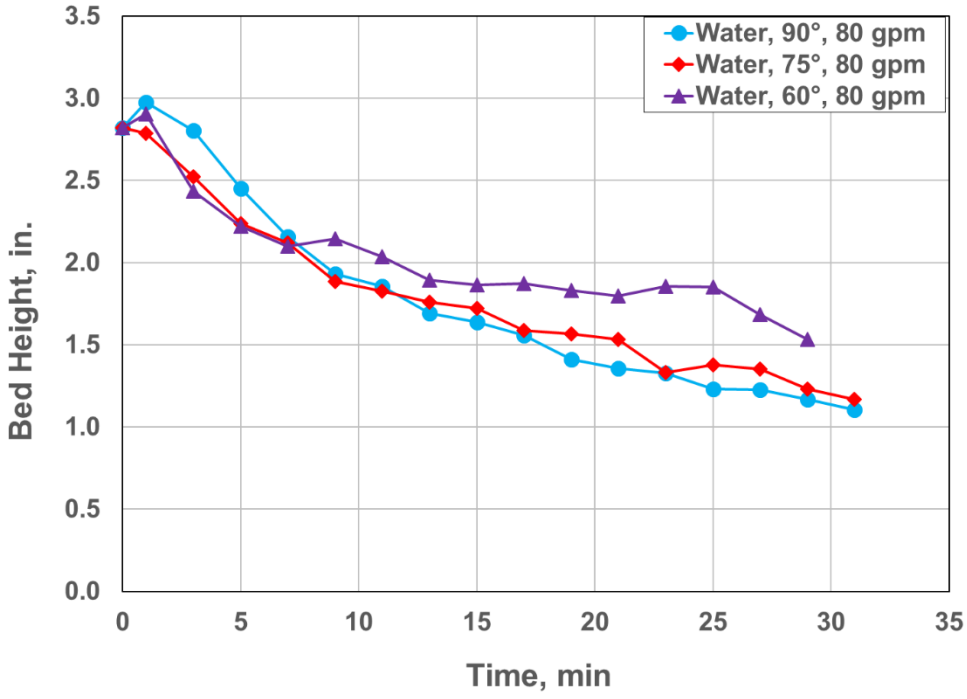

Figure 4.39: Bed erosion curves for water at 80 gpm (TS 2)

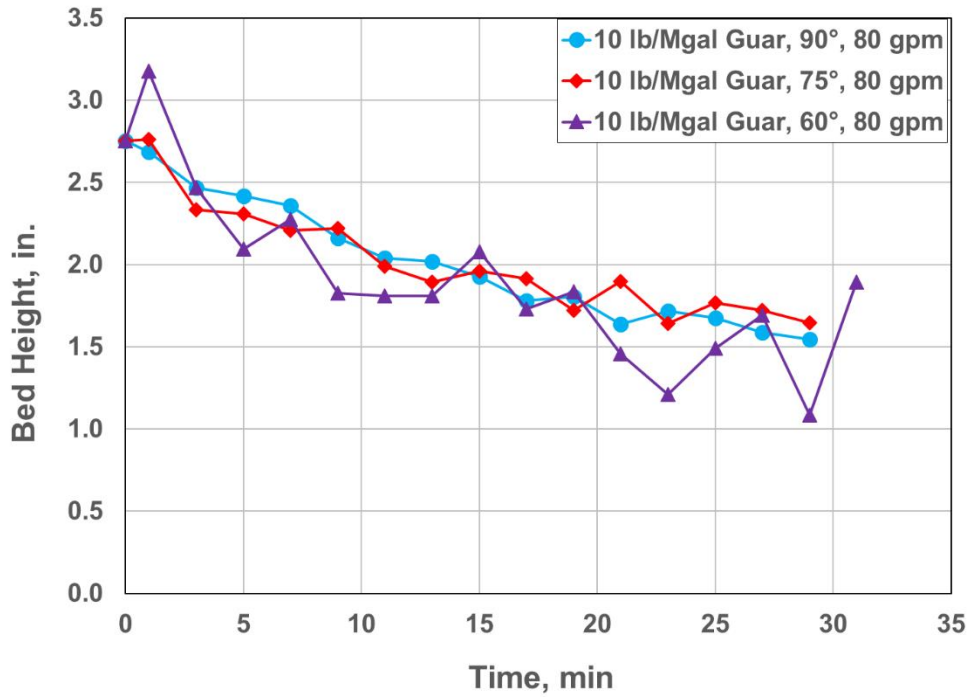

Figure 4.40: Bed erosion curves for 10 lb/Mgal at 80 gpm (TS 2)

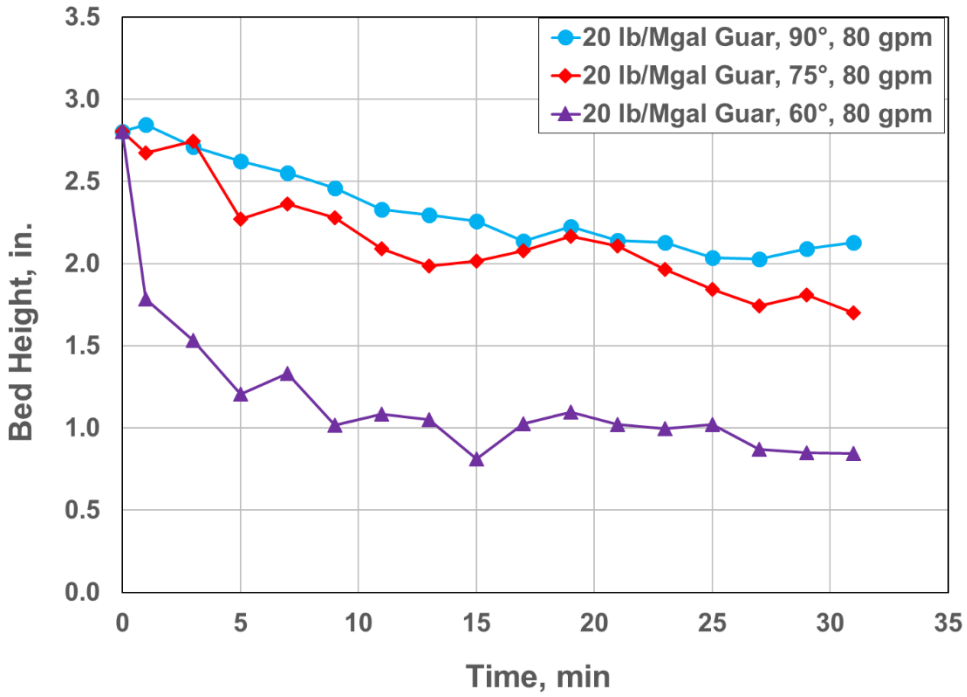

Figure 4.41: Bed erosion curves for 20 lb/Mgal at 80 gpm (TS 2)

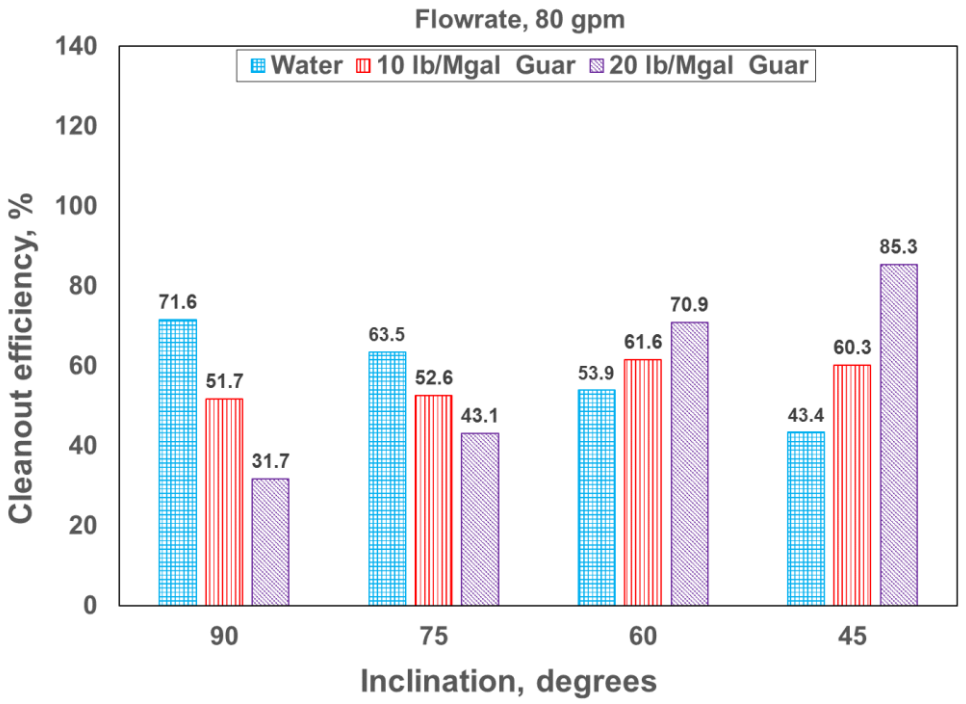

Figure 4.42: Cleanout efficiency of different fluids at 80 gpm (TS 2)

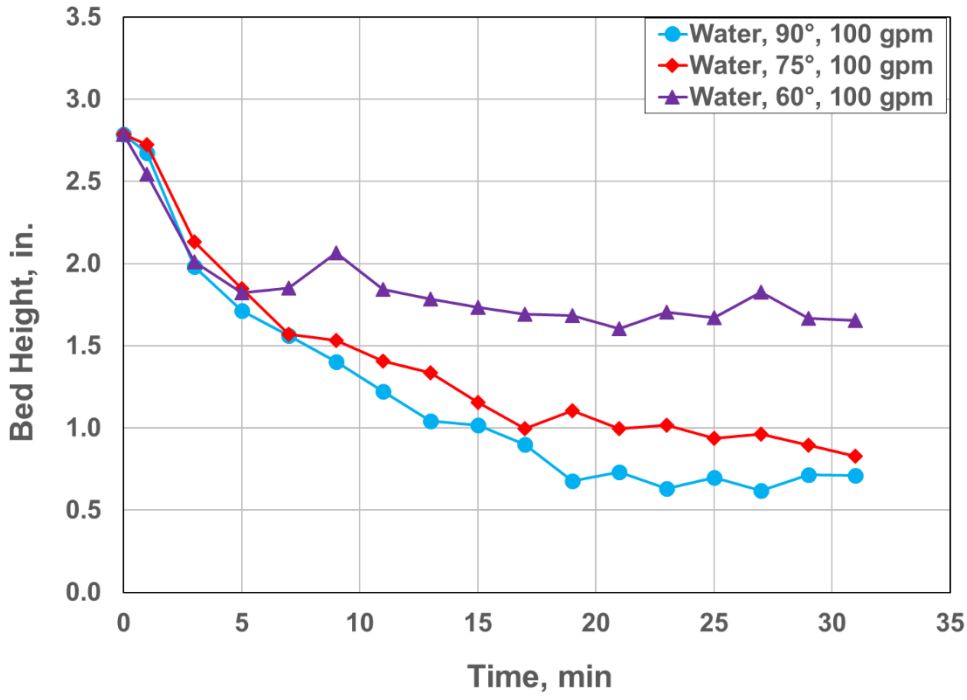

Figure 4.43: Bed erosion curves for water at 100 gpm (TS 2)

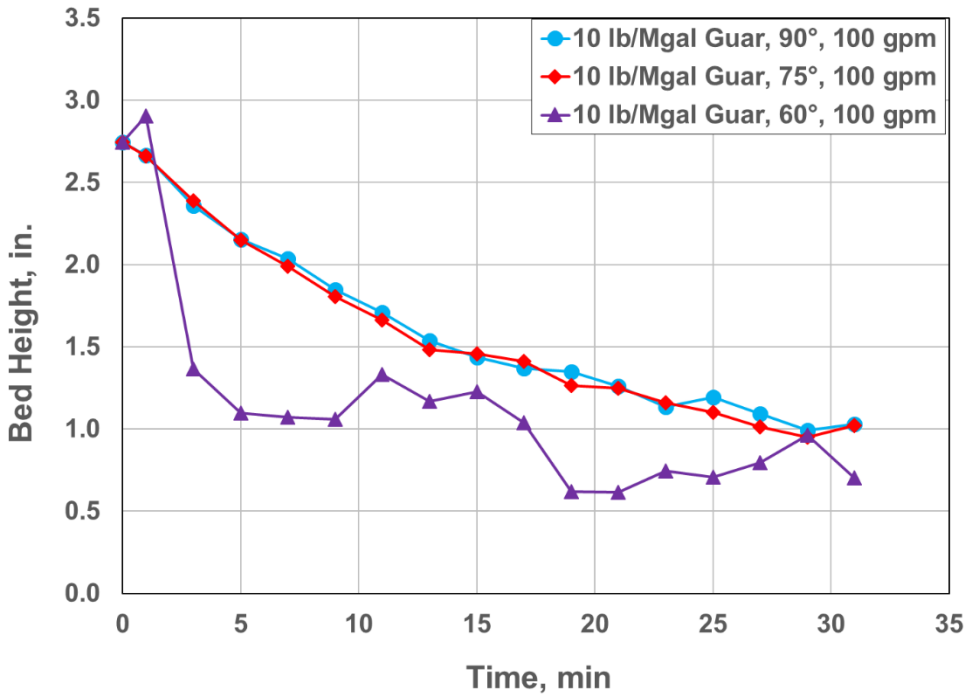

Figure 4.44: Bed erosion curves for 10 lb/Mgal Guar at 100 gpm (TS 2)

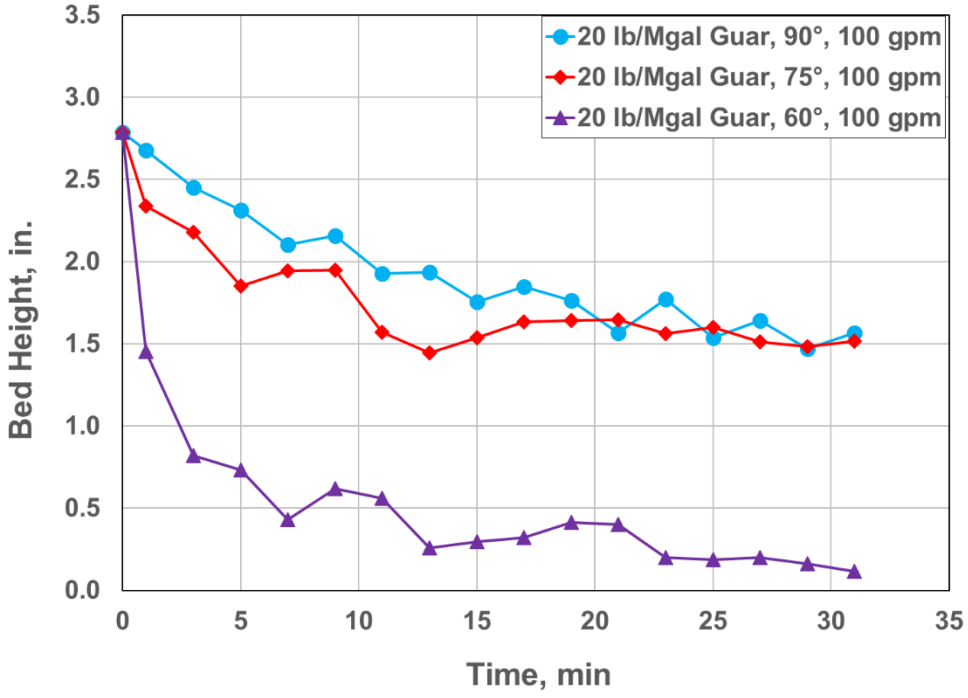

Figure 4.45: Bed erosion curves for 20 lb/Mgal Guar at 100 gpm (TS 2)

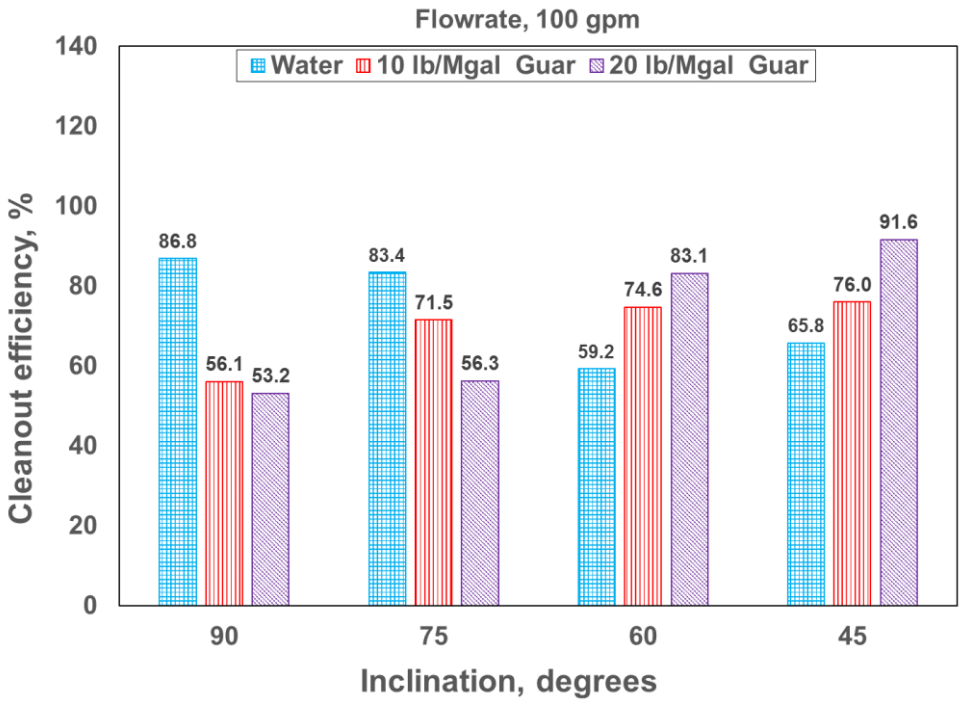

Figure 4.46: Cleanout efficiency of different fluids at 100 gpm (TS 2)

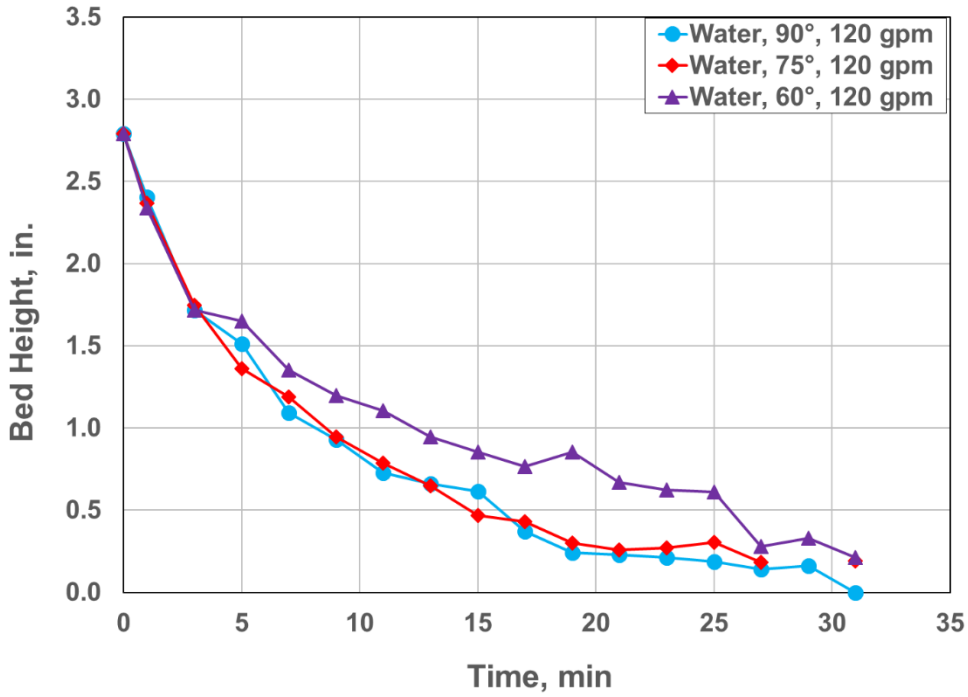

Figure 4.47: Bed erosion curves for water at 120 gpm (TS 2)

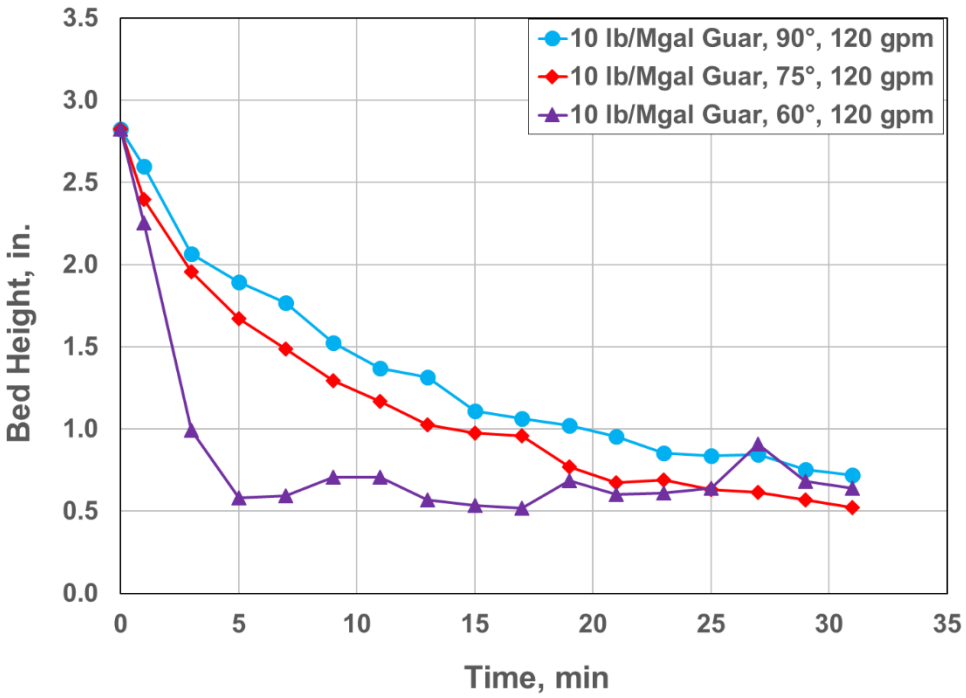

Figure 4.48: Bed erosion curves for 10 lb/Mgal Guar at 120 gpm (TS 2)

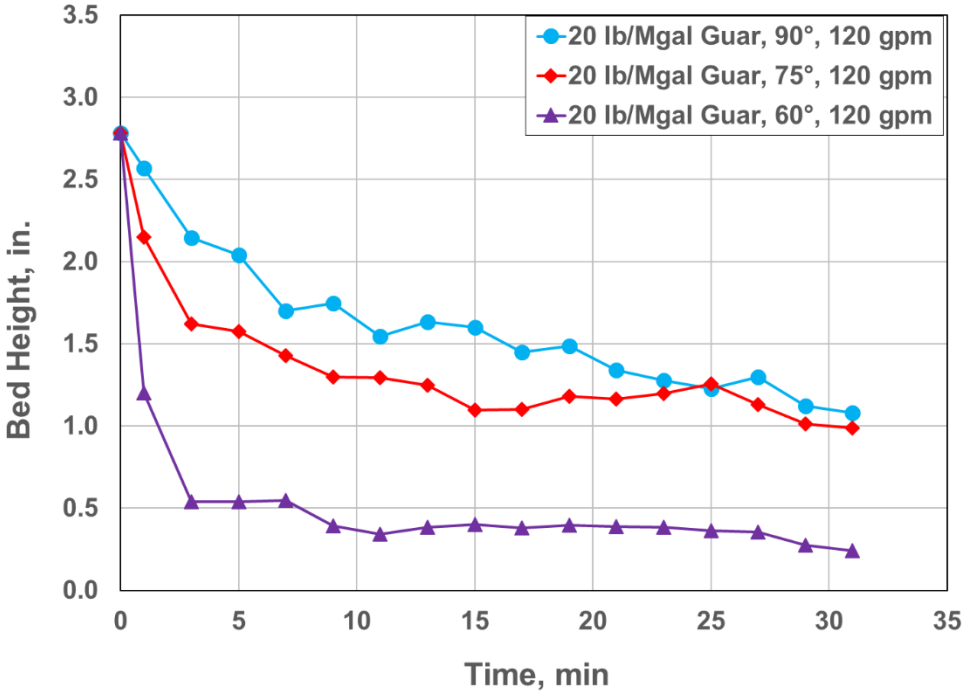

Figure 4.49: Bed erosion curves for 20 lb/Mgal Guar at 120 gpm (TS 2)

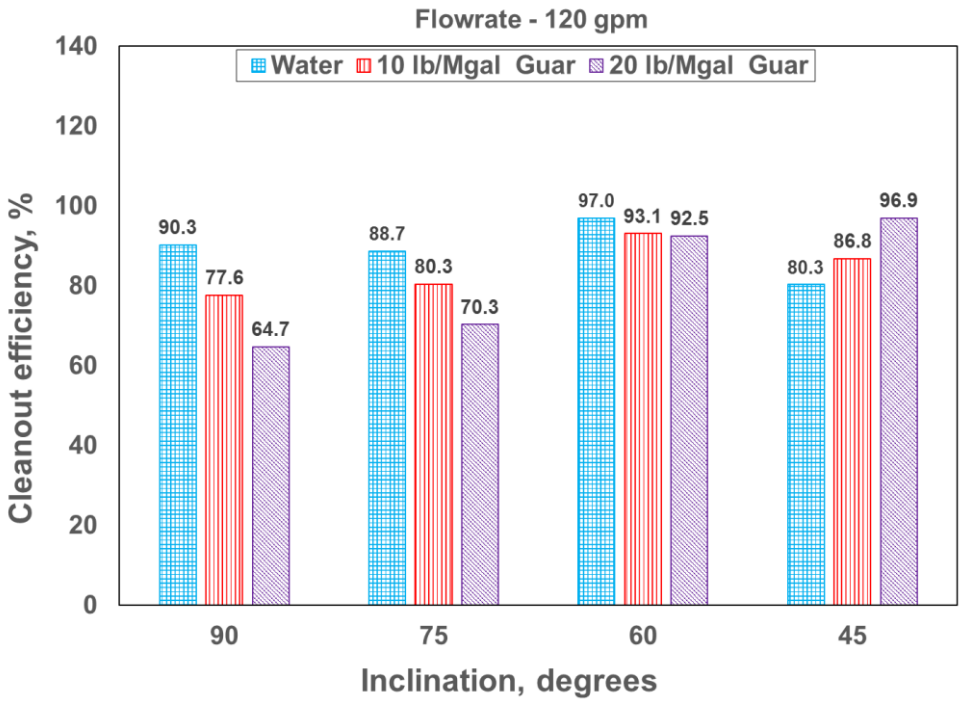

Figure 4.50: Cleanout efficiency of different fluids at 120 gpm (TS 2)

CHAPTER 5

CORRELATION DEVELOPMENT

5.1 Development of empirical correlation

The data of solids bed height as a function of time was used to develop a correlation to predict circulation time required to clean a solids bed for a given set of fluid rheology and flow rate. It should be noted that if the flow rate is insufficient, there will be a critical solids bed height below which solids will not be removed. An exponential function is used to model this non-linear relationship of decreasing solids bed height with time coupled with a critical solids bed height. Martins et al. (1997) suggested that compared to a polynomial equation, exponential function is preferable to model solids bed decrease since it is a solution for first order differential equations.

Therefore, the rate of reduction of bed height was modeled here as exponential decay function; it decreases at a rate proportional to its present value. Similar model was used by Adari (1999). Mathematically, it can be expressed as,

$$\frac{d[h(t)-h_f]}{dt} = -\lambda h(t) \tag{5.1}$$

where, h_f is the steady state bed height.

Upon rearrangement of Eq. 5.1, we get,

$$\frac{d[h(t)-h_f]}{h(t)} = -\lambda dt$$

Integrating,

$$\int \frac{d[h(t)-h_f]}{h(t)} = -\int \lambda dt + c \tag{5.2}$$

$$\ln[h(t)-h_f] = -\lambda t + c \tag{5.3}$$

or,

$$[h(t)-h_f] = e^{-\lambda t} + e^{c} \tag{5.4}$$

where 'c' is the integration constant.

At time t = 0, the bed height, h(t) = h_i

Substituting this into Eq. 3.6

$$[h_i - h_f] = e^{-\lambda(0)} + e^{c}$$

or,

$$c = \ln(h_i - h_f) \tag{5.5}$$

Substituting 'c' into Eq. 5.4

$$[h(t)-h_f] = [h_i - h_f]e^{-\lambda t}$$

$$h(t) = h_f + [h_i - h_f]e^{-\lambda t} \tag{5.6}$$

The proposed model therefore, is

$$h = \alpha + \beta e^{-\lambda t} \tag{5.7}$$

where, $\alpha = h_f$ (steady state bed height); $\beta = (h_i - h_f)$; λ = Reciprocal of time constant; t = time.

The time constant ($1/\lambda$), is the time required for a system to achieve 36.8 % of its initial value. The proposed model is used to fit experimental data to obtain regression

coefficients α, β and λ using a statistical software, MINITAB 16. The regression coefficients of model and the absolute percent deviation between predicted and measured values from experiments are listed in Table 3.2. The predictions from correlation are within 10 % of measured values for all fluids at inclinations of 75° and 90°. The absolute percentage deviation is higher for inclination at 60°; maximum of 30.5%. An unstable bed coupled with dunes at this inclination leads to instantaneous change in bed height, thereby making bed height readings highly variable across the length. With increasing flow rate, α reduces which suggests higher flow rates lead to better solids transport. Also, with increasing flow rate, β and γ increased for each case.

Table 5.1: Correlation Coefficients and Absolute percentage deviation (TS 1)

Fluid	**Flow rate, gpm**	**α**	**β**	**λ**	**Absolute deviation, %**
Water	80	1.007	1.470	0.063	1.9
	100	0.584	2.118	0.079	5.3
	120	0.180	2.570	0.110	14.6
2.16 lb/Mgal HE 150	80	1.891	1.070	0.104	2.5
	100	0.727	1.790	0.041	3.6
	120	0.817	1.813	0.113	7.0
10 lb/Mgal Guar	80	1.838	0.941	0.065	2.4
	100	0.742	2.099	0.049	3.2
	120	1.075	1.632	0.120	4.7
20 lb/Mgal Guar	80	2.167	0.607	0.036	2.9
	100	1.990	0.805	0.170	2.4
	120	1.578	1.207	0.156	4.5

Table 5.2: Correlation Coefficients and Absolute percentage deviation (TS 2)

Fluid	Inclination	Flow rate, gpm	α	β	λ	Absolute deviation, %
Water	90°	80	0.805	2.050	0.068	2.6
		100	0.591	2.215	0.123	6.0
		120	0.053	2.568	0.125	8.7
Water	75°	80	1.058	1.784	0.073	2.9
		100	0.867	1.937	0.130	4.2
		120	0.166	2.550	0.138	8.2
Water	60°	80	1.653	1.138	0.126	3.5
		100	1.599	0.517	0.085	5.8
		120	0.299	2.248	0.100	14.9
10 lb/Mgal Guar	90°	80	1.23	1.526	0.054	1.7
		100	0.787	1.932	0.071	2.1
		120	0.651	2.042	0.100	3.0
10 lb/Mgal Guar	75°	80	1.558	1.104	0.093	3.3
		100	0.753	1.988	0.072	2.0
		120	0.525	2.170	0.115	4.3
10 lb/Mgal Guar	60°	80	1.348	1.366	0.080	11.1
		100	0.844	1.825	0.250	19.2
		120	0.618	1.808	0.378	13.7
20 lb/Mgal Guar	90°	80	1.947	0.928	0.072	1.6
		100	1.446	1.324	0.084	3.3
		120	1.164	1.534	0.111	4.9
20 lb/Mgal Guar	75°	80	1.615	1.065	0.070	4.1
		100	1.491	1.101	0.205	4.8
		120	1.125	1.494	0.306	6.1
20 lb/Mgal Guar	60°	80	0.916	1.005	0.197	9.8
		100	0.281	1.761	0.326	30.5
		120	0.375	1.962	0.847	11.5

5.1.1 Procedure for calculating circulation time

The stepwise procedure for calculating circulation time using the developed correlation is discussed. The correlations developed in test section 2 are used since readings are recorded on both sides of test section, which ensures a more realistic value compared to test section 1 in which readings were taken only on one side.

The following steps should be followed:

1. Note the initial solids bed height (h_i) and desired bed height (h) required after cleanout operation.
2. If h > α, where 'α' is steady state bed height for a combination of fluid and flowrate given in Table 5.2, then proceed with cleanout operation.
3. If h < α, for a combination of fluid and flow rate, then cleanout operation will be unsuccessful. This is because 'α' represents the minimum bed height which can be achieved with a given fluid – flow rate combination.
4. If h > α, then calculate $\beta = h_i - \alpha$.
5. Substitute the values of h, α and β into Eq 5.7.
6. The values of α and λ are constant for a given combination of flow rate and fluid, whereas the value of β depends on the initial bed height.
7. Solving Eq 5.7, will provide the circulation time required to clean a required wellbore to a desired solids bed height using a given combination of fluid and flow rate.

5.2 Correlation development using dimensional analysis

Dimensional analysis is used to relate various process parameters in any operation using the fundamental dimensions (mass, length and time). It is used to analyze large sets of data and for scale up studies. In field operations, the fluid and solids properties and annular configurations may be different than those employed in the present study. Dimensional analysis can be a valuable tool to predict solids erosion rate for an operation

whose parameters are different than those used in the present study. The solids erosion rate is a function of fluid and solid properties, and wellbore parameters.

The solids erosion rate depends on the following:

- Flow rate (q), gpm
- Fluid density (ρ_f), lb/gal
- Fluid viscosity (μ_a) @ 511sec^{-1}, cP
- Solids diameter (d_s), microns
- Solids density (ρ_s), lb/gal
- Circulating time (t), min
- Hydraulic diameter (d_h), in.
- Solids bed height (h) at time 't', in.
- Initial solids bed height (h_i), in.
- Length of the wellbore (l), ft
- Acceleration due to gravity (g), m^2/sec
- Inclination (θ)

Dimensional analysis was performed using Buckingham Pi method and Rayleigh method. The detailed procedures used for both methods are described in Appendix A.

5.2.1 Buckingham Pi method

Buckingham Pi method involves forming (p - q) dimensionless groups (known as π groups), where p is the number of variables and q is number of primary or basic dimensions such as mass, length and time. The different π groups can be related in the

form of $\pi_1 = f(\pi_2, \pi_3, \ldots. \pi_{p-q})$ where f is an arbitrary function. Since there are twelve variables and three basic dimensions; Buckingham Pi method states that nine π groups can be formed.

The nine π groups formed are:

$$\pi_1 = (\frac{\mu_a d_h}{q\rho_f}), \pi_2 = (\frac{\rho_s}{\rho_f}), \pi_3 = (\frac{d_s}{d_h}), \pi_4 = (\frac{h}{d_h}), \pi_5 = (\frac{gd_h^5}{q^2}), \pi_6 = (\frac{l}{d_h}), \pi_7 = (\frac{qt}{d_h^3}),$$

$$\pi_8 = (\frac{h_i}{d_h}), \pi_9 = (\theta).$$

These π groups can be related as,

$$\frac{h}{d_h} = f[(\frac{\rho_s}{\rho_f}), (\frac{\mu_a \mathrm{d}_h}{q\rho_\mathrm{f}}), (\frac{qt}{d_h^3}), (\frac{l}{d_h}), (\frac{d_s}{d_h}), (\frac{gd_h^5}{q^2}), (\frac{h_i}{d_h}), (\theta)] \quad (5.8)$$

where, f is an arbitrary function.

5.2.2 Rayleigh method

This method was used to verify the dimensionless groups formed using Buckingham Pi method. It expresses a relationship between the parameters as an exponential equation. The form of this equation is

$$\pi_1 = A\pi_2^B \pi_3^C \pi_4^D \pi_5^E \pi_6^F \pi_7^G \pi_8^H \pi_9^I \quad (5.9)$$

where, A is an arbitrary constant and B, C, D, E, F, G, H and I are the exponents for π groups.

As it can be seen in Appendix A, this method also produce the same π groups as those obtained from the Buckingham Pi method. A logarithmic transformation is used for developing correlation using Rayleigh method. This transformation is as follows:

$$log\pi_1 = logA + \mathrm{B}log\pi_2 + \mathrm{C}log\pi_3 + \mathrm{D}log\pi_4 + \mathrm{E}log\pi_5 + \mathrm{F}log\pi_6 + \mathrm{G}log\pi_7 + \mathrm{H}log\pi_8 + \mathrm{I}log\pi_9$$

$$\pi_1 = 10^{logA+\mathrm{B}log\pi_2+\mathrm{C}log\pi_3+\mathrm{D}log\pi_4+\mathrm{E}log\pi_5+\mathrm{F}log\pi_6+\mathrm{G}log\pi_7+\mathrm{H}log\pi_8+\mathrm{I}log\pi_9} \quad (5.10)$$

Using non-linear regression analysis, the values of the coefficients and intercept are determined. Three correlations applicable to 60, 75 and 90° are developed. Two different correlations for each inclination, one for water and another for polymeric fluids are developed. These equations are developed by including data for both water and polymeric fluids obtained from test conducted in both test sections.

The correlation for water at 60° is given by,

$$\frac{h}{d_h} = 10^P \quad (5.11)$$

where, $P = -7.244 - 4.021\log\left(\frac{\mu_a d_h}{q\rho_f}\right) + 2.964\log\left(\frac{gd_h^5}{q^2}\right) - 0.297\log\left(\frac{qt}{d_h^3}\right)$

The correlation for polymeric fluids at 60° is given by,

$$\frac{h}{d_h} = 10^Q \quad (5.12)$$

where, $Q = -27.936 - 0.778\log\left(\frac{\mu_a d_h}{q\rho_f}\right) + 117.09\log\left(\frac{\rho_s}{\rho_f}\right) + 1.707\log\left(\frac{gd_h^5}{q^2}\right) - 0.342\log\left(\frac{qt}{d_h^3}\right)$

The correlation for water at 75° is given by,

$$\frac{h}{d_h} = 10^R \quad (5.13)$$

where, $R = -5.192 - 3.263\log\left(\frac{\mu_a d_h}{q\rho_f}\right) + 2.883\log\left(\frac{gd_h^5}{q^2}\right) - 0.486\log\left(\frac{qt}{d_h^3}\right)$

The correlation for polymeric fluids at 75° is given by,

$$\frac{h}{d_h} = 10^S \quad (5.14)$$

where, $S = 11.5293 + 0.10695\log\left(\frac{\mu_a d_h}{q\rho_f}\right) - 44.678\log\left(\frac{\rho_s}{\rho_f}\right) + 0.3454\log\left(\frac{gd_h^5}{q^2}\right) - 0.2428\log\left(\frac{qt}{d_h^3}\right) - 3.5071\log\left(\frac{h_i}{d_h}\right)$

The correlation for 90° for water is given by,

$$\frac{h}{d_h} = 10^T \tag{5.15}$$

where, $T = 2337.90 - 126.41 \log\left(\frac{\mu_a d_h}{q\rho_f}\right) - 11176.98 \log\left(\frac{\rho_s}{\rho_f}\right) +$

$60.84851 \log\left(\frac{g d_h^5}{q^2}\right) + 90.34 \log\left(\frac{l}{d_h}\right) - 0.55 \log\left(\frac{qt}{d_h^3}\right) - 14.77 \log\left(\frac{h_i}{d_h}\right)$

The correlation for 90° for polymeric fluids is given by,

$$\frac{h}{d_h} = 10^U \tag{5.16}$$

where, $U = 12.48 - 0.151 \log\left(\frac{\mu_a d_h}{q\rho_f}\right) - 54.57 \log\left(\frac{\rho_s}{\rho_f}\right) + 0.335 \log\left(\frac{g d_h^5}{q^2}\right) -$

$0.004 \log\left(\frac{l}{d_h}\right) - 0.196 \log\left(\frac{qt}{d_h^3}\right) - 0.197 \log\left(\frac{h_i}{d_h}\right)$

The absolute percentage deviation of predictions from Eqs. 5.11 through 5.16 with the experimental values are 18.13, 21.14, 20.85, 14.64, 21.57 and 8.82 % respectively.

Out of the nine dimensionless groups, π_9 is neglected since the correlations are developed for a specific inclination. The term π_3 is the ratio of solids size to hydraulic diameter, both of which were held constant in all the tests. Hence, the coefficient of π_3 was zero in all the three correlations. Similarly, since tests at inclination of 60 and 75° were conducted only in test section 2, the coefficient of π_6 ($\pi_6 = l/d_h$) is zero for their respective correlations. Also, while conducting tests at 60°, the initial bed height is assumed to be the average of all the bed height for each test conducted at 75 and 90. This is a reasonable assumption since, 200 lbs of sand were added in each case. Since, the initial height is same, so the coefficient of π_8 is zero in the correlation for 60°.

CHAPTER 6

FIELD APPLICATION OF CORRELATION

6.1 Case Study

This section details the procedure for calculating circulation time using the exponential decay equation for a given fluid. Since the developed correlation is to be used for the case study, it is assumed that the annular wellbore configuration, solids size and density, and cleanout fluids are similar to those used in our study.

Problem: Initial Bed height, h_i = 3-in, Fluids: water and 10 lb/Mgal guar, Inclination = 90°. Calculate the circulation time required to reduce the bed height from 3-in. to 0.9-in. with water and 10 lb/Mgal guar? Repeat the calculations when the initial bed height is 4-in.?

Solution:

Exponential Decay Equation:

Refer to Table 5.2, and compare the values of α for water and 10 lb/Mgal guar with the desired bed height, h = 0.9-in.

The desired bed height can be achieved with water at 80, 100 and 120 gpm and with 10 lb/Mgal guar at 100 and 120 gpm.

Consider the first case of cleanout operation with water at 80 gpm.

The form of the exponential decay equation is given by,

$$h = \alpha + \beta e^{-\lambda t} \tag{5.14}$$

From Table 5.2, α = 0.805, λ = 0.068

$\beta = (h_i - h_f)$

or, $\beta = (h_i - \alpha)$

$\beta = 3 - 0.9$

$\beta = 2.1$

Substituting the values of h, α, β and λ into Eq 5.14

$0.9 = 0.805 + 2.1e^{-0.068t}$

Solving for t,

$2.1e^{-0.068t} = 0.095$

t = 45.53 min.

Similarly for water at 100 and 120 gpm, the circulation times required are 16.7 and 10 minutes respectively.

Similarly the circulation times with 10 lb/Mgal guar at 100 and 120 gpm are calculated to be 39.38 min and 22.44 min.

Repeating the above procedure for the case of h_i = 4-in.

Circulation time required for water at 80 gpm:

α = 0.805,

β = hi - α

β = 4-0.805 = 3.195

$\gamma = 0.068$

$0.9 = 0.805 + 3.195e^{-0.068t}$

Solving for t,

t = 51.71 mins

Similarly circulation time required for water at 100 and 120 gpm are 19.52 and 12.31 min respectively.

Similarly with 10 lb/Mgal guar fluid at 100 and 120 gpm, the circulation time required are 47.15 and 26 min.

Hence, it can be concluded that circulation time required decreases with increase in the flow rate given the initial and final bed height are similar. Also, at inclination of 90°, water cleans the bed faster compared to polymeric fluids. The circulation time required increases if the difference between the initial and the final bed height increases.

CHAPTER 7

CONCLUSIONS AND RECOMMENDATIONS

7.1 Conclusions

1. A wellbore cleanout setup with two interchangeable test sections, TS 1 and TS 2, was designed and fabricated for this study. TS 1 is a 54 ft long annular section with 5.5-in. OD x 5-in. ID outer pipe and 2 3/8-in OD inner pipe. TS 2 is a 34 ft long setup with a similar outer pipe-inner pipe configuration as TS 1. This setup allows to conduct solids bed erosion tests with various types of solids and fluids at variable inclination (45 to 90°).
2. Solids bed erosion tests are conducted with fresh water, and 10 and 20 lb/Mgal guar fluids each at flow rates of 80, 100 and 120 gpm and inclinations of 45, 60, 75 and 90° in both TS 1 and 2. Additional tests with 2.16 lb/Mgal HE 150 at 80,100 and 120 gpm were carried out at 90° in TS 1.
3. With increasing flow rate, rate of solids erosion and cleanout efficiency increased for all fluids and inclinations considered. Higher flow rate exerts higher drag force on entrained solids and a higher interfacial shear stress on solids bed leading to improved solids transport. As expected, solids erosion rate and cleanout efficiency were higher at 120 gpm than 80 gpm for all cases considered.
4. Fluids with higher viscosity performed better at 45° compared to low viscosity fluids at all flow rates. The solids erosion rate was higher with 20 lb/Mgal than 10 lb/Mgal and water at 60°. The cleanout efficiency increased with fluid viscosity for 80 and 100 gpm at 60°. At 120 gpm, the cleanout efficiency at 60° for all fluids were similar (92-97%) as the higher drag force compensated for lower viscosity. The solids erosion

rate was higher with water compared to polymeric fluids at 75 and 90° for similar flow rates. Cleanout efficiencies with water were higher compared to polymeric fluids at 75° and 90° for the flow rates considered.

5. For all flow rates considered, rate of solids erosion for water increased with inclination whereas for polymeric fluids it increased with decrease in inclination. With decreasing inclination, the cleanout efficiency increases with fluid viscosity. A 20 lb/Mgal guar fluid performed better at 45° and water performed better at 90° at all flow rates considered.
6. The reduction in solids bed height with time is modeled with an exponential decay equation. The parameters of the equation, namely, steady state bed height (α), the difference in the initial and steady state bed height (β), and reciprocal of time constant (λ), are calculated for different test conditions. With increasing flow rate, 'α' decreased, whereas 'β' and 'λ' increased for each case (for tests conducted in TS 2).
7. The predictions from correlation are within 10% of measured values for all fluids at inclinations of 75 and 90° at all the flow rates considered. The absolute percentage deviation is higher for inclination at 60°, due to the formation of an unstable bed coupled with dunes.
8. Nine different dimensionless groups are developed using the Buckingham Pi method and Rayleigh method. Non-linear regression analysis is performed to develop a generalized correlation model each for inclination of 60, 75 and 90° (each for water and polymeric fluids). The absolute percentage deviation of predictions with the experimental values are 18.13, 21.14, 20.85, 14.64, 21.57 and 8.82 % respectively.

7.2 Recommendations

1. It is observed that there is a critical angle between the 45° and 75°, between which the polymeric fluids perform better than water depending on the flow rate. Additional cleanout studies should be conducted to identify the critical angle as a function of flow rate.
2. Solids bed erosion tests with various initial bed height values, annular configurations, wellbore length, and solids size and density should be undertaken to quantify their effect of wellbore cleanout.
3. Solids bed erosion test in TS 1 should be repeated by recording measurements on both sides of the test section. Since, the bed height readings were recorded on both sides in TS 2, a discrepancy may be observed while comparing the results of TS 2 with TS 1.

NOMENCLATURE

A-I	Coefficients in Eq. 5.9
P-U	Coefficients in Eq. 5.11-5.16
A_p	Projected area of the solid particle
a	Bed arc length measured from top, in.
b	bed arc length measured from bottom, in.
C_D	Drag Coefficient, dimensionless
C_L	Lift Coefficient, dimensionless
D_b	Diameter of bob, mm
D_c	Diameter of cup, mm
D_c	Diameter of cup, mm
d_h	Hydraulic diameter, in.
d_s	Solids diameter, in.
F_b	Buoyancy force
F_d	Drag Force
F_g	Gravitational force
F_l	Lift force
f	Arbitrary function
g	Gravitational acceleration, m/s^2
h_i	Initial bed height, in.
h_f	Steady state bed height, in.
h	Bed height at a given time ‘t’, in.
K_v	Viscometer consistency index, $lbf\text{-}s^n/ft^2$
k	Fluid consistency index, $lbf\text{-}s^n/ft^2$
l	Length of test section, ft
m	Mass of solid particle
N	Spring factor, equals 0.2 for 1/5 spring

n	Flow behavior index, dimensionless
q	Flow rate, gpm
r	Radius of outer pipe, in.
t	Circulation time, min or sec.
u	Fluid velocity, ft/sec

GREEK SYMBOLS

α	Steady state bed height, in.
β	Difference in the initial and final bed height, in.
δ	Distance between the centers of the two pipes, in.
ε	Eccentricity, dimensionless
γ	Shear rate, s^{-1}
γ_w	Wall shear rate, s^{-1}
θ	Wellbore Inclination
θ_i	Fann 35 viscometer reading at i^{th} rpm, dimensionless
λ	Reciprocal of time constant, s^{-1}
μ_a	Apparent viscosity, cP
π	Dimensionless groups
ρ_f	Fluid density, lb/gal
ρ_s	Solids density, lb/gal
τ	Shear stress, lb_f/ft^2
τ_w	Wall shear stress, lb_f/ft^2

ABBREVIATIONS

CT	Coiled Tubing
CDV	Critical Deposition Velocity
CRV	Critical Re-suspension Velocity
CTFV	Critical Transport Fluid Velocity
ID	Inner diameter
LSRV	Low shear rate viscosity
MTV	Minimum Transport Velocity
NI CDAQ	National Instruments Compact Data Acquisition System
OD	Outer diameter
PV	Plastic Viscosity
PVC	Polyvinyl chloride
RPM	Revolutions per minute
TS 1	Test Section 1
TS 2	Test Section 2
YP	Yield Point

REFERENCES

Adari, R.B. 1999. Development of Correlations Relating Bed Erosion to Flowing Time for Near Horizontal Wells. MS thesis, University of Tulsa, USA.

Aitken, B., and Li, J. 2013. Solids Cleanout Analysis Reduces Screen Out Risk. Presented at SPE/ICoTA Coiled Tubing & Well Intervention Conference & Exhibition, The Woodlands, Texas, USA, 26-27 March. SPE 163895.

Bagnold, R.A. 1954. Experiments on a Gravity-Free Dispersion of Large Solid Spheres in a Newtonian Fluid under Shear. Proceedings of the Royal Society of London, Series A: Mathematical and Physical Sciences 225 (1160): 49-63.

Becker, T.E. 1982. The Effects of Mud weight and Hole geometry variations on Cutting transport in Directional Drilling. MS thesis, University of Tulsa,USA.

Brown, N.P., Bern, P.A., and Weaver, A. 1989. Cleaning Deviated Holes: New Experimental and Theoretical Studies. Presented at SPE/IADC Drilling Conference, New Orleans, Louisiana, USA, 28 February-3 March. SPE 18636

Cho, H., Shah, S. N., and Osisanya, S.O. 2001. Effects of Fluid Flow in a Porous Cuttings-Bed on Cuttings Transport Efficiency and Hydraulics. Presented at SPE Annual Technical Conference and Exhibition, New Orleans, Louisiana, USA, 30 September-3 October. SPE 71374.

Cho, H. 2001. Development of a three-segment hydraulic model for cuttings transport in horizontal and deviated wells. Ph.D Dissertation. University of Oklahoma, USA.

Clark, R. K., and Bickham, K. L. 1994. A Mechanistic Model for Cuttings Transport. Presented at SPE Annual Technical Conference and Exhibition, New Orleans, Louisiana, USA, 25-28 September. SPE 28306.

Doron, P., Granica, D., and Barnea, D. 1987. Slurry flow in horizontal pipes - Experimental and Modeling. International Journal of Multiphase Flow 13 (4): 535-547.

Doron, P., and Barnea, D. 1993. A three-layer model for solid-liquid flow in horizontal pipes. International Journal of Multiphase Flow 19 (6): 1029-1043.

Duan, M., Miska., S.Z., Yu, M. et al. 2008. Transport of small cutting in extended reach drilling. SPE Drilling and Completion 23 (3): 258-265. SPE 104192.

Duan, M., Miska, S. Z., Yu, M. et al. 2009. Critical Conditions for Effective Sand-Sized Solids Transport in Horizontal and High-Angle Wells. SPE Drilling and Completion 24 (2): 229-238. SPE 106707.

Gavignet, A. A., and Sobey, I. J. 1989. Model Aids Cuttings Transport Prediction. Journal of Petroleum Technology 41(9): 916-921. SPE 15417.

Jalukar, L.S. 1990. A study of Hole Size Effect on Critical and Sub-critical Drilling Fluid velocities in Cuttings Transport for Inclined Wellbores. MS Thesis, University of Tulsa, USA.

Kamp, A. M., and Rivero, M. 1999. Layer Modeling for Cuttings Transport in Highly Inclined Wellbores. Presented in Latin American and Caribbean Petroleum Engineering Conference, Caracas, Venezuela, 21-23 April. SPE 53942.

Kelessidis, V. C., and Mpandelis, G. E. 2003. Flow Patterns and Minimum Suspension Velocity for Efficient Cuttings Transport in Horizontal and Deviated Wells in Coiled-Tubing Drilling. Presented at SPE/ICoTA Coiled Tubing Conference and Exhibition, Houston, Texas, 8-9 April. SPE 81746.

Kenny, P., Sunde, E., and Hemphill, T. 1996. Hole Cleaning Modelling: What's 'n' Got To Do With It? Presented at SPE/IADC Drilling Conference,New Orleans, Louisiana, 12-15 March. SPE 35099.

Khan, M.U. 2008. Transient Cuttings Transport Focused on Bed Erosion for Horizontal Wells. MS thesis, University of Tulsa, USA.

Larsen, T. I., Pilehvari, A. A., and Azar, J.J. 1997. Development of a New Cuttings-Transport Model for High-Angle Wellbores Including Horizontal Wells. SPE Drilling & Completion **12**(2): 129-136. SPE 25872.

Leising, L. J., and Walton, I. C. 2002. Cuttings-Transport Problems and Solutions in Coiled-Tubing Drilling. SPE Drilling & Completion 17 (1): 54-66. SPE 77261.

Li, J., and Walker, S. 1999. Sensitivity analysis of Hole Cleaning parameters in Directional Wells. Presented at SPE/IcoTA Coiled Tubing Roundtable, Houston, Texas, 25-26 May. SPE 54498.

Li, J., Walker, S., and Aitken, B. 2002. How to Efficiently Remove Sand from Deviated wellbores with a solids transport simulator and a Coiled Tubing Cleanout Tool. Presented at the SPE Annual Technical Conference and Exhibition, San Antonio, Texas, 29 September-2 October, 2002. SPE 77527.

Li, J., Wilde, G., and Crabtree, A.R. 2005. Do Complex Super-Gel Liquids Perform Better Than Simpled Linear liquids in Hole Cleaning with Coiled Tubing ? Presented at the SPE/ICoTA Coiled Tubing Conference and Exhibition, The Woodlands, Texas, 12-13 April. SPE 94185.

Li, J., and Wilde, G. 2005. Effect of Particle Density and Size on Solids Transport and Hole Cleaning With Coiled Tubing. Presented at SPE/ICoTA Coiled Tubing Conference and Exhibiton, The Woodlands, Texas, 12-13, April. SPE 94187.

Li, J., Misselbrook, J., and Sach, M. 2010. Sand Cleanout with Coiled Tubing : Choice of Process, Tools or Fluids ? Journal of Canadian Petroleum Technology 49 (8): 69-82. SPE 113267.

Li, J., and Luft, B. 2014. Overview of Solids Transport Study and Application in Oil-Gas Industry: Theoretical Work. Presented at International Petroleum Technology Conference, Kuala Lumpur, Malaysia, 10-12 December 2014. IPTC 17832.

Martins, A. L., and Santana, C. C. 1992. Evaluation of Cuttings Transport in Horizontal and Near Horizontal Wells-A Dimensionless Approach. Presented at the SPE Latin America Petroleum Engineering Conference, Caracas, Venezuela, 8-11 March. SPE 23643.

Martins, A.L., Campos, W., Liporace, F.S. et al. 1997. On Erosion Velocity of a Cuttings Bed During Circulation of Horizontal and Highly Inclined Wells. Presented at Latin American and Carribean Petroleum Engineering Conference, Rio de Janiero, Brazil, 30 August-3 Spetember. SPE 39021.

Moore, Preston L. 1974. “Drilling Practice Manual”, The Petroleum Publishing Co., Tulsa.

Nguyen, D., and Rahman, S.S. 1998. A Three Layer Hydraulic Program for Effective Cuttings Transport and Hole Cleaning in Highly Deviated and Horizontal Wells. SPE Drilling and Completion 13 (3):182- 189. SPE 51188.

Nguyen, T.N. 2007. Study of Effective Hole Cleaning Using “ Conventional and Enhanced Sweeps” in Horizontal Wellbores. MS thesis, University of Tulsa, USA.

Okrajni, S., and Azar, J. J. 1986. The Effects of Mud Rheology on Annular Hole Cleaning in Directional Wells. SPE Drilling Engineering **1**(4): 297-308. SPE 14178.

Ozbayoglu, E.M., Miska, S.Z., Reed, T. et al. 2003. Cuttings Transport with Foam in Horizontal and Highly Inclined Wellbores. Presented at SPE/IADC Drilling Conference, Amsterdam, Netherlands,19-21 February. SPE 79856.

Ozbayoglu, M. E., Miska, S. Z., Reed, T. et al. 2004. Analysis of the Effects of Major Drilling Parameters on Cuttings Transport Efficiency for High-Angle Wells in Coiled Tubing Drilling Operations. Presented at SPE/ICoTA Coiled Tubing Conference and Exhibition, Houston, Texas, 23-24 March. SPE 89334.

Ozbayoglu, M. E., Sorgun, M., Saasen, A. et al. 2010. Hole Cleaning Performance of Light-Weight Drilling Fluids During Horizontal Underbalanced Drilling. Journal of Canadian Petroleum Technology 49 (4): 21-26. SPE 136689.

Peden, J.M., Ford, J.T., and Oyeneyin, M.B. 1990. Comprehensive Experimental Investigation of Drilled Cuttings Transport in Inclined Wells Including the Effects of Rotation and Eccentricity. Presented in European Petroleum Conference, The Hague, Netherlands, 21-24 October. SPE 20925.

Ramadan, A., Skalle, P., and Saasen, A. 2005. Application of a three-layer modeling approach for solids transport in horizontal and inclined channels. Chemical Engineering Science 60 (10): 2557-2570.

Rubiandini, R. 1999. Equation for Estimating Mud Minimum Rate for Cuttings Transport in an Inclined-Until-Horizontal Well. Presented at SPE/IADC Middle East Drilling Technology Conference, Abu Dhabi, United Arab Emirates, 8-10 November. SPE 57541.

Sapru, A. 2001. Study of Effect of Drill pipe rotation on cuttings bed erosion in horizontal wells. MS thesis, University of Tulsa, USA.

Seeberger, M.H., Matlock, R.W., and Hanson, P.M. 1989. Oil Muds in Large Diameter, Highly Deviated Wells: Solving the Cuttings Removal Problem. Presented at SPE/IADC Drilling Conference, New Orleans, Louisiana, 28 Feb-3 March. SPE 18635.

Sifferman, T.R., and Becker, T.E. 1992. Hole Cleaning in Full Scale Inclined Wellbores. SPE Drilling Engineering 7 (2):115-120. SPE 20422.

Tomren, P. H., Iyoho, A. W., and Azar, J. J. 1986. Experimental Study of Cuttings Transport in Directional Wells. SPE Drilling Engineering 1 (1): 43-56. SPE 12123.

Walker, S., and Li, J. 2001. Coiled-Tubing Wiper Trip Hole Cleaning in Highly Deviated Wellbores. Presented at SPE/ICoTA Coiled Tubing Roundtable, Houston, Texas, 7-8 March. SPE 68435.

Zamora, M., and Hanson, P. 1990. Selected Studies in High Angle Hole Cleaning. Nineteenth Annual Convention Proceedings, Indonesian Petroleum Association. 411-425.

APPENDIX

Formulation of dimensionless groups:

Buckingham Pi theorem

Variables included in the analysis are q, ρ_f, μ, ρ_s , d_s, h, h_i, d_h, g, θ, l and t.

Since, θ is dimensionless, it can be considered as one of the dimensionless groups.

Hence, excluding θ, 11-3 = 8 dimensionless groups can be formed.

Repeating variables considered in this analysis are q, ρ_f and d_h.

The seven Π groups can be formed as shown,

$$\pi_1 = (q)^a(\rho_f)^b(d_h)^c(\mu)^d$$

Substituting the basic dimensions of each variable,

$$M^0L^0T^0 = (L^3T^{-1})^a(ML^{-3})^b(L)^c(ML^{-1}T^{-1})^d$$

$$M^0L^0T^0 = (M)^{b+d}(L)^{3a-3b+c+d}(T)^{-a-d}$$

Comparing the terms of M, L and T on both sides,

M: b = -d ; L: 3a-3b+c+d=0 ; T:-a - d =0

a= -d, b=-d, c= d

$$\pi_1 = \left(\frac{\mu d_h}{q\rho_f}\right) \qquad (1)$$

$$\pi_2 = (q)^a(\rho_f)^b(d_h)^c(\rho_s)^d$$

Substituting the basic dimensions of each variable,

$$M^0L^0T^0 = (L^3T^{-1})^a(ML^{-3})^b(L)^c(ML^{-3})^d$$

$$M^0L^0T^0 = (M)^{b+d}(L)^{3a-3b+c-3d}(T)^{-a}$$

Comparing the terms of M, L and T on both sides,

M: b+d=0; L: 3a-3b+c-3d =0 ; T:-a =0

a = 0; b = -d; c = 0

$$\pi_2 = (\frac{\rho_s}{\rho_f}) \tag{2}$$

$$\pi_3 = (q)^a (\rho_f)^b (d_h)^c (d_s)^d$$

Substituting the basic dimensions of each variable,

$$M^0 L^0 T^0 = (L^3 T^{-1})^a (ML^{-3})^b (L)^c (L)^d$$

$$M^0 L^0 T^0 = (M)^b (L)^{3a-3b+c+d} (T)^{-a}$$

Comparing the terms of M, L and T on both sides,

M: b =0; L: 3a - 3b + c + d= 0; T: -a=0

a = 0; b = 0; c =d

$$\pi_3 = (\frac{d_s}{d_h}) \tag{3}$$

$$\pi_4 = (q)^a (\rho_f)^b (d_h)^c (h)^d$$

Substituting the basic dimensions of each variable,

$$M^0 L^0 T^0 = (L^3 T^{-1})^a (ML^{-3})^b (L)^c (L)^d$$

$$M^0 L^0 T^0 = (M)^b (L)^{3a-3b+c+d} (T)^{-a}$$

Comparing the terms of M, L and T on both sides,

M: b =0; L: 3a - 3b + c + d= 0; T: -a=0

a = 0; b = 0; c =d

$$\pi_4 = (\frac{h}{d_h}) \tag{4}$$

$$\pi_5 = (q)^a (\rho_f)^b (d_h)^c (g)^d$$

Substituting the basic dimensions of each variable,

$$M^0 L^0 T^0 = (L^3 T^{-1})^a (ML^{-3})^b (L)^c (LT^{-2})^d$$

$$M^0 L^0 T^0 = (M)^b (L)^{3a-3b+c+d} (T)^{-a-2d}$$

Comparing the terms of M, L and T on both sides,

M: b = 0; L: 3a - 3b + c + d= 0; T: -a - 2d = 0

a = -2d; b = 0; c = 5d

$$\pi_5 = (\frac{g d_h^5}{q^2}) \qquad (5)$$

$$\pi_6 = (q)^a (\rho_f)^b (d_h)^c (l)^d$$

Substituting the basic dimensions of each variable,

$$M^0 L^0 T^0 = (L^3 T^{-1})^a (ML^{-3})^b (L)^c (L)^d$$

$$M^0 L^0 T^0 = (M)^b (L)^{3a-3b+c+d} (T)^{-a}$$

Comparing the terms of M, L and T on both sides,

M: b =0; L: 3a - 3b + c + d= 0; T: -a=0

a = 0; b = 0; c =d

$$\pi_6 = (\frac{l}{d_h}) \qquad (6)$$

$$\pi_7 = (q)^a (\rho_f)^b (d_h)^c (t)^d$$

Substituting the basic dimensions of each variable,

$$M^0 L^0 T^0 = (L^3 T^{-1})^a (ML^{-3})^b (L)^c (T)^d$$

$$M^0L^0T^0 = (M)^b(L)^{3a-3b+c}(T)^{-a+d}$$

Comparing the terms of M, L and T on both sides,

M: b =0; L: 3a - 3b + c = 0; T: -a+d=0

a = d; b = 0; c = -3d

$$\pi_7 = (\frac{qt}{d_h^3}) \tag{7}$$

The final dimensionless group is

$$\pi_8 = \frac{h_i}{d_h} \tag{8}$$

So, the final list of dimensionless group of variables is,

$\pi_1 = (\frac{\mu d_h}{q\rho_f})$, $\pi_2 = (\frac{\rho_s}{\rho_f})$, $\pi_3 = (\frac{d_s}{d_h})$, $\pi_4 = (\frac{h}{d_h})$, $\pi_5 = (\frac{gd_h^5}{q^2})$, $\pi_6 = (\frac{l}{d_h})$, $\pi_7 = (\frac{qt}{d_h^3})$ and

$\pi_8 = (\frac{h_i}{d_h})$, $\pi_9 = (\theta)$.

Rayleigh Method:

Variables included in the analysis are q, ρ_f, μ, ρ_s , d_s, h, h_i, d_h, g, θ, l and t.

Since, θ is dimensionless, it can be considered as one of the dimensionless groups.

The bed height is the dependent variable, hence,

h = f (q, ρ_f, μ, ρ_s, d_s, h_i, d_h, g, l, t)

$h = (q)^a(\rho_f)^b(\mu)^c(\rho_s)^d(d_s)^e(d_h)^f(g)^g(l)^h\ (t)^i(h_i)^j$ (9)

Writing each variable using their fundamental dimensions,

$$M^0L^1T^0 = (L^3T^{-1})^a(ML^{-3})^b(ML^{-1}T^{-1})^c(ML^{-3})^d(L)^e(L)^f(LT^{-2})^g(L)^h(T)^i(L)^j$$

(10)

Equating the coefficients of the M, L and T on both sides of Eq. 10,

M: b + c + d = 0

L: 3a - 3b - c - 3d + e + f + g +h +j= 1

T: - a - c -2g +i = 0

Expressing a, b and f in terms of e, c, d, g, h and i,

a = - c - 2g + i, b = - c - d, f = 1 + c - e + 5g - h -3i

Substituting a, b and f in A-9,

$h = (q)^{-c-2g+i}(\rho_f)^{-c-d}(\mu)^c(\rho_s)^d(d_s)^e(d_h)^{1+c-e+5g-h-3i}(g)^g(l)^h(t)^i$

Grouping the terms with similar coefficients,

$$h = (\frac{\rho_s}{\rho_f})(\frac{\mu d_h}{q\rho_f})(\frac{qt}{d_h^3})(\frac{l}{d_h})(\frac{d_s}{d_h})(\frac{h_i}{d_h})(\frac{gd_h^5}{q^2})d_h$$

$$\frac{h}{d_h} = f[(\frac{\rho_s}{\rho_f})(\frac{\mu d_h}{q\rho_f})(\frac{qt}{d_h^3})(\frac{l}{d_h})(\frac{d_s}{d_h})(\frac{h_i}{d_h})(\frac{gd_h^5}{q^2})] \quad (11)$$

Hence, the groups are

$$(\frac{h}{d_h}),(\frac{\rho_s}{\rho_f}),(\frac{\mu d_h}{q\rho_f}),(\frac{qt}{d_h^3}),(\frac{l}{d_h}),(\frac{d_s}{d_h}),(\frac{h_i}{d_h}),(\frac{gd_h^5}{q^2})and(\theta)$$

Hence, the dimensional groups obtained from Rayleigh method and Buckingham theorem are similar.